Rebeca Bailo Vergara

Characterization of the MmpL4/MmpS4 efflux system in *Mycobacterium bovis* and *Mycobacterium tuberculosis*

Departamento

Bioquímica y Biología Molecular y Celular

Director/es

Aínsa Claver, José Antonio

CHARACTERIZATION OF THE MMPL4/MMPS4 EFFLUX SYSTEM IN *MYCOBACTERIUM BOVIS* AND *MYCOBACTERIUM TUBERCULOSIS*

Autor

Rebeca Bailo Vergara

Director/es

Aínsa Claver, José Antonio

UNIVERSIDAD DE ZARAGOZA

Bioquímica y Biología Molecular y Celular

2015

Universidad Zaragoza
1542

Tesis Doctoral

Characterization of the MmpL4/MmpS4 efflux system in *Mycobacterium bovis* and *Mycobacterium tuberculosis*

Autor

Rebeca Bailo Vergara

Director/es

José A. Aínsa Claver

UNIVERSIDAD DE ZARAGOZA
Bioquímica y Biología Molecular y Celular

2015

Universidad Zaragoza
1542

FACULTAD DE MEDICINA

DEPARTAMENTO DE MICROBIOLOGÍA, MEDICINA
PREVENTIVA Y SALUD PÚBLICA

Characterization of the MmpL4/MmpS4 efflux system in *Mycobacterium bovis* and *Mycobacterium tuberculosis*

Memoria presentada por Rebeca Bailo Vergara

Licenciada en Bioquímica

Para optar al grado de Doctor por la Universidad de Zaragoza

Director: José A. Aínsa Claver

Curriculum vitae

Personal details

Surname: Bailo
Name: Rebeca
Phone number: + 34 637269523
Email: rebecab@unizar.es

EDUCATION

09/2015
(Expected)

Ph.D. in Biochemistry and Cell and Molecular Biology
University of Zaragoza - Spain

07/2011

Master in Cell and Molecular Biology
University of Zaragoza - Spain

07/2010

Degree in Biochemistry
University of Zaragoza - Spain

AWARDS

03/2011 – 03/2015

PhD studentship
- Granted by the regional Government of Aragón (Spain), Department of Education, Science and Technology; BOA 11/02/2011.
- Mycobacterial Genetics Group, Department of Microbiology. Faculty of Medicine. University of Zaragoza.

02/2014

Short term fellowship
- Granted by EMBO (European Molecular Biology Organization) in order to make a predoctoral research visit in Birmingham (UK).
- 20th January – 25th April 2014.

11/2013

President's Fund 2013 for Research Visit Grant
- Granted by SGM (Society for General Microbiology) so as to make a predoctoral research visit in Birmingham (UK).
- 20th January – 25th April 2014.

09/2012   **Young Scientist Meeting Grant (YSMG)**
- Granted by FEMS (Federation of European Microbiological Societies) in order to attend the FEMS meeting: Tuberculosis 2012, Biology, Pathogenesis, Intervention strategies.
- Paris (France), 11-15th September 2012.

11/2010   **2º Extraordinary Award "Francisco Grande Covián"**
- Second-best record in the degree on Biochemistry from University of Zaragoza.

RESEARCH VISITS

01/2014 – 04/2014   **Predoctoral research visit**
- School of Bioscience, University of Birmingham, Birmingham, United Kingdom.
- Supervised by Prof. Apoorva Bhatt and Prof. Gurdyal S. Besra.
- 20th January – 25th April 2014.
- Phenotypic characterization of efflux pump mutants from *Mycobacterium tuberculosis*.
- Funded by Society for General Microbiology and EMBO.

LABORATORY SKILLS

Microbiology
- Basic microbiology procedures: cultures staining, storage, drug susceptibility testing…
- Work in BSL-1, BSL-2 and BSL-3 laboratories: culture and manipulation of pathogenic (*Mycobacterium tuberculosis*) and no-pathogenic microorganisms.
- 5 years of experience in genetic manipulation of mycobacteria.

Cell culture
- Manipulation, seeding and infection of cells lines.

Molecular biology and genetic engineering
- Genomic and plasmid DNA extraction and analysis.
- RNA, protein and lipid extraction and analysis.
- Cloning and transformation of *E.coli* and mycobacteria.
- PCR, qRT-PCR, gel electrophoresis, sequence analysis, Southern and Western Blot hybridization.

Other techniques
- Accumulation and susceptibility assays.
- Flow cytometry assays.
- Optical and fluorescence microscopy.

PUBLICATIONS

Role of the Mmr efflux pump in drug resistance in _Mycobacterium tuberculosis_.
Liliana Rodrigues, Cristina Villellas, Rebeca Bailo, Miguel Viveiros, José Antonio Ainsa.
ANTIMICROBIAL AGENTS AND CHEMOTHERAPY.57 - 2,pp. 751 - 757.2013.

Lipid transport in _Mycobacterium tuberculosis_ and its implications in virulence and drug development.
Rebeca Bailo, Apoorva Bhatt, José Antonio Ainsa.
Biochemical pharmacology. Accepted.

RESEARCH PROJECTS

02/2011 – 01/2016   **"More Medicines for Tuberculosis (MM4TB)"**
- Funded by the European Union 7th Framework Programme. Ref: 260872.
- Coordinator Stewart T. Cole.
- Principal investigator: José Antonio Aínsa.

01/2010 – 12/2012   **"Study of membrane transporters of _Mycobacterium tuberculosis_: implications in resistance and virulence"**
- Funded by the Spanish Ministry of Science and Innovation (BIO-2009-09405).
- Principal investigator: José-Antonio Aínsa.

01/2007 to date   **"Corporate Research Programme on Tuberculosis"**
- Funded by CIBERes (Spanish Network for Research on Respiratory Diseases).
- Principal investigator: Carlos Martín.

01/2003 to date   **"Research on Mycobacterial Genetics"**
- Funded by Regional Government of Aragon.
- Principal investigator: Carlos Martín.

02/2015
VII National Conference BIFI2015.
- Zaragoza (Spain), 4-6th February 2015.
- Poster. "New (and not so new) drugs against tuberculosis".
José Antonio Ainsa; Cristina Villellas; Rebeca Bailo; Ainhoa Lucia; Santiago Ramón-García; Begoña Gracia.

11/2012
IX Meeting of Molecular Microbiology (Spanish Society for Microbiology).
- Palma de Mallorca (Spain), 14-16th November 2012.
- Poster. **"**Characterization of the MmpL4 Knockout Mutant of *Mycobacterium tuberculosis*".
Rebeca Bailo; Cristina Villellas; José Antonio Aínsa.
- Poster. "Rv1258c and Rv1410c efflux pumps contribute to antibiotic resistance and virulence in *Mycobacterium tuberculosis*".
Cristina Villellas; Rebeca Bailo; Ainhoa Arbués; Nacho Aguiló, Carlos Martín; José Antonio Aínsa.
- Poster. "Role of the Mmr efflux pump in drug resistance in *Mycobacterium tuberculosis*".
Liliana Rodrigues, Cristina Villellas, Rebeca Bailo, Miguel Viveiros, José Antonio Aínsa.

09/2012
EMBO Conference Tuberculosis 2012: Biology, pathogenesis, intervention, strategies.
- Paris (France), 11-15th September 2012.
- Poster. "Characterization of the MmpL4 Knockout Mutant of *Mycobacterium tuberculosis*".
Rebeca Bailo; Cristina Villellas; Carlos Martín; José Antonio Aínsa.

02/2012
Protein Targets: Discovery of Bioactive Compounds.
- Zaragoza (Spain), 1-4th February 2012.
- Poster. **"**Novel compounds active against Mycobacterium tuberculosis: Testing competitive inhibitors of type II Dehydroquinase".
Begoña Gracia; Liliana Rodrigues; Cristina Villellas; Rebeca Bailo; Jesús A. Gonzalo-Asensio; L. Tizón; C. González-Bello; José Antonio Aínsa.

10/2012	**Workshop Novel vaccines against tuberculosis.**
	Tuberculosis Vaccine Iniciative, University of Zaragoza and Fundación Ramón Areces.
	• Madrid (Spain), 17-18th October 2011.

06/2010	**Workshop Research and development of new vaccines against tuberculosis.**
	Tuberculosis Vaccine Iniciative, University of Zaragoza y Fundación Ramón Areces.
	• Zaragoza (Spain), 3-4th June 2010.

TRAINING COURSES

06/2015	**Introductory Course of Biostatistics.**
	Health Research Institute of Aragon (IIS Aragón).
	20 hours.

05/2015	**Introductory Course of Immunology and Immunotherapy and Cancer.**
	Forum Debate "Oncology". Miguel Servet University Hospital.
	2.5 hours.

02/2015	**Training course for directing and designing experimental procedures with laboratory animals. Category C.**
	Ethical advisory commission for animal experimentation.
	80 hours.

| 06/2013 | **B1 certificate in English.** |
| | Official School for Foreign Languages – Zaragoza, Spain. |

01/2013	**English conversation course.**
	University Modern Languages Centre – University of Zaragoza.
	12 hours.

10/2011	**IV Training Seminars on Respiratory Diseases of CIBERes.**
	Spanish Network for Research on Respiratory Diseases.
	• Palma de Mallorca (Spain), 27-28th October 2011.
	• Poster. "Study of the effect of transport mechanism of molecules through cell envelope of *Mycobacterium tuberculosis* in drug discovery". Rebeca Bailo; Cristina Villellas; Carlos Martín; José Antonio Aínsa.

12/2011	**Online course on Biotechnology and Microbiological Safety of Food**
	Spanish Society for Microbiology.
	• 3th October-20th December 2011.
06/2011	**XV Introductory Course in Microbiology Research.**
	Spanish Society for Microbiology.
	• Oviedo (Spain), 6-10th June 2011.
08/2010	**Internship on Genitourinary Pathogens Diagnostic and Techniques.**
	Microbiology Service of University Clinical Hospital "Lozano Blesa".
	150 hours.

TEACHING EXPERIENCE

2012 - 2015	180 hours (three academic years) of teaching practical courses for undergraduate students of the Degree on Biochemistry (Molecular Genetics and Genetic Engineering), Degree on Biotechnology (Microbiology, Genetic Engineering, Microbial Biotechnology), and for graduate students of the Master on Molecular and Cell Biology (Wine Microbiology). University of Zaragoza.

LANGUAGES

Spanish: mother tongue.
English: fluent.

REFERENCES

Prof. **José Antonio Aínsa**. Grupo de Génetica de Micobacterias. Departamento de Microbiologia, Medicina Preventiva y Salud Pública. Universidad de Zaragoza. CIBA-Centro de Investigación Biomédica de Aragón, Av San Juan Bosco, 13. 50009-Zaragoza, Spain. +34 876 55 43 43. ainsa@unizar.es

Prof. **Carlos Martín Montañes**. Grupo de Génetica de Micobacterias. Departamento de Microbiologia, Medicina Preventiva y Salud Pública. Universidad de Zaragoza. C/ Domingo Miral s/n. 50009-Zaragoza, Spain. +34 976 76 17 59. carlos@unizar.es

Prof. **Apoorva Bhatt**. School of Bioscience, University of Birmingham, Edgbaston, Birmingham, B15 2TT, United Kingdom. +44 (0)121 41 45893. a.bhatt@bham.ac.uk

Index of Contents

2

Index of Figures

Index of Tables

Abbreviations list

Abbreviation	Meaning
7AAD	7-actinomycinD
ABC	ATP-Binding Cassette
Abs	Absorbance
ADC	Albumin, dextrose, catalase
AES	Allelic Exchange Substrate
Amp	Ampicillin
ATP	Adenosine triphosphate
BAC	Bacterial Artificial Chromosome
BCG vaccine	Bacille Calmette-Guerin vaccine
Bdq	Bedaquiline
Bp	Base pair
BSA	Bovine Serum Albumin
BSL-2	Biosafety level 2
BSL-3	Biosafety level 3
C	Cytosine
cDNA	Complementary DNA
CFU	Colony Forming Units
CHCA	*alpha*-Cyano-4-hydroxycinnamic acid
Clo	Clofazimine
Cm	Chloramphenicol
CPZ	Chlorpromazine
CTAB	Cetyltrimethylammonium bromide
DAT	Diacyltrehaloses
DC	Dendritic cell
DFO	Desferrioxamine
DIP	2,2'-dipyridyl

DMEM	Dulbecco's modified Eagle medium
DNA	Deoxyribonucleic acid
dsDNA	Double stranded DNA
DTT	Dithiothreitol
EDTA	Ethylene-diamine-tetraacetic acid
Emb	Ethambutol
EtBr	Ethidium bromide
Eth	Ethionamide
FAMEs	Fatty Acid Methyl Esters
FBS	Fetal Bovine Serum
FC	Fold change
FDR	False Discovery Rate
FQs	Fluoroquinolones
G	Guanine
GMM	Glucose monomycolate
HIV	Human Immunodeficiency Virus
Hyg	Hygromycin
IEF	Isoelectric focusing
IGRAs	Interferon Gamma Release Assays
Inh	Isoniazid
IPTG	Isopropyl-β-thiogalactopyranoside
Km	Kanamycin
LAM	Lipoarabinomannan
LB	Luria Bertani
LM	Lipomannan
Log-phase	Logarithmic phase
MAMEs	Mycolic Acid Methyl Esters
Man-LAM	Mannose-capped Lipoarabinomannan
MATE	Multidrug And Toxic-compound Extrusion
MDR	Multidrug Resistant

MFS	Major Facilitator Super-family
MH-S	Murine alveolar macrophages
MIC	Minimum Inhibitory Concentration
MMDAG	Monomeromycolyl diacylglycerol
MmpL	Mycobacterial Membrane Protein Large
MmpS	Mycobacterial Membrane Protein Small
MOI	Multiplicity of infection
MPA	Molybdophosphoric acid
Mtb	*Mycobacterium tuberculosis*
OADC	Oleic acid, albumin, dextrose, catalase
OD	Optical Density
Ofx	Ofloxacin
PAMPs	Pathogen-Associated Molecular Patterns
PAT	Polyacyltrehaloses
PBS	Phosphate-buffered saline
PCR	Polymerase Chain Reaction
PDIM	Phthiocerol dimycocerosate
PE	Proline-glutamic acid
PFA	Paraformaldehyde
PGL	Phenolic glycolipid
PIMs	Phosphatidylinositol mannosides
PPE	Proline-proline-glutamic acid
PRRs	Pattern Recognition Receptors
Pza	Pyrazinamide
qRT-PCR	Real-Time Quantitative PCR
REMA	Resazurin Microtiter Assay
Rif	Rifampicin
RNA	Ribonucleic acid
RND	Resistance Nodulation Division
RNI	Reactive Nitrogen Intermediates

RQ	Relative quantification
RT	Room Temperature
RT-PCR	Real-Time PCR
SCID	Severe Combined Immune Deficient
SD	Standard deviation
SDS	Sodium Dodecyl Sulfate
SDS-PAGE	SDS polyacrylamide gel electrophoresis
SL	Sulpholipid
Sm	Streptomycin
SMR	Small Multidrug Resistance
Spc	Spectinomycin
SSC	Saline Sodium Citrate
TAG	Triacyl glycerol
TAT	Triacyltrehaloses
TB	Tuberculosis
TBAH	Tetrabutylammonium hydroxide
TBE	Tris-Borate-EDTA
TCA	Trichloroacetic acid
TDM	Trehalose dimycolate
TDR	Totally Drug Resistant
TE	Tris-EDTA
Tet	Tetracycline
TFA	Trifluoroacetic acid
TLC	Thin Layer Chromatography
TMD	Transmembrane domain
TMM	Trehalose monomycolate
Tpp	Tetraphenylphosphonium
VP	Verapamil
WHO	World Health Organization
XDR	Extensively Drug Resistant

Summary

Mycobacterium tuberculosis has got several proteins of the MmpL family (Mycobacterial Membrane Protein Large) belonging to the RND (Resistance Nodulation Division) superfamily of transporters. The efflux system MmpL4/MmpS4 (Rv0450c y Rv0451c) may contribute to virulence and possibly to lipid transport, in addition to transport of siderophores and/or other compounds. The main objective of this thesis has been the characterization of this efflux system in *M. bovis* and *M. tuberculosis*.

First, we constructed a mutant strain of *M. tuberculosis* deleted in *rv0450c* gene, a second strain deleting *rv0450c* and *rv0451c* genes, and derivatives of these mutants in which wild-type genes were complementing the deletions. Further, we produced a strain overexpressing *rv0450c* and *rv0451c* genes. All these strains have been used for investigating the role of this efflux system.

Regarding *in vitro* tests, antibiotic susceptibility assays indicated that the efflux system MmpL4/MmpS4 of *M. tuberculosis* is not involved in intrinsic drug resistance, but we have got evidences of its ability to transport ethidium bromide. In addition, we have determined that deletion of the efflux system MmpL4/MmpS4 of *M. tuberculosis* does not affect the ability to grow in iron-deficient media, probably because bacteria still have the efflux system MmpL5/MmpS5, which may compensate the deletions. However, overexpression of the MmpL4/MmpS4 efflux system in *M. tuberculosis* caused a morphological change in its colonies, and a decrease in its *in vitro* growth rate, suggesting that structure and/or composition of the mycobacterial membrane has been affected notably.

M. tuberculosis strains with altered levels of expression of the MmpL4 and MmpS4 efflux system, either by overexpression or by deletion, are affected in their capability for surviving inside macrophages, showing lower cytotoxicity than the parental strain H37Rv. These results indicate that efflux system MmpL4/MmpS4 is needed for virulence of *M. tuberculosis,* and that its level of expression is critical.

The deletion of *mmpL4* gene in *M. tuberculosis* alters expression of other genes encoding transport proteins of the same family, such as *mmpL5*/*mmpS5* and *mmpL10*. Phenotypically, main lipids of *M. tuberculosis* were not affected significantly by the loss of *mmpL4*, the loss of both *mmpL4* and *mmpS4,* or the overexpression of *mmpL4* and *mmpS4*. Proteomic analysis of strains having altered levels of these genes or the complemented mutants showed that there were relevant changes in the levels of proteins related to fatty acid metabolism.

In *M. bovis*, we observed that overexpression of the MmpL4/MmpS4 efflux system changed production of PDIM*,* an important lipid for mycobacterial virulence.

Resumen

Mycobacterium tuberculosis posee varias proteínas de la familia MmpL (Mycobacterial Membrane Protein Large) que pertenecen a la superfamilia de transportadores RND (Resistance Nodulation Division). El sistema de eflujo MmpL4/MmpS4 (Rv0450c y Rv0451c) puede contribuir a su virulencia y posiblemente al transporte de lípidos, además de al transporte de sideróforos y/o de otros compuestos. El objetivo principal de esta tesis ha sido la caracterización de este sistema de eflujo en *M. bovis* y *M. tuberculosis.*

En primer lugar, hemos construido una cepa mutante de *M. tuberculosis* en la que se ha delecionado el gen *rv0450c*, una cepa mutante en la que se han delecionado los genes *rv0450c* y *rv0451c*, y cepas derivadas de las anteriores, en la que los genes wild-type complementan la deleción. Además, se ha generado una cepa que sobreexpresa los genes *rv0450c* y *rv0451c*. Con estas cepas se han realizado diversos ensayos encaminados a identificar la función de este sistema de eflujo.

En cuanto a los experimentos *in vitro*, los ensayos de susceptibilidad a antibióticos indican que el sistema de eflujo MmpL4/MmpS4 en *M. tuberculosis* no estaría implicado en la resistencia intrínseca a fármacos, pero sí se ha puesto en evidencia su capacidad para transportar bromuro de etidio. Además, hemos determinado que la delección del sistema de eflujo MmpL4/MmpS4 en *M. tuberculosis* no afecta la capacidad de la bacteria para crecer en medios deficientes en hierro, probablemente debido a que las bacterias todavía conservan el sistema de eflujo MmpL5/MmpS5 que compensa las delecciones realizadas. Sin embargo, la sobreexpresión del sistema de eflujo MmpL4/MmpS4 en *M. tuberculosis* provoca cambios en la morfología de las colonias y disminuye su velocidad de crecimiento, lo que sugiere que la estructura y/o composición de la membrana se ha visto alterada de forma importante.

Las cepas de *M. tuberculosis* con alteraciones en la expresión del sistema de eflujo MmpL4/MmpS4, tanto por sobreexpresión como por delección, se vieron afectadas en su capacidad para sobrevivir en el interior de macrófagos, presentando una menor citotoxicidad que la cepa parental H37Rv. Estos resultados indican que el sistema de eflujo MmpL4/MmpS4 es necesario para la virulencia de *M. tuberculosis*, y que su nivel de expresión es crítico.

La delección del gen *mmpL4* en *M. tuberculosis* ha provocado la alteración de los niveles de expresión de otros genes que codifican transportadores de la misma familia, entre ellos *mmpL5*/*mmpS5* y *mmpL10*. A nivel fenotípico, no pudo observarse ninguna variación significativa en la producción de los principales lípidos de *M. tuberculosis* causados por la pérdida del gen *mmpL4* o de ambos genes *mmpL4* y *mmpS4,* ni tampoco por la sobreexpresión de los genes *mmpL4* y *mmpS4*. Con el análisis proteómico de las cepas con alteraciones en la

expresión de estos genes, o de los mutantes complementados, se encontraron cambios relevantes en los niveles de proteínas relacionadas con el metabolismo de ácidos grasos.

En *M. bovis*, se observó que la sobreexpresión del sistema de eflujo MmpL4/MmpS4 provocó alteraciones en la producción de PDIM, un lípido importante para la virulencia de las micobacterias.

1. Introduction

1.1. Immersion in tuberculosis world

1.1.1. Significance of tuberculosis

Mycobacterium tuberculosis (Mtb) is the causative agent of tuberculosis (TB) and has been present in the human population since antiquity. Initially, it was thought that *Mycobacterium bovis* strains jumped from infected cattle to humans during the domestication of animals in the Neolithic period, hence originating human TB [1]. However, it is now widely accepted that the ancients Mtb strains were originated from environmental mycobacteria 70,000 years ago in Africa [2, 3]. The introduction of agriculture, civilization and the increase in human population density led to the selection of virulent and transmissible Mtb strains. These modern Mtb strains spread throughout the world causing the TB epidemics that ravaged mankind for centuries [4].

Nowadays, 9 million people fell ill with TB and 1.5 million died in 2013 (including 360,000 deaths among HIV-positive people) according to the World Health Organization (WHO) [5]. At present, TB is the second leading cause of death from an infectious agent worldwide, after the Human Immunodeficiency Virus (HIV), in spite of the fact that we have powerful tools in order to face TB: vaccination, diagnostics and treatments.

1.1.2. Vaccination

BCG (Bacille Calmette-Guerin) was first developed in the 1920s and it is the only vaccine currently available for TB disease. BCG vaccine provides children with excellent protection against the disseminated forms of TB, especially against meningitis; however protection against pulmonary TB in adults is variable. Several hypotheses attempt to explain this variability: differences in protection between BCG substrains (which originated by subculturing the original vaccine strain in different laboratories or countries around the world), an inadequate dosage of BCG in some trials, interference with environmental mycobacteria, genetic differences in human populations, and geographic differences in clinical isolates of *M. tuberculosis* [6].

Due to its variable effectiveness, the inability to prevent primary infection and reactivation of latent TB, which is the principal source of disease transmission, great efforts are being made by governments, research institutions and private foundations for constructing and testing new promising vaccine candidates.

1.1.3. Diagnostics

The most common methods for diagnosing TB worldwide are sputum smear microscopy and the Mantoux tuberculin skin test. These methods are simple, inexpensive and quick, but their main drawbacks are low specificity and sensitivity. It is necessary to carry out more tests such as chest radiography, Interferon Gamma Release Assays (IGRAs), and culturing, to confirm the infection with Mtb [7]. Diagnosing TB using culture involves the identification of Mtb by biochemical tests [8], and molecular identification methods. Moreover, cultures can also be used for drug susceptibility testing [8], which is important to get successful treatment in drug-resistant TB patients.

Early identification of people with symptomatic TB not only allows therapy to be administered before serious lung damage occurs, but also helps to prevent the spread of the bacteria to other susceptible people. For this purpose, there are several new diagnostic technologies under development [9].

1.1.4. Treatment and drug resistance

Drug treatment is the only effective therapy for TB. Drugs are classified into three groups based on evidence of efficacy, potency and experience of use [10].

- First-line anti-TB drugs are the most effective and widely used drugs for the treatment of drug-susceptible TB (which is not drug resistant).
- Second-line anti-TB drugs are reserved for resistant bacilli to first-line therapy. A drug may be classed as second-line instead of first-line for being less effective than the first-line drugs (e.g. para-aminosalicylic acid), having toxic side-effects (e.g. cycloserine) or being effective, but unavailable in many developing countries (e.g. fluoroquinolones).
- Third-line anti-TB drugs are characterized for not being very effective (e.g. clarithromycin) or because their efficacy has not been proven (e.g. clofazimine).

Table 1. Drugs used in the treatment of TB [10].

First-line drugs	Second-line drugs	Third-line drugs
Isoniazid	Aminoglycosides (Streptomycin, Kanamycin, Amikacin)	Clofazimine
Rifampicin	Polypeptides (Capreomycin, Viomycin)	Linezolid
Pyrazinamide	Fluoroquinolones (Ciprofloxacin, Levofloxacin, Moxifloxacin, Ofloxacin, Gatifloxacin)	Amoxicillin plus clavulanate
Ethambutol	Para-aminosalicylic acid	Imipenem plus cilastatin
Rifapentine	Cycloserine	Clarithromycin
Rifabutin	Terizidone	
	Ethionamide	
	Prothionamide	
	Thioacetazone	
	Linezolid	

With appropriate antibiotic treatment, around 90% of HIV-negative patients with drug-susceptible TB can be cured in 6 months using a combination of rifampicin (Rif), isoniazid (Inh), pyrazinamide (Pza) and ethambutol (Emb) for 2 months, followed by a four-month continuation phase of Rif and Inh [5]. The main reason for prescribing this combination of medicines in the treatment of TB is because the likelihood of the emergence of multiple drug resistance bacteria is virtually impossible [11], apart from the fact that the distinct anti-TB drugs have different modes of action: Inh are bactericidal against replicating bacteria; Emb is bacteriostatic at low doses, but is used in TB treatment at higher, bactericidal doses; Rif is bactericidal and has a sterilizing effect; and Pza is only weakly bactericidal, but is very effective against bacteria located in acidic environments, inside macrophages, or in areas of acute inflammation.

Monotherapy, irregular drug supply, poor drug quality, inappropriate prescription, poor adherence to treatment and unsuitable supervision and support on the part of health personnel, can contribute to appearance, selection and multiplication of drug-resistant TB strains. This phenomenon is called acquired resistance [11]. The traditional mechanisms by which bacteria in general acquire drug resistance are: barrier mechanisms (decreased permeability/efflux), degrading/inactivating enzymes, modification of pathways involved in drug activation/metabolism, and drug target modification (mutations) or target amplification [12]. Mtb in particular is able to acquire drug resistance by spontaneous mutations in its chromosomal genes, but no horizontal transfer of resistance genes had been reported [13].

Table 2. The commonly used TB drugs with the genes associated with their respective resistance and major mechanism of resistance [12].

Drug or drug class	Resistance genes	Rv number	Gene function	Mechanism of drug resistance
Rifamycins	rpoB	Rv0667	RNA polymerase B	Target modification
Isoniazid	katG	Rv1908c	Catalase-peroxidase enzyme	Decreased drug activation
	inhA	Rv1484	NADH-dependent enoyl-acyl carrier protein	Target amplification or modification
Pyrazinamide	pncA	Rv2043c	Pyrazinamidase	Decreased drug activation
Ethambutol	embCAB operon	Rv3793-5	Arabinosyltransferases	Target modification
Streptomycin	rpsL	Rv0682	12S ribosomal protein	Target modification
	rrs	n/a	16S rRNA	Target modification
	gidB	Rv3919c	7-Methylguanosine methyltransferase	Target modification
Kanamycin/amikacin	rrs	n/a	16S rRNA	Target modification
	eis	Rv2416c	Aminoglycoside acetyltransferase	Inactivating mutation
Capreomycin	rrs	n/a	16S rRNA	Target modification
	tylA	Rv1694	rRNA methyltransferase	Target modification
Quinolones	gyrA	Rv0006	DNA gyrase A	Target modification
	gyrB	Rv0005	DNA gyrase B	Target modification
Ethionamide	ethA	Rv3854c	Mono-oxygenase	Decreased drug activation
	ethR	Rv3855	Transcriptional regulatory repressor protein (TetR family)	Decreased drug activation
	inhA	Rv1484	NADH-dependent enoyl-acyl carrier protein	Target amplification and modification
Para-aminosalicylic acid	thyA	Rv2764c	Thymidylate synthase	
	ribD	Rv2671	Enzyme in riboflavin biosynthesis	
Cycloserine	alr	Rv3423c	Alanine racemase	
	ddl	Rv2981c	D-Alanine-D-alanine ligase	
	cycA	Rv1704c	Bacterial D-serine/L- and D-alanine/glycine/D-cycloserine proton symporter	
Bedaquiline	atpE	Rv1305	ATP synthase	
Linezolid	rrl	n/a	23S rRNA	Target modification
	rplC	Rv0701	50S ribosomal protein L3	Target modification

1.1.5. New drugs to treat tuberculosis

The advent of antibiotics for the treatment of TB represented a major breakthrough in the fight against the disease. However, since its very first use, antibiotic therapy has been associated with the emergence of resistance to drugs. Drug-resistant bacilli can be classified in three groups:

- Multidrug-resistant (MDR) strains are resistant to Inh and Rif. In 2013, the highest levels of MDR-TB were found in Eastern Europe and central Asia, where in some countries more than 20% of new TB cases and more than 50% of those previously treated for TB have MDR-TB [5].
- Extensively drug-resistant (XDR) strains are resistant to not only Inh and Rif, but also a quinolone and one of the second-line injectable drugs (kanamycin, amikacin or capreomycin). In 2006, the first XDR-TB outbreak was described in KwaZulu-Natal in South Africa. The mortality rate among HIV-positive patients, with limited or no access to highly active antiretroviral therapy was 98%, after a median survival period from diagnosis of only 16 days [14].

- Totally drug-resistant (TDR) refers to strains that are resistant to all available TB drugs, although the number and level of resistance to each drug has not yet been precisely defined. To date, only a limited number of TDR-TB cases have been confirmed in Iran, India, South Africa and Italy [15].

Apart from multidrug resistance, there are other aspects that further underscore the urgency to discover new TB drugs, such as the long treatment duration, complex regimens that involve expensive and toxic drugs, and toxic effects when given with antiretroviral therapy. Consequently, a great effort is being done by academic laboratories, non-profit organizations and pharmaceutical companies to research in drug development. The result of this common work is reflected in the following figure, which represents the list of compounds that are currently in the pipeline of candidate drugs for the treatment of TB [16].
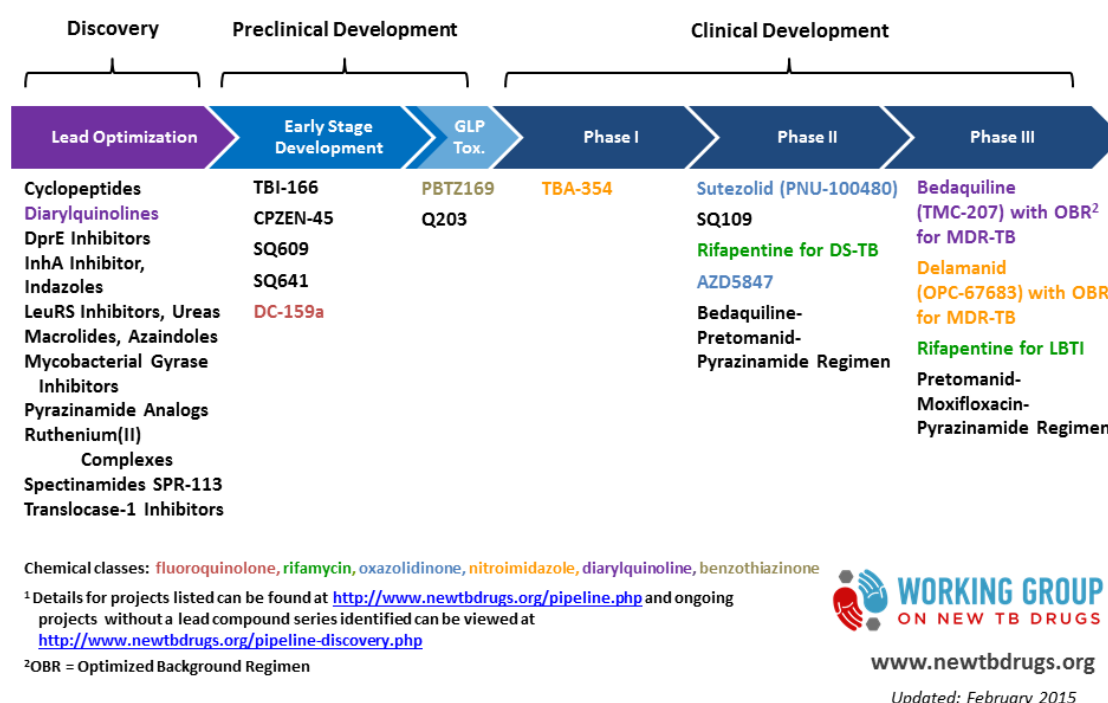
Figure 1. The development pipeline for new TB drugs [16].

It should be pointed out that although advances in drug discovery are significant, it is still necessary more anti-TB drugs that target new pathways or enzymes, new targets to avoid cross-resistance to existing medicines, and inhibitors that could enhance the activity of the current and new drugs. Given the current burden of TB, it would be a mistake to stop researching on new anti-TB drugs.

1.2.   The tubercle bacillus

1.2.1.   General characteristics of *Mycobacterium tuberculosis*

Mtb is an acid-fast, rod-shape and aerobe bacteria belonging to the family *Mycobacteriaceae*, included into the suborder *Corynebacterineae*, order *Actinomycetales* [17].

Mtb is not classified as either Gram-positive or Gram-negative since it gives the appearance of "ghost" cells when it is Gram stained [18]. Phenotypically it is catalase and nitrate reductase positive, non-motile and non-spore forming bacillus of 2-5 μm in length and 0.2-0.5 μm in width. Mtb is slow-growing mycobacteria with a generation time of ~15-20 hours. It takes 4 weeks to get visual colonies on solid medium. In smears made from *in vitro*-grown colonies, chains of cells often form distinctive serpentine cords, which is called cording, and it is related to virulent strains of the bacterium.

1.2.2.   Genome and genetic manipulation of *Mycobacterium tuberculosis*

The complete genome sequence of the best-characterized strain of Mtb, H37Rv [19], was obtained in 1998 [20] and it is in continuous revision since then [21, 22]. The genome comprises 4,411,532 base pairs, and has an unusually high G+C (guanine plus cytosine) content of 65.9%. The last re-annotation identifies 4,111 genes thought to encode 4,018 proteins and 80 stable RNAs [23]. The most striking feature of Mtb genome is the abundance of genes involved in lipid metabolism, both in lipid biosynthesis and lipolysis, which occupy about 7% of the coding capacity of the genome. Besides, the Pro-Glu motif containing (PE) and Pro-Pro-Glu motif containing (PPE) family of proteins represents 4% of the genome. They are highly expanded in pathogenic mycobacteria and have been linked to virulence [24, 25], but their function remains unknown.
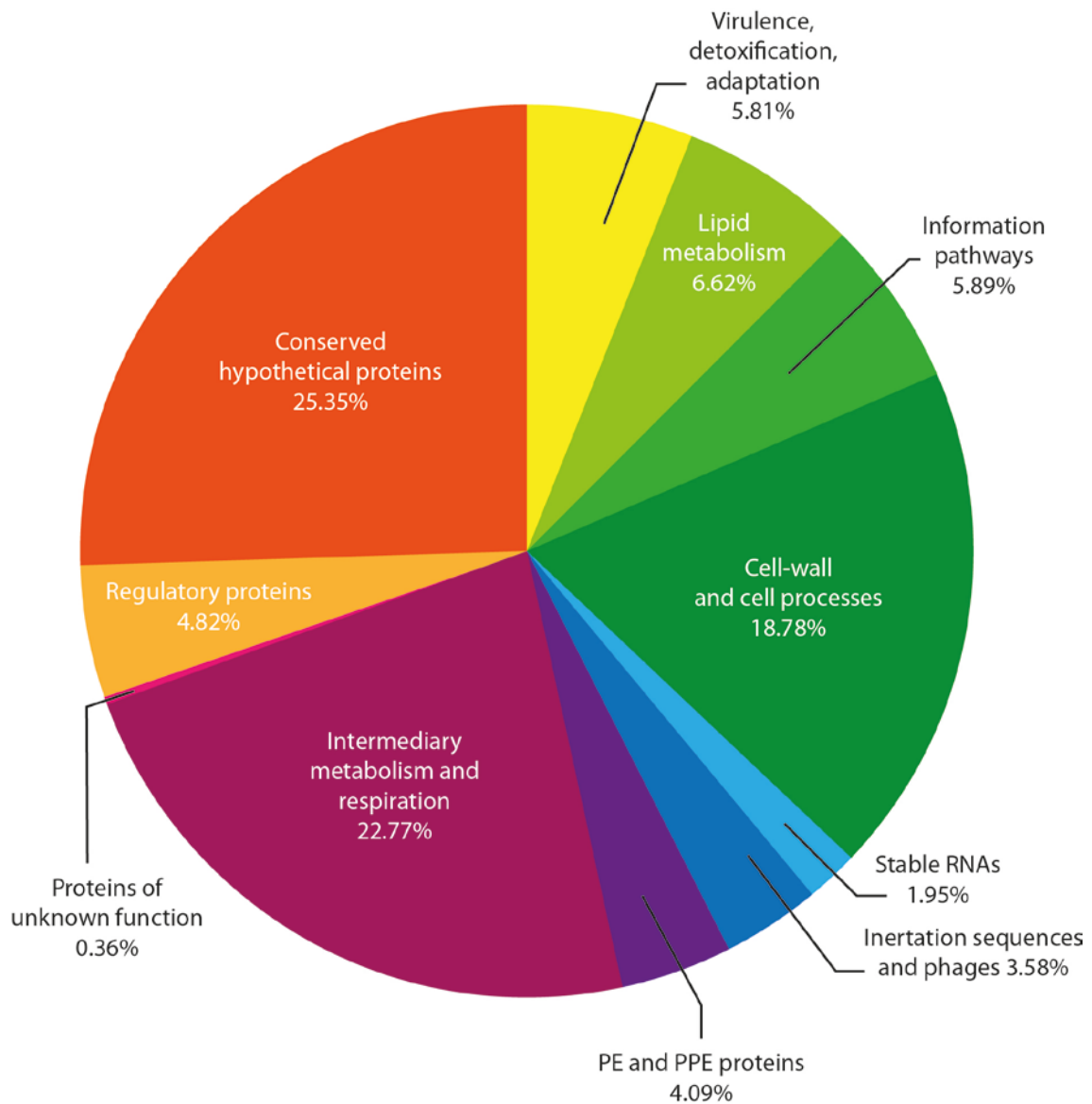
Figure 2. Functional classification of *Mycobacterium tuberculosis* genes. Adapted from [21, 23].

Genetic manipulation of DNA remains one of the most powerful approaches for understanding the molecular basis of survival, virulence, and pathogenicity of a bacterium. It should be noticed that genetic manipulation of slow-growing mycobacteria such as Mtb is complicated by its pathogenesis, slow growth rate, inefficient DNA uptake and high level of illegitimate recombination. Eventually, the discovery of mycobacteriophages and plasmids, the development of mycobacterial vectors and transposons, transformation by electroporation, and successful methods to generate knockout mutant strains allowed the study gene function in mycobacteria. A variety of genetic methods have been developed such as those based on homologous recombination: counter-selection with *sacB*, specialized transduction, and recombineering.

- Counter-selection with *sacB* [26]: this two-step strategy consists of the integration of a suicide vector carrying an inactivated copy of the target gene through a single crossover under antibiotic pressure. The suicide vector contains a genetic marker (usually encoding resistance to an antibiotic) and *sacB* gene, which is lethal to mycobacteria in the presence of sucrose. The antibiotic resistant colonies are plated on sucrose to remove the vector sequence by a second crossover event.
- Specialized transduction [27]: The target gene of interest is interrupted with a selectable marker and cloned into a cosmid vector in *E. coli*. This construct is cloned into a mycobacteriophage vector and packaged by transducing *M. smegmatis*. A high-titer stock can then be prepared to infect Mtb and obtain mutant strains.
- Recombineering [28]: This strategy consists of the electroporation of a linear dsDNA allelic exchange substrate (AES), which contains two small portions of sequence identity to the target *locus* flanking an antibiotic resistance gene. Using Che9c gp60 and gp61 recombinases stimulate homologous recombination.

1.2.3. Mycobacterial cell envelope

The mycobacterial envelope is unique, both in molecular composition and in the architectural arrangement of its constituents. Its complex structure is composed of a typical phospholipid bilayer plasma membrane, an outer membrane called mycomembrane and an outermost layer known as the capsule. The plasma membrane is composed mainly of anionic phospholipids in a bilayer arrangement with proteins. The mycomembrane consists of an asymmetric lipid bilayer made of long chain (C60-C90) mycolic fatty acids in the inner leaflet, and free intercalating glycolipids and waxy components on the outer leaflet. Cryo-electron microscopy images support a folded or compact configuration of these mycolic chains, which reminiscent of Gram-negative bacterial cell walls [29-31], and also confirm that the measured thickness of the outer membrane is consistent with the size of mycobacterial porins, such as MspA from *M. smegmatis*, which may therefore form channels in this bilayer [29]. The outer and inner membrane form a periplasmic space, with the presence of a thin layer of peptidoglycan covalently linked to arabinogalactan and lipoarabinomannan, which in turn are bound to mycolic acids. Peptidoglycan, arabinogalactan and mycolic acids form the cell wall skeleton. The capsule is mainly composed of polysaccharides, proteins and small amounts of lipids, and it is considered to have a different molecular composition in pathogenic and non-pathogenic species [32]. The outermost layer is visible in conventional electron microscopy preparations only when cultures have been grown in free detergent medium. It is thought that mycobacterial growth under routine culturing conditions (with a detergent as Tween-80) promotes removing of this layer [33].

Free glycolipids are important components of the mycobacterial cell wall. Among them can be found trehalose dimycolate (TDM), often referred as cord factor, trehalose monomycolate

(TMM), glucose monomycolate (GMM), glycerol monomycolate, diacyltrehaloses (DAT), triacyltrehaloses (TAT), polyacyltrehaloses (PAT), the recently characterized family of mannosyl-b-1-phosphomycoketides, sulpholipids (SLs), phenolic glycolipids (PGLs) and phthiocerol dimycocerosate (PDIM). Other major glycolipids are lipomannan (LM), lipoarabinomannan (LAM) and phosphatidylinositol mannosides (PIMs).

Ultrastructure of mycobacterial envelope is unclear yet; therefore, the spatial location of many lipid components is still mere speculation. A proposed model of the mycobacterial cell envelope is shown in the following figure.
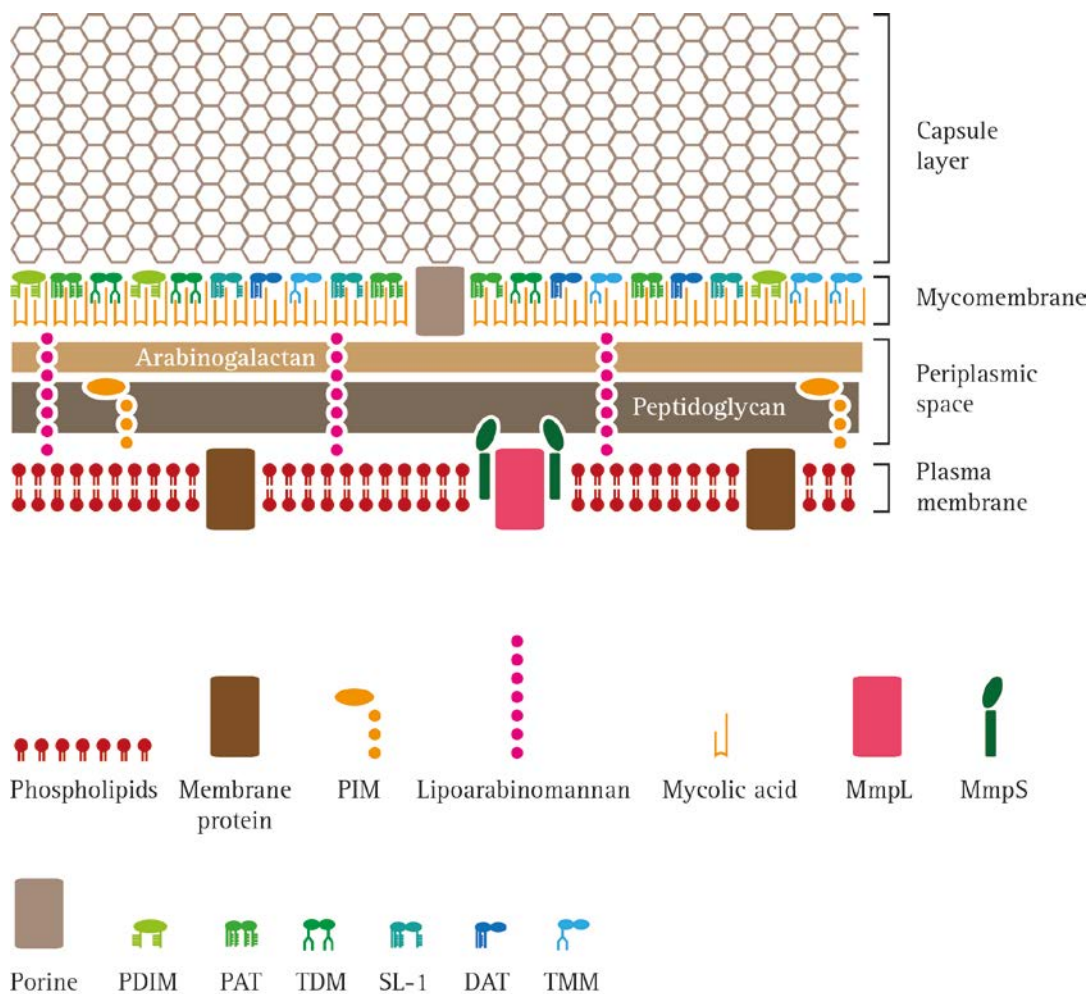
Figure 3. Schematic representation of the cell envelope of *Mycobacterium tuberculosis*. Adapted from [34].

The mycobacterial envelope is involved in important roles, such as defining the shape of the cell and providing mechanical and osmotic protection. Its unusual high hydrophobicity makes it an efficient barrier for chemotherapeutic agents. Other important function is the transport of molecules, including nutrients, ions and toxic metabolites. During infection, cell-wall compounds have been shown to trigger a set of biological effects including adjuvanticity, toxicity, immune down-modulation, and arrest of phagosome maturation [35].

1.3. Pathogenesis and virulence

1.3.1. Progress of the disease

Early in infection, TB follows a relatively reproducible course. Mtb bacilli are inhaled from droplets aerosolized by individuals with active pulmonary TB into the alveoli of the lung. Once there, macrophages and dendritic cells (DCs) express numerous pattern recognition receptors (PRRs) that recognize antigenic molecules expressed on Mtb called pathogen-associated molecular patterns (PAMPs) to internalize the bacilli [36, 37]. This event induces a localized proinflammatory response that leads to recruitment of inflammatory cells [38]. Over time, the granuloma becomes a stratified lesion which includes blood-derived infected and uninfected macrophages, foamy macrophages, epithelioid cells (uniquely differentiated macrophages), and multinucleated giant cells (Langerhans cells), B and T lymphocytes, and fibroblasts [39]. In many lesions these cell populations are separated by a fibrous layer of extracellular matrix [40].

The main function of the granuloma is to localize and contain Mtb while concentrating the immune response to a limited area. Thanks to this strategy 90% of infected individuals defeat the disease or are successful in controlling TB (latent TB) [38]. People with latent TB are still infected but are non-infectious and asymptomatic. However, in 10% of the cases, when the host's immune status changes as consequence of aging, malnutrition, stress, cancer, immunosuppressive drugs or co-infection with HIV among other factors, this situation leads to active disease in which the centre of the granuloma becomes necrotic, liquefies (caseous necrosis), and viable bacilli can be released and spread to the lung, other parts of the body and the atmosphere [39].
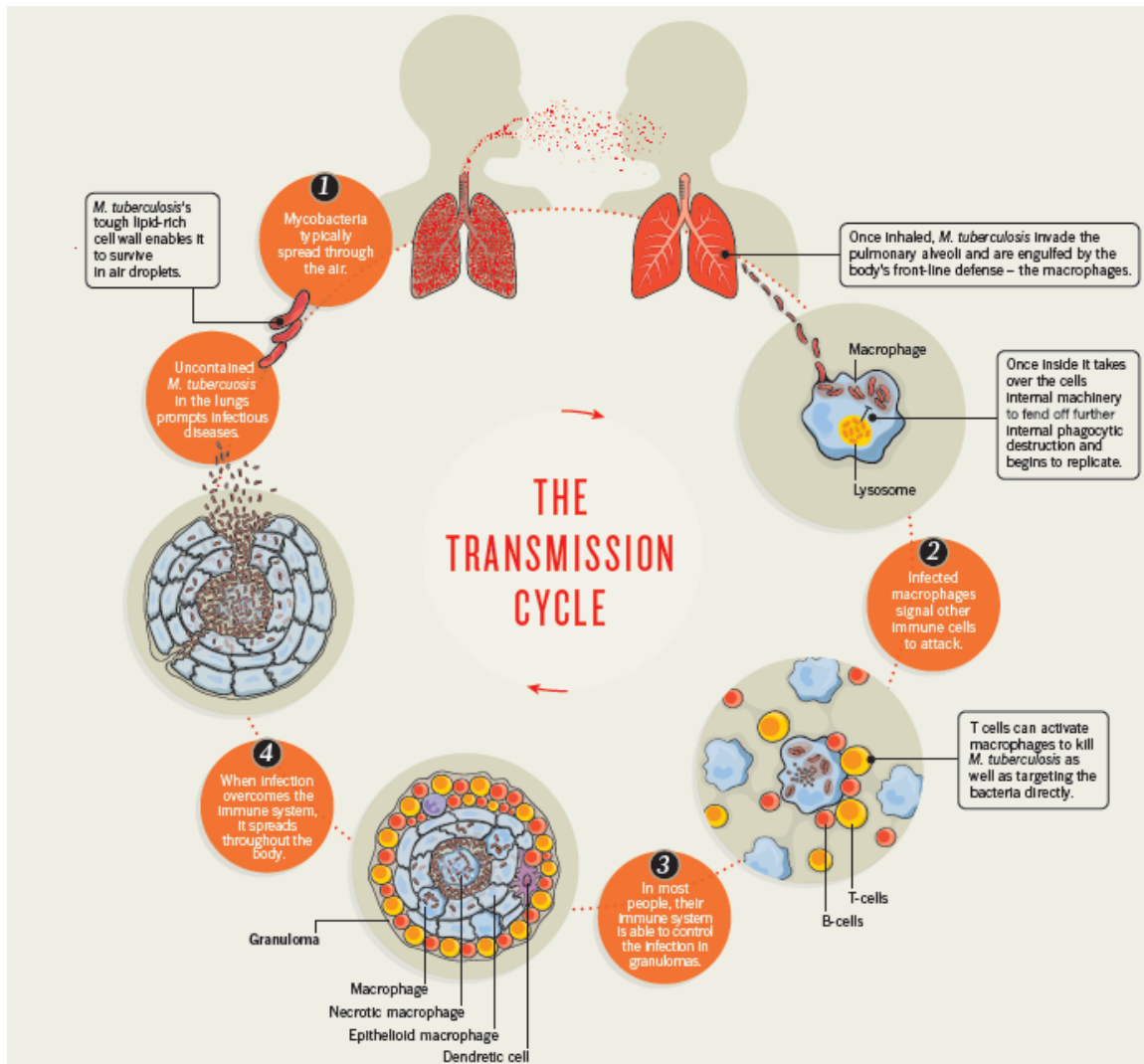
Figure 4. The transmission cycle of *Mycobacterium tuberculosis* [41].

1.3.2. Life inside the phagosome

In the lungs, Mtb bacilli are phagocytosed by alveolar macrophages, in which the bacteria are contained in phagosomes. Under normal circumstances, phagosomes are fused to lysosomes and other endosomes in a process called phagosome maturation [42]. The resultant compartment is among other attributes, iron limiting, carbon poor, hypoxic, nitrosative, and oxidative [43]. The mechanisms that Mtb have evolved to counteract the hostile environment of the macrophage, such as inhibiting phagosome-lysosome fusion or to escape into the cytosol are part of its virulence factors. The cytosol likely offers a more permissive environment, where the bacteria can replicate and induce the infected macrophages to undergo necrosis instead of apoptosis, a strategy that allows the bacteria to infect neighbouring cells, thereby enabling the perpetuation of the infection process [44].

1.3.3. Virulence factors

Mtb virulence determinants can be defined as factors that are important for the progression of the TB disease.

In recent years, there have been considerable advances in the understanding of the molecular bases of pathogenicity, virulence and persistence of mycobacteria. The use of transposon mutant libraries in combination with different *in vivo* screening methods has allowed the identification of mycobacterial virulence genes, and factors, whose role in virulence is clear. For example, the nucleoside diphosphate kinase Ndk [45, 46] and the phosphatase SapM [47] both affect the maturation of the mycobacterial-containing phagosome; enzymes such as AhpC, SodC, KatG and TpX contribute to the detoxification of reactive oxygen intermediates (ROI) and reactive nitrogen intermediates (RNI) [48, 49]; and isocitrate lyase enzyme is essential for the metabolism of fatty acids [50].

Other genes have been identified as encoding potential virulence factors in Mtb. For instance, the inactivation of LipF resulted in attenuated mutant in mice [51, 52], possibly due to the metabolic shift suffered by Mtb during infection, from carbohydrates (*in vitro*) to fatty acids (*in vivo*). Deletion of at least three of the four phospholipases C genes results in an attenuated phenotype in the late phase of the infection in mice [53]. Mutants in two important two-component regulatory systems, RegX3/SenX3 and PhoP/PhoR, were attenuated in mice [54]. Nevertheless, the deletion of *kdpDE*, *tcrS*, *dosR* and *tcrXY* led to a hypervirulent phenotype when tested in severe combined immune-deficient (SCID) mice [55].

A great variety of secreted and cell wall-associated proteins has been demonstrated to play a key role in bacterial survival and immune modulation in the host. For example, ESAT-6 is secreted in the early stages of Mtb infection and induces strong cell mediated and humoral immune responses [56]. The Ag85 complex (Ag85A, Ag85B, and Ag85C, also known as FbpA, FbpB and FbpC, respectively) is the major secreted protein constituent of mycobacterial cell culture, and contributes to the biosynthesis of TMM and TDM [49]. The *fbpA* mutant showed to be attenuated in growth in human and murine macrophages, unlike *fbpB* and *fbpC* mutants, but also vaccinogenic against TB [57]. Several *pks* genes along with *fadD26*, *fadD28* and *drrC*, take part in biosynthesis or transport of PDIM, a major virulence factor of Mtb, in particular during the early step of infection when bacilli encounter their host macrophages. Mutant strains in these genes showed attenuated phenotypes in mice [49]. PIMs and mannose-capped lipoarabinomannan (Man-LAM) both interfere with phagosome maturation [58].

Other proteins integrated into the membrane participate in the transport of virulence factors and drugs across the mycobacterial cell wall. In the following section, this and other roles of efflux proteins will be detailed.

1.4. Functional diversity of efflux pumps in *Mycobacterium tuberculosis*

Efflux pumps are membrane proteins that transport actively a wide variety of compounds across bacterial envelope. They have been classified into five superfamilies: ATP-binding cassette (ABC), major facilitator super-family (MFS), resistance nodulation division (RND), small multidrug resistance (SMR) and multidrug and toxic-compound extrusion (MATE). While MFS, SMR, RND and MATE members are secondary transporters, typically energized by the proton motive force (H^+ or Na^+), members of the ABC superfamily use ATP as the energy source and are considered as primary transporters [59]. Whereas efflux pumps are mostly known because of the transport of drugs from the cytoplasm, other efflux pump substrates are sugars, lipids, proteins, synthetic compounds, toxic metabolites, host-defence molecules, virulence factors, etc. Such a heterogeneous substrate profile allows bacterial efflux pumps to play diverse roles in drug resistance, virulence, bacterial cell physiology, and detoxification [59], among others.

1.4.1. Drug resistance

In mycobacteria, intrinsic resistance to different drugs is conferred by mycobacterial efflux pumps as well as the low permeability of the mycobacterial envelope, enzymes like β-lactamases [60], and transcriptional activators like *whiB7* [61], among others. The following table summarizes our current knowledge on drug efflux pumps in Mtb that have been related to low-level resistance to drugs or whose expression increases in response to exposure to drugs. Most studies have been done by determining drug resistance levels after overexpressing genes encoding efflux pumps from multicopy plasmids or after deleting genes in the bacterial chromosome; others have been done by genomic and transcriptomic approaches in response to exposure to drugs.

Table 3. Efflux pumps related to drug resistance.

Drug efflux pump	Transporter family	Drugs related	References
Rv1258c (Tap)	MFS	Rif, Ofx, aminoglycosides, Tet	[62-65]
RV1410c (P55)	MFS	Inh, Emb, Rif, Cfz	[63, 66, 67]
Rv2333c (Stp)	MFS	Spc, Tet	[68]
Rv1634	MFS	FQs	[69]
Rv2459 (JefA)	MFS	Inh, Emb	[70]
Rv2846c (EfpA)	MFS	Inh, Eth	[63, 71]
Rv2936-Rv2937-Rv2938 (DrrABC)	ABC	Emb, FQs, Sm	[72]
Rv2686c-Rv2687c-Rv2688c	ABC	FQs	[73]
Rv1217c-Rv1218c	ABC	Inh, Rif	[74]
Rv3065 (Mmr)	SMR	Inh, EtBr, Tpp, CTAB	[63, 75]
Rv2942 (MmpL7)	RND	Inh	[63, 76]
Rv0676c-Rv0677c (MmpL5-MmpS5)	RND	Bdq, Cfz, azole	[77-79]

Ofx, ofloxacin; Tet, tetracycline; Clo, clofazimine; Spc, spectinomycin; FQs, fluoroquinolones; Eth, ethionamide; Sm, streptomycin; EtBr, ethidium bromide; Tpp, tetraphenylphosphonium; CTAB, cetyltrimethylammonium bromide; Bdq, bedaquiline.

It is worth noting that in other bacterial pathogens efflux pumps are frequent mechanisms of acquired drug resistance, conferring high levels of resistance to the drugs transported by the efflux pumps. In contrast, in mycobacteria most efflux pumps contribute to intrinsic drug resistance by providing the bacterial cells with basal levels of resistance to the drugs transported by the efflux pumps. Recently, MmpL5-MmpS5 and Tap have been related to acquired drug resistance due to genomic mutations increasing their expression and conferring Bdq and Sm resistance, respectively [65, 77].

1.4.2. Drug tolerance

Unlike intrinsic and acquired drug resistance, tolerance is a transitional situation, in which the bacteria change its physiological state to show phenotypic resistance or non-susceptibility to a drug, yet being genetically identical to drug-susceptible bacteria in the same population.

It is widely accepted that drug-tolerant bacilli have slowed growth and quiescent metabolism. In this non-replicating state, most of anti-TB drugs are unable to kill drug-tolerant mycobacteria, which make necessary to prolong treatment courses, and consequently increases the chances of emergence of genetic drug resistance. For example with Inh, greater than 99% of the initial sputum bacillary load is killed during the first two days of treatment, after which the rate of killing decreases markedly due to the residual drug-tolerant mycobacteria [80]. Recently, a new insight in the mechanism leading to drug tolerance in mycobacteria has been demonstrated [81]. In this model, drug tolerance appears in actively replicating mycobacteria due to bacterial efflux pumps whose expression is likely induced by antimicrobial peptides upon macrophage entry, and is retained for a period of time after bacteria resume extracellular growth.

1.4.3. Virulence

Not only efflux pumps have a role in drug resistance and drug tolerance, but also in virulence. LpqY, which is among these virulence-related proteins, is a component of a putative sugar ABC transporter of Mtb and *lpqY* forms an operon with *sugC*, *sugB* and *sugA*. It has been shown that this importer plays a role in recycling of extracellular trehalose, released from trehalose-containing molecules (such as DAT, PAT, etc) synthesized by the bacillus. Moreover, the attenuation of the *lpqY* mutant in mice suggests that sugars may be relevant for infection [82].

Mce proteins are ABC transporters implicated in virulence. The Mce proteins are encoded by the *mce1*, *mce2*, *mce3* and *mce4* operons in the genome of Mtb. The involvement of Mce4 transport system in cholesterol import and intracellular survival has been confirmed [83, 84], but the role of *mce1*, *mce2* and *mce3* operons is not clearly established, especially in the case of the *mce3* operon. As regards to *mce1* operon, it has been suggested that these proteins may serve as a mycolic acid re-importer [85], and *mce2* operon might be related to sulpholipid transport [86]. Due to their most probable implication in lipid metabolism, the Mce proteins may modulate pathogenicity through changes in Mtb lipid pathways.

The Mtb genome possesses 15 different genes encoding for RND proteins [87], 13 of which belong to MmpL (Mycobacterial Membrane Protein Large) protein family. Mutants with disruptions in *mmpL2*, *mmpL4*, *mmpL5*, *mmpL7*, *mmpL8*, *mmpL10*, and *mmpL11* showed significant attenuation for growth in mice lungs [51, 88-90]; only the MmpL4 mutant showed a survival defect in the spleen [88]. It should be noted that Mtb mutants harbouring deletions of *mmpL8* and *mmpL11* are attenuated for survival in the chronic stages of infection [90]. It is even more striking the fact that MmpL4 and MmpL7 knockout mutants appear to be avirulent [90].

Four *mmpL* genes appear to be in operons also containing an *mmpS* gene. The latter encode for proteins equivalent to the MFPs in other bacterial RND systems [91]. MmpL and MmpS (Mycobacterial Membrane Protein Small) protein families mediate transport of important cell wall lipids across the mycobacterial membrane, which are known to play a significant role in

pathogenesis. In Mtb, MmpL3 [92, 93], MmpL7 [94, 95] and MmpL8 [89, 96] have been shown to transport TMM, PDIM and SL-1 respectively. Moreover, the translocation of DAT and biosynthesis of PAT is likely due to MmpL10 [97]. In other mycobacteria, *M. smegmatis*, MmpL11 is responsible for the mycolic acid-containing lipids monomeromycolyl diacylglycerol (MMDAG) export [98]. Besides drug efflux and lipid transport, MmpL and MmpS proteins are involved in siderophore export [99] (MmpL4/MmpS4 and MmpL5/MmpS5), and heme uptake [100, 101] (MmpL3 and MmpL11); the acquisition of iron is an essential attribute of pathogenic bacteria so as to establish a successful infection.

Interestingly, some efflux pumps have a dual role in Mtb contributing to drug resistance and virulence. It has been proven that Rv1258c efflux pump induces tolerance to Rif, and promotes intracellular bacterial growth as well, contributing to Mtb virulence [81]. Moreover, LprG (an antigenic lipoprotein) and P55 (a MFS efflux pump) are encoded in an operon that is related to the transport of toxic compounds, including some drugs, and the cell wall permeability of the bacterium [66, 67, 102, 103].

1.5. The MmpL4-MmpS4 efflux system

In this work, we have studied the efflux system composed by Rv0450c (MmpL4) and Rv0451c (MmpS4) proteins of Mtb. Identical proteins can be found in *M. bovis* AF2122/97 strain (http://genolist.pasteur.fr/BoviList/), which are named BCG_0489c and BCG_0490c, respectively, in the genome of *M. bovis* BCG strain.

MmpL4, a protein of 967 amino acids with a molecular mass of 105.2 kDa, has been predicted to have 11 transmembrane domains (TMDs), a short cytoplasmic loop between TMD 1 and TMD 2, and a large extra-cytoplasmic loop between TMD 6 and TMD 7. All of these characteristics are similar to those described as typical of RND efflux pumps [104].
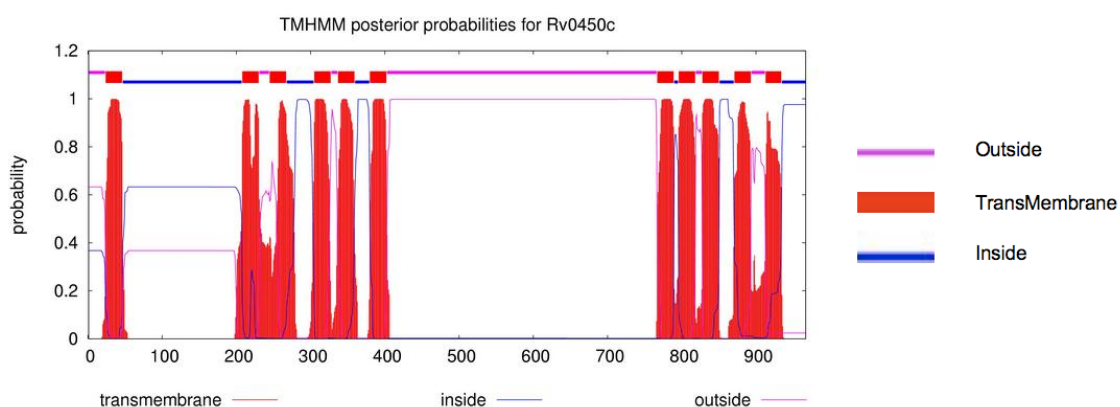
Figure 5. Prediction of TMS of Rv0450c efflux pump, using Hidden Markov Models (http://www.cbs.dtu.dk/services/TMHMM/).
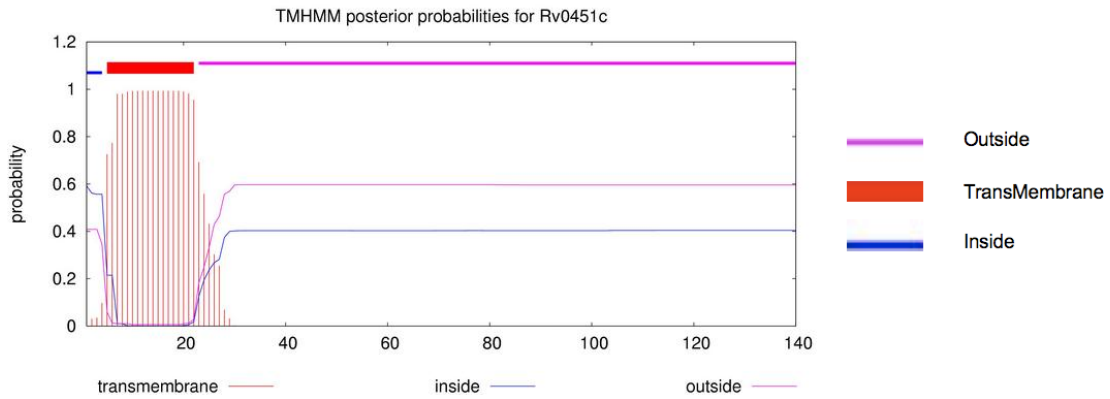
Figure 6. Prediction of TMS of Rv0451c efflux pump, using Hidden Markov Models (http://www.cbs.dtu.dk/services/TMHMM/).

However, MmpS4, a small protein of 423 amino acids with a molecular mass of 15.4 kDa, shows no structural similarity to any periplasmic adapter proteins from RND drug efflux systems of Gram-negative bacteria, indicating that the mycobacterial MmpS proteins constitute a novel class of accessory proteins in complex transporter systems [99]. MmpS4 has been predicted to have a TMD in the extreme N-terminal region, and an extra-cytoplasmic domain that has seven consecutive β-strands [99].

As it has been mentioned in the previous section, MmpL4/MmpS4 and MmpL5/MmpS5 are components of siderophore export systems that have been demonstrated to be essential for virulence of Mtb. These apparently redundant pairs of transporters are not only required for export but also for efficient siderophore synthesis [99]. The mutants' attenuation is due to two effects: the restricting access to iron, and the toxic intracellular siderophore accumulation [105].

Furthermore, it has been demonstrated that *mmpL4a*, *mmpL4b* and *mmpS4* are involved in glycopeptidolipid biosynthesis and transport in other mycobacteria. In *M. smegmatis*, single mutants deleted in *mmpL4a*, *mmpL4b* and *mmpS4* have altered colony morphology, reduced sliding motility and biofilm formation [106-108]. Apart from these phenotypic characteristics, *M. abscessus mmpL4b* knockout mutants have shown immunostimulatory and invasive bacterial phenotype [109].

2. Objectives

The main objective of this work is the characterization of the MmpL4/MmpS4 efflux system in *Mycobacterium tuberculosis*. To deal with this issue, the following objectives will be tackled:

- To construct the *M. tuberculosis* H37Rv knockout mutants deleted in *rv0450c,* in *rv0451c*, and in both *rv0450c* and *rv0451c,* besides their complemented strains.

- To overexpress both *rv0450c* and *rv0451c* in *M. tuberculosis* H37Rv wt.

- To discover whether this efflux system is involved in intrinsic drug resistance in *M. tuberculosis*.

- To characterise the *in vitro* phenotype of the *M. tuberculosis* strains covering cell and colony morphology and growth in synthetic media.

- To study the *in vivo* phenotype of the *M. tuberculosis* strains including growth and cytotoxicity in infected macrophages.

- To find out the influence of MmmpL4 and MmpS4 efflux pumps in the expression of the MmpL and MmpS protein families.

- To figure out the involvement of MmpL4/MmpS4 efflux system in lipid transport by lipidomics.

- To analyse the proteome of the *M. tuberculosis* strains.

- To carry out complementary analyses in *M. bovis* so as to improve the knowledge of the MmpL4/MmpS4 efflux system.

3. Material and Methods

3.1. Basic procedures

3.1.1. Bacterial strains, growth media and general culture conditions

E. coli HB101, XL1-Blue, DH10β, and TOP10 strains were used for cloning experiments. Strains were grown at 37ºC in Luria-Bertani (LB) broth or LB agar supplemented with ampicillin (Amp; 100µg/ml), kanamycin (Km; 20µg/ml), chloramphenicol (Cm; 15µg/ml), hygromycin (Hyg; 50µg/ml), when necessary. Isopropyl-β-thiogalactopyranoside (IPTG) (0.1mM) and X-Gal (40µg/ml) were added when it was required to check Lac phenotype. Liquid cultures were grown in glass tubes in a shaker.

M. smegmatis mc^{2}155 strains were grown at 37ºC in tryptic soy broth (Difco) containing 0.05% Tween-80. For propagation of mycobacteriophages, Middlebrook 7H9 (Difco) medium supplemented with 1.5% Bacto Agar (Difco) was used as a bottom agar and with 0.75% as a top agar. Liquid cultures were grown in inkwells in a shaker.

M. bovis BCG strains were grown at 37ºC in Middlebrook 7H9 medium supplemented with 10% OADC (0.05% oleic acid, 0.5% bovine serum albumin, 0.2% dextrose, 0.085% NaCl, 0.0003% beef catalase) (Difco) and 0.05% Tween-80 (7H9T OADC), or on solid Middlebrook 7H10 medium supplemented with 10% OADC (7H10 OADC). Km (20µg/ml), or Hyg (50µg/ml) were added if appropriate. Liquid cultures were done in cell culture flasks without shaking.

M. tuberculosis strains were grown at 37ºC in Middlebrook 7H9 supplemented with ADC (0.2% dextrose, 0.5% BSA fraction V, 0.0003% beef catalase) (Difco). In order to keep the culture clump-free, Tween-80 was added to a final concentration of 0.05% (7H9T ADC), except for the media used in drug susceptibility assays, which were supplemented with glycerol 0.5% (7H9G ADC). Solid medium was Middlebrook 7H10 supplemented with ADC (7H10 ADC), and also with 0.05% Tween-80 for colony morphology assays. When required, Km or Hyg were used at concentration of 20µg/ml. For obtaining knockout mutants by recombineering method, Middlebrook 7H9 supplemented with 0.2% succinate were used to grow the recombineering strain Mtb H37Rv pJV53 and 24h before preparing their competent cells, acetamide final concentration 0.2% was added. Middlebrook 7H9 supplemented with 0.2% dextrose and 0.085% NaCl were used for protein extraction. Liquid cultures were done in cell culture flasks without shaking.

Storage of strains was done at -80ºC in 7H9T ADC supplemented with 15% glycerol.

M. tuberculosis manipulation was carried out in a biosafety level 3 (BSL3) laboratory.

3.1.2. Neutral-red staining

This method was adapted from Soto *et al.* [110]. Mycobacterial strains were grown on 7H10 ADC medium for 3 to 4 weeks. Cells were placed and gently disaggregated in 15ml Falcon tubes containing 4ml of 50% aqueous methanol, and incubated for 1h at 37ºC. Cells were pelleted by centrifugation (4,000rpm, 5min), and methanol removed. Then, 4ml barbital buffer (1% sodium barbital in 5% NaCl, pH=9.8) were added. Subsequently, 150µl of a solution of 0.05% aqueous neutral red were added. Results were evaluated after 1h incubation at 37ºC.

3.1.3. Auramine/rodamine staining and microscopic examination

Mtb cultures were grown to the late-logarithmic phase in 7H9T ADC medium devoid of Tween-80. 50µl of each culture were placed on a microscope slide and warmed at 65ºC for 10min to fix the cells. After fixation, 200µl of auramine solution (1% auramine O, 0.5% rodamine B in 50% glycerol-7% phenol) was added over the cells and incubated for 30min at room temperature (RT) in the dark. Slides were rinsed with an acid-alcohol solution (0.5% HCl in 70% ethanol) in order to eliminate the excess of auramine not retained by the cells, then rinsed with water and finally covered with a solution of 0.5% $KMnO_4$. After 5min at RT slides were again rinsed with water. Stained cells were examined under a Nikon Eclipse E400 fluorescent microscope with an attached MOTICAM 2500 digital camera. The resulting images are representative of the whole slide at a magnification of 1000x.

3.1.4. *In vitro* growth

In order to characterize the growth rate of Mtb H37Rv wt (wild type) and Mtb H37Rv mutants, growth curves were performed in 7H9T ADC. Mtb strains were grown until log-phase and then inoculated at 10^5 CFU (colony forming units)/ml. OD_{600nm} was measured at different time points for 1 month. When OD_{600nm} reached 1, the culture was diluted ½ and ¼ and OD corrected depending on the dilution.

So as to compare the growth rate of Mtb H37Rv wt and Mtb H37Rv mutants in low iron conditions, growth curves were performed in 7H9T ADC 0.1mM 2,2'-dipyridyl (DIP) and 7H9T ADC 0.2mM desferrioxamine (DFO). Mtb strains were grown until log-phase and then inoculated at 10^5 CFU/ml. OD_{600nm} was measured for 2 weeks.

3.2. Nucleic acid and genetic engineering techniques

3.2.1. DNA extraction

3.2.1.1. Extraction of genomic DNA from mycobacteria

Genomic DNA of mycobacterial strains was isolated using CTAB method [111]. Briefly, mycobacteria were resuspended in 400µl TE (100mM Tris/HCl, 10mM EDTA, pH=8.0) and heated for 10min at 85ºC. Samples were slightly cooled at RT before adding 50µl of 10mg/ml lysozyme and were then incubated for at least 1h at 37ºC. Subsequently, 75µl of a solution containing 72.5µl of 10% SDS and 2.5µl of 20mg/ml proteinase K were added and the suspension warmed for 10min at 65ºC. Hereafter, 100µl 5M NaCl and 100µl CTAB/NaCl (10% CTAB in 0.7M NaCl) pre-warmed at 65ºC were added and samples incubated for further 10min at 65ºC. Genomic DNA was extracted by adding 750µl of chloroform:isoamylalcohol 24:1. Samples were mixed by vortexing for 10s before centrifugation (13,000rpm for 5min). The upper (aqueous) phase was transferred to a fresh tube containing 450µl isopropanol and samples incubated overnight at -20ºC. Precipitated nucleic acids were collected by centrifugation (13,000rpm for 10min at 4ºC). The pellets were dissolved in 50µl double-distilled water and treated with RNAse. DNA was quantified by Abs_{260nm} readings using a ND-1000 spectrophotometer (NanoDrop Technologies).

3.2.1.2. Plasmid DNA extraction from *E. coli*

3.2.1.2.1. Mini-preparation (Mini-prep)

1.5ml of a liquid culture grown overnight were centrifuged (10,000rpm for 3min) and the pellet resuspended in 100µl of Solution I (50mM glucose, 10mM EDTA, 25mM Tris HCl pH=8). 200µl of freshly made Solution II (0.2M NaOH, 1% SDS) were added, and the content mixed by inverting the tube several times, until it becomes transparent and viscous. After incubation on ice for 5min, 150µl of cold Solution III (5M KAc, 11.5% glacial HAc) were added and the tubes were mixed by inversion; as a result, a white pellet is formed. This mix was incubated on ice for 5min, followed by centrifugation (12,000rpm for 10min). Supernatants (400µl approx.) were then transferred to a fresh tube and mixed with the same volume of chloroform: isoamyl alcohol 24:1. After centrifugation, the aqueous phase was transferred to a tube containing 900µl EtOH and 50µl 3M NaAc and incubated at -20ºC for 30min. By centrifugation (12,000rpm for 5min) small nucleic acids (plasmids and RNA) were pelleted, and then washed with 100µl 70%EtOH. Finally, the pellet was dried in a vacuum drier and resuspended in 30µl double distilled water.

RNA, which co-purifies with plasmidic DNA, was removed by adding 1μl RNAse 1mg/ml and incubating for 15min at 37ºC. Plasmidic DNA was kept at -20ºC.

3.2.1.2.2. Maxi-preparation (Maxi-prep)

This method was used to obtain large quantities of plasmid. The process is the same as the mini-preparation, but starting with 100ml of liquid culture. Larger volumes of solutions are needed: 5ml Solution I, 10ml Solution II and 7.5ml Solution III. Besides, precipitation of plasmid DNA is done by adding 0.7 volumes of isopropanol instead of ethanol. Finally, nucleic acids are dissolved in 350μl of double distilled water and treated with 10μl RNase 1mg/ml for 15min at 37ºC.

3.2.1.3. BAC DNA extraction from *E. coli*

We have available a BAC library derived from vector pBeloBAC11 [112] containing the chloramphenicol resistance marker, which contains the genome of *M. tuberculosis* H37Rv. BAC DNA extraction was done as previously described by Birnboim *et al.* [113] with minor modifications. Briefly, 100ml of BAC-transformed *E. coli* was prepared in LB medium containing 15μg/ml Cm, and the cultures were grown overnight at 37ºC with vigorous and continuous agitation. Then, the bacterial cells were collected by centrifugation. The bacterial pellet was softly resuspended in 5ml of Solution I, 5ml of Solution II (see section 3.2.1.2.1 for composition of solutions I and II) was added to the tube, and 4ml of ice-cold NaAc pH=4.8 was added to the mixture. The tube was placed on ice and the precipitated debris was removed by centrifugation. Then, 14ml of chloroform: isoamyl alcohol 24:1 were added to the supernatant, and after centrifugation the aqueous phase was transferred to a new microfuge tube. DNA of the BACs was precipitated adding the same volume of isopropanol and finally obtained by centrifugation.

3.2.2. Mycobacterial RNA isolation

Mtb cultures were grown in 7H9T ADC at 37ºC to mid-logarithmic phase (OD_{600nm}=0.4-0.5) or to stationary phase (4 weeks). Cells from 10ml of culture were harvested (4,000rpm for 5min at 37ºC). To minimize RNA degradation, cells were resuspended in 1ml of RNA protect reactive (Qiagen). Cellular suspensions were incubated for 5min at RT and were centrifuged (14,000rpm for 5min at RT). Pellets were resuspended in 400μl of lysis buffer (0.5% SDS, 20mM NaAc, 0.1mM EDTA) and 1ml of acid-phenol:clorophorm (5:1, pH=4.5) was added. Bacterial suspensions were transferred to tubes containing glass beads (Qbiogene) and were lysed by mechanical traction (Fast-prep instrument) in two cycles (45s at speed 6.5m/s) cooling the samples on ice for 5min between the pulses. Samples were centrifuged (14,000rpm for 5min at 4ºC). The upper phase (aqueous) was recovered and transferred to a fresh tube that contained pre-chilled chloroform:isoamyl alcohol 24:1. Tubes were inverted carefully before centrifugation

(14,000 rpm for 5min at 4ºC). The upper (aqueous) phase was then transferred to a fresh tube containing 90µl of 0.3 M NaAc (pH=5.5) and 900µl of isopropanol and samples were incubated overnight at -20ºC. Precipitated nucleic acids were collected by centrifugation (14,000rpm for 1 hour at 4ºC). The pellets were rinsed with 70% ethanol and air dried before being re-dissolved in RNase-free water. DNA was removed from RNA samples using Turbo DNA free (Ambion) by incubation at RT for 1 hour 30 min. Then RNA was purified with acid-phenol:chloroform (5:1, pH=4.5) and the same steps to precipitate, collect and dry were repeated to dissolve RNA in RNase-free water. The concentration and purity of the extracted RNA was estimated from the Abs_{260}/Abs_{280} readings using a ND-1000 spectrophotometer. RNA integrity was assessed by agarose gel electrophoresis. RNA samples were stored at -80ºC.

3.2.3. Construction of plasmids

DNA fragments for cloning purposes were amplified by PCR using the Pwo high fidelity DNA polymerase (Roche) or the PrimeSTAR HS DNA polymerase (Takara Bio) for larger fragments, and gel-purified by using QIAquick Gel Extraction Kit (Qiagen). Plasmids were cut by restriction endonucleases and gel-purified by using QIAquick Gel Extraction Kit (Qiagen). Ligations were done using T4 DNA ligase (Invitrogen). Allelic exchange substrates (AES) were obtained by digestion of plasmid containing AES or amplified by PCR using the PrimeSTAR HS DNA polymerase.

3.2.3.1. Construction of the replicative plasmid pRBZ13

A 4,390bp DNA fragment containing the operon *rv0451c-rv0450c* from Mtb H37Rv was amplified by PCR with oligonucleotides mmpL4S4-rFw4 and mmpL4S4-rRv (Table 4).

Table 4. Oligonucleotides to amplify the region containing the operon *rv0451c-rv0450c* from Mtb H37Rv.

Oligonucleotide	Sequence 5' → 3'	Characteristics
mmpL4S4-rFw4	TTTTAAGCTTCACTTCTTT GTGCGAGGTGA	HindIII site underlined.
mmpL4S4-rRv	TTTTAAGCTTACATCGAC ATTTCCGACTCC	HindIII site underlined.

The previous PCR fragment was digested with the restriction enzyme HindIII and inserted into pSUM36 replicative vector digested with HindIII. The amplified DNA fragment includes the promoter of the operon; consequently, the overexpression of *mmpL4* and *mmpS4* is due to the presence of multiples copies of this plasmid. To confirm the absence of PCR-induced mutations

in the final plasmid pRBZ13 (Figure 7), it was sequenced using the oligonucleotides included in Table 5.
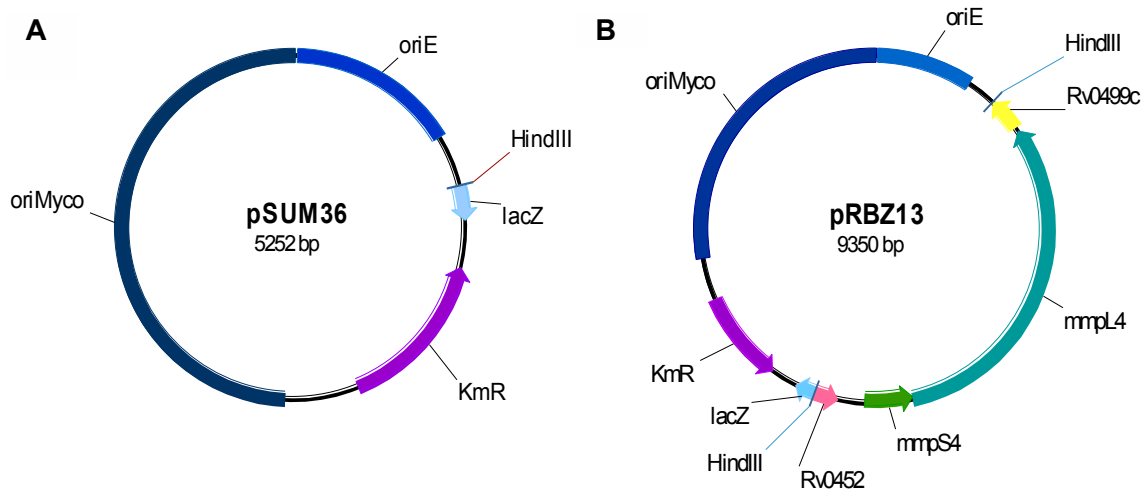
Figure 7. Replicative plasmid pSUM36 and its derivative pRBZ13. (A) pSUM36 has replication origins in *E. coli* and mycobacteria, Km[R] and *lacZ* marker genes. (B) pRBZ13 comprises *M. tuberculosis* H37Rv *mmpL4* and *mmpS4* genes.

Table 5. Oligonucleotides used for sequencing the replicative plasmid pRBZ13.

Oligonucleotide	Sequence 5' → 3'
mmpL4-1r	TTTTTACTAGTGACACCGATCGCTCTTGG
mmpL4-2fa	GCAGCGGCCACCAGAAC
mmpL4-a	TCCGAAGACAGGAACGACTT
mmpL4-b	CCTGCTTCAGCATGTCGTT
mmpL4-c	GACTTTGAGGAGCCGCTTAG
mmpL4-d	GTGATTGCTGCACATCCTGT
mmpS4KO-Rv	CCACCGTGATCAGCAGGAG
pSUR1-Rv	GACTCTGGGGGTTCGAAATGA
RP-180	ATGCAGCTGGCACGACAGGT

3.2.3.2. Construction of the integrative plasmid pRBV2

In order to generate pRBV2 (Figure 8), a 4,104bp DNA fragment containing the operon *rv0451c-rv0450c* from Mtb H37Rv was amplified by PCR with oligonucleotides mmpL4S4-iFw and mmpL4S4-iRv (Table 6).

Table 6. Oligonucleotides to amplify the region containing the operon *rv0451c-rv0450c* from Mtb H37Rv.

Oligonucleotide	Sequence 5' → 3'	Characteristics
mmpL4S4-iFw	TTTTGCTAGCCACTTC TTTGTGCGAGGTGA	NheI site underlined.
mmpL4S4-iRv	TTTTGCTAGCACATCG ACATTTCCGACTCC	NheI site underlined.

The previous PCR fragment was digested with restriction enzyme NheI and inserted into pMV361 integrative vector digested with NheI. The resulting plasmid was sequenced with oligonucleotides included in Table 7 to verify the sequence.
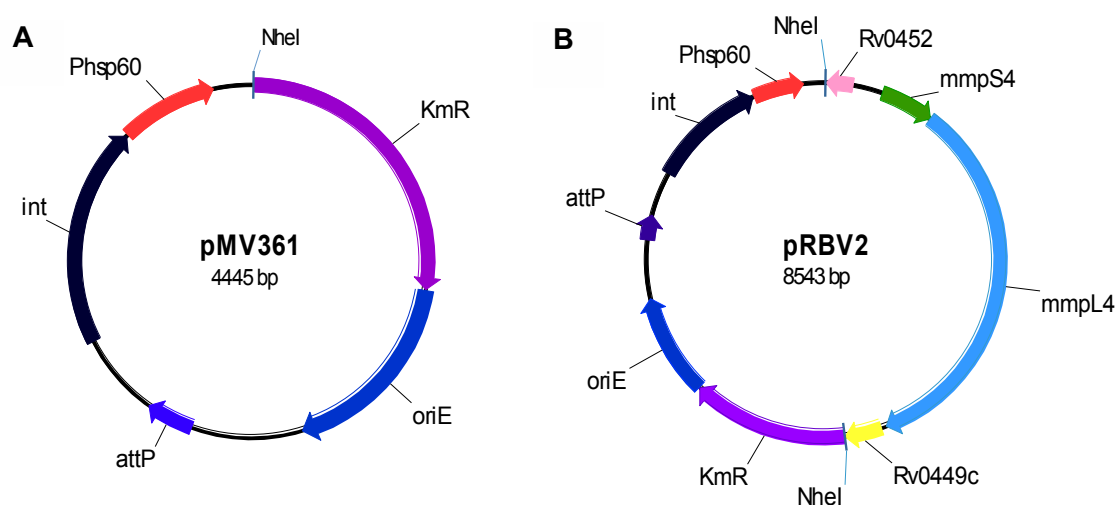
Figure 8. Integrative plasmid pMV361 and its derivative pRBV2. (A) pMV361 contains a origin of replication in *E. coli*, a Km[R] marker, the strong promoter *hsp60* and attP site and *int* gene that mediate integration process. (B) pRBZ2 includes *M. tuberculosis* H37Rv *mmpL4* and *mmpS4* genes.

Table 7. Oligonucleotides used for sequencing the integrative plasmid pRBV2.

Oligonucleotide	Sequence 5' → 3'
mmpL4-1f	TTTTGGATCCGCGGCTTCTTC
mmpL4-2fa	GCAGCGGCCACCAGAAC
mmpL4-a	TCCGAAGACAGGAACGACTT
mmpL4-b	CCTGCTTCAGCATGTCGTT
mmpL4-c	GACTTTGAGGAGCCGCTTAG
mmpS4-1f	TTTTAGATCTTGCGCAGACCTGCGACAGCCGTTAAC
mmpS4KO-Rv	CCACCGTGATCAGCAGGAG

pMV361-B	GGAAACGTCTTGCTCGAGG
pMV361-C	GATCCGGAGGAATCACTTC

3.2.4. Electrotransformation of *E. coli* and mycobacteria

To prepare *E. coli* electrocompetent cells, bacteria were grown to an OD_{600nm} of 0.4 to 0.6. Then, the growth was stopped for 30min on ice, and bacteria were washed twice in chilled-cold water, and once in chilled-cold 10% glycerol. Cells are finally resuspended in 1ml chilled-cold 10% glycerol. Aliquots of 40μl were directly used or stored at -80ºC for further use. Aliquots of 40μl were electroporated with 20-30ng of purified plasmid DNA in 0.2cm gap cuvettes (Bio-Rad) with a single pulse (2.5kV, 25μF, 200Ω) in a GenePulser XcellTM (Bio-Rad). Cells were resuspended in LB to a final volume of 1ml and incubated for 1h at 37ºC if required before plating several dilutions on plates containing the needed antibiotic. Colonies appeared after incubation overnight.

M. smegmatis electrocompetent cells were grown to an OD_{600nm} of 0.8 to 1.0, and then were incubated on ice for 30min to 2h. After centrifugation, cells were washed thrice in 10% glycerol at 4ºC; first wash was done in a half of the initial culture volume, second in a quarter and third in an eighth. Subsequently, bacteria were resuspended in 1ml of 10% glycerol, and aliquots of 100μl were electroporated with 400ng of phasmid DNA using 0.2cm gap cuvettes with a single pulse (2.5kV, 25μF, 1000Ω) in a GenePulser XcellTM. Cells were recovered with 1ml of LB and incubated at 30ºC for 6h. Then, 100μl and 300μl of the transformed mc^{2}155 were diluted to 200μl actively growing mc^{2}155 culture. The dilutions were added to 4ml top agar and pour onto 7H9 agar bottom plates. The plates were incubated at 30ºC for 3 days until plaques were observed. Importantly, *M. smegmatis* cells should be kept cold by using ice-cold glycerol, centrifuging at 4°C, and placing tubes on ice whenever possible.

M. bovis and *M. tuberculosis* electrocompetent cells were prepared as described by Wards *et al.* [114]. Bacteria were grown until an OD_{600nm} of 0.6 to 0.8. Glycine was added to the cells to a final concentration of 0.2M and incubated at 37ºC for 24 hours more. All the process was performed at RT. Bacterial pellet was washed twice with 0.05% Tween-80 and once with 10% glycerol 0.05% Tween-80, and finally resuspended in 2ml of 10% glycerol 0.05% Tween-80. Aliquots of 200-400μl were electroporated with 100-200ng of replicative or integrative plasmid DNA (previously purified), using 0.2cm gap cuvettes with a single pulse (2.5kV, 25μF, 1000Ω) in a GenePulser XcellTM. Cells were recovered with 1ml of 7H9T ADC and incubated for 24h at 37ºC, to allow expression of the antibiotic resistance genes, before plating serial decimal dilutions on plates containing the relevant antibiotic. Colonies typically appeared in 3-4 weeks.

For recombineering method, Mtb H37Rv containing the plasmid pJV53 was grown in 50ml 7H9T 0.2% succinate until an OD_{600nm} of 0.5. Then, acetamide was added to a final concentration of

0.2%, and the culture was grown at 37°C overnight. After three washes with 10% sterile glycerol, cells were resuspended in 2ml of 10% glycerol. Aliquots of 100µl were directly electroporated with 100ng AES in 0.2cm cuvettes with a single pulse in a GenePulser XcellTM (2.5 kV, 25 µF, 1000 Ω). Cells were recovered with 1ml of 7H9T ADC, and incubated for 72h at 37°C before plating the entire reaction on 7H10 ADC Km Hyg plates. Colonies typically appeared in 3-4 weeks.

3.2.5. Specialised transduction in *E. coli* and mycobacteria

To prepare *E. coli* cells for transduction process, 5ml of LB medium supplemented with 10mM MgSO$_4$ and 0.2% maltose were inoculated with 100µl of fresh *E. coli* culture, incubated at 37°C and shaken at 200rpm, until OD$_{600nm}$ reached 0.8-1.0. The culture was centrifuged at 3,000rpm at 4°C for 10min and resuspended in 500µl. The *E. coli* cells can be stored at 4°C for 1 week until ready to use.

Regarding *M. bovis* BCG, 500ml of 7H9T OADC were inoculated with 10ml of BCG culture, incubated at 37°C till the OD$_{600nm}$ reached 0.8-1.0. The culture was centrifuged at 4,000rpm for 15min. The pellet was washed twice with MP buffer (50mM Tris–HCl, pH=7.6, 150mM NaCl, 10mM MgCl$_2$ and 2mM CaCl$_2$), resuspended in 5ml of MP buffer, and 5 aliquots of 1ml were obtained.

Washes with MP buffer are necessary to remove traces of the Tween-80 detergent, which can inhibit phage infection.

3.2.6. Construction of knockout mutant strains of mycobacteria

3.2.6.1. Recombineering

Knockout mutants of Mtb H37Rv were constructed following the method described by van Kessel and Hatfull [115].

Firstly, it was necessary to construct AES for each gene of interest: *rv0450c* (*mmpL4* AES) and both *rv0450c* and *rv0451c* (*mmpL4-mmpS4* AES).

The general procedure for obtaining AES for homologous recombination by using the recombineering method is depicted in the following figure:
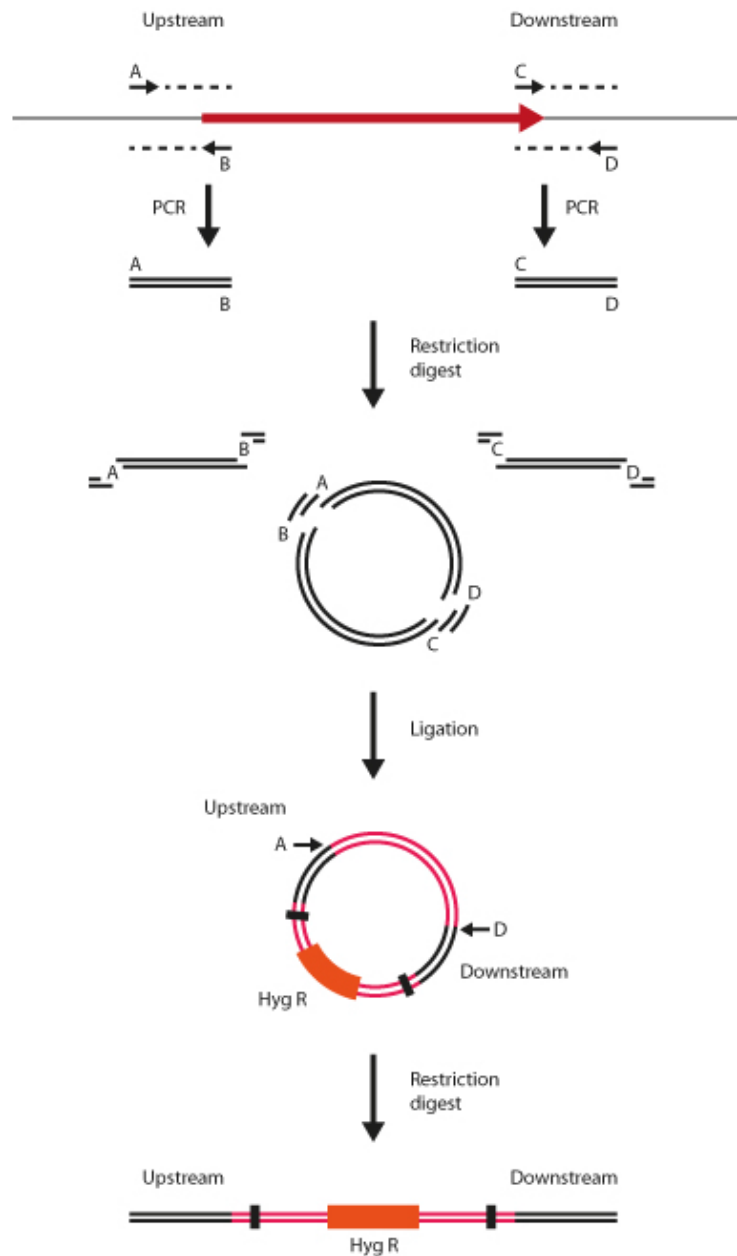
Figure 9. Construction and preparation of targeting substrate for recombineering. Primers are designed with restriction sites (A–D) to amplify upstream and downstream regions flanking the target gene. The amplification products are digested, and directionally cloned into a vector flanking a Hyg^R cassette. The plasmid is then linearized by double-digestion with enzymes A and D at the ends of the targeting substrate. Black boxes indicate γδ res sites that can be used to remove the hygromycin cassette after mutagenesis [115].

Specifically, for obtaining the *mmpL4* AES, primers were designed with restriction sites to amplify upstream and downstream regions flanking *mmpL4 gene*; mmpL4-1f (BamHI) and mmpL4-1r (SpeI) primers amplified a 540bp region upstream *mmpL4*, and mmpL4-2f (KpnI) and mmpL4-2r (KpnI) a 549bp region downstream *mmpL4*, using H37Rv genomic DNA as the template (Table 8). The PCR products were cloned into pWM27 vector flanking a Hyg-

resistance cassette in the same orientation as they are in the H37Rv genomic DNA and sequenced (Table 8). The resulting plasmid pRBZ2 (Figure 10) was linearized by restriction digest with BamHI and FspI.

Table 8. Oligonucleotides to amplify upstream and downstream regions flanking *mmpL4* and to sequence these regions in pRBZ2.

Oligonucleotide	Sequence 5' → 3'	Use
mmpL4-1f	TTTTGGATCCGCGGCTTCTTC	To amplify and sequence. BamHI site underlined.
mmpL4-1r	TTTTTACTAGTGACACCGATC GCTCTTGG	To amplify and sequence. SpeI site underlined.
mmpL4-2f	TTTTGGTACCGTTCTGGTGGC CGCTGC	To amplify and sequence. KpnI site underlined.
mmpL4-2r	TGCACAGGTACCGTGGC	To amplify. KpnI site underlined.
pWM27-Rv	CACGACGTTGTAAAACGACG	To sequence.

The fragment that contains the Hyg-cassette flanked by the two regions adjacent to *mmpL4* gene was separated by gel extraction, microdialized and quantified by Abs_{260nm} readings using a ND-1000 spectrophotometer.
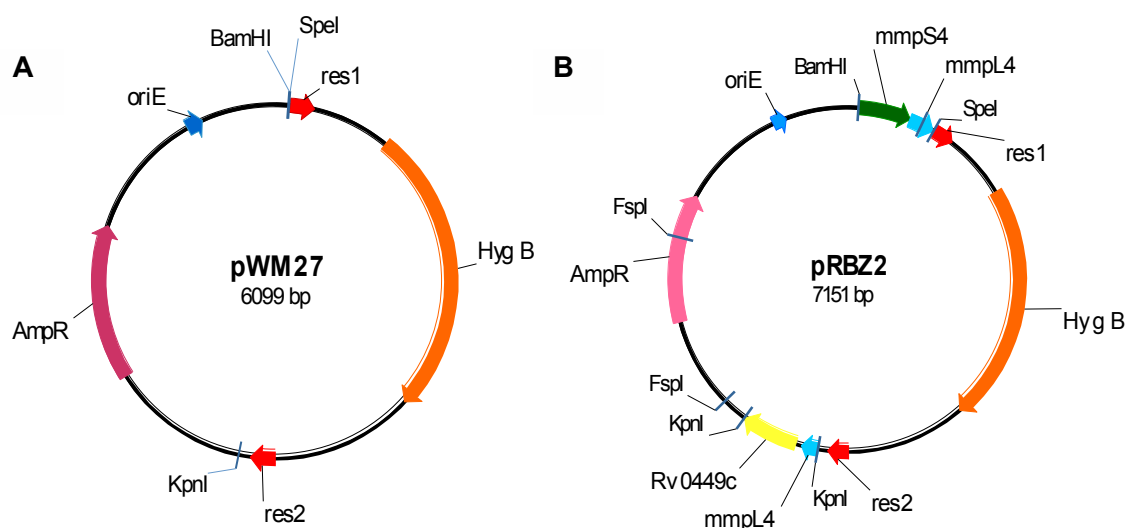
Figure 10. Vector pWM27 and its derivate pRBZ2. (A) pWM27 has a origin of replication in *E. coli*, recombination sites res1 and res2, and Amp[R] and Hyg[R] marker genes. (B) pRBZ2 carries the *mmpL4* AES.

For deleting both *mmpL4* and *mmpS4* genes, a different approach was followed: the *mmpL4-mmpS4* AES was constructed using the λ-Red system [116] to manipulate a BAC, which contains the region with the targeted gene, through homologous recombination.

E. coli DH10β containing the BAC313 [112, 117], which has a large fragment of DNA where *mmpL4-mmpS4* are included, was transformed with pKD46. The recombinogenic plasmid, pKD46, contains the λ-Red recombinase under control of the inducible arabinose operon (Figure 11).
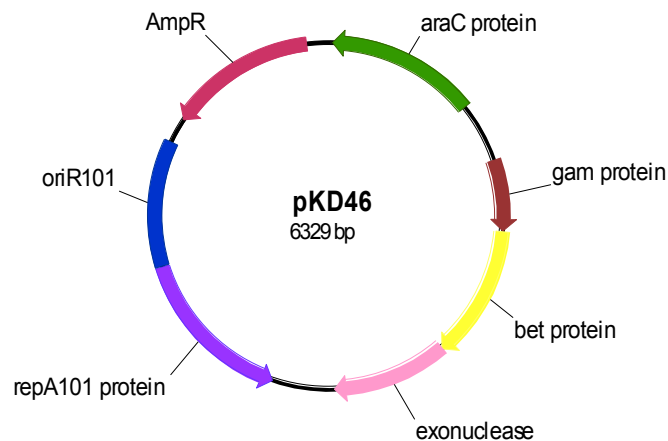
Figure 11. pKD46 plasmid and its components. pKD46 includes λ-Red genes (λ exonuclease, β protein and δ protein), its repressor AraC, RepA temperature sensitive origin in *E. coli* and Amp[R] cassette.

L4S4-bacFw primer was designed to include 20bp of the end region of Hyg[R] cassette of pYUB854 in its 3' end, and 50bp of the region upstream of *mmpS4* in its 5' end. Similarly, L4S4-bacRv primer includes 20bp of the other end region of Hyg[R] cassette in its 3' end and 50bp of the region downstream *mmpL4* in its 5' end. Using the plasmid pYUB854 as a template, these primers amplified a 2,182bp fragment containing the Hyg cassette flanked by 50bp regions identical to sequences adjacent to *mmpL4* and *mmpS4* genes. A culture of DH10β BAC313 pKD46 strain was induced with arabinose for 3h to trigger expression of λ-Red recombinase, and competent cells were prepared. This strain was transformed with the PCR product described above, which integrated in BAC313 replacing the original *mmpL4* and *mmpS4* genes. From the Hyg[R] colonies, the recombinant BAC313::Hyg was extracted and the *mmpL4-mmpS4* AES, which contains regions of 1,000bp upstream and downstream of the target genes flanking a Hyg[R] cassette was amplified with L4S4aes-Fw and L4S4aes-Rv oligonucleotides (Figure 12) (Table 9).
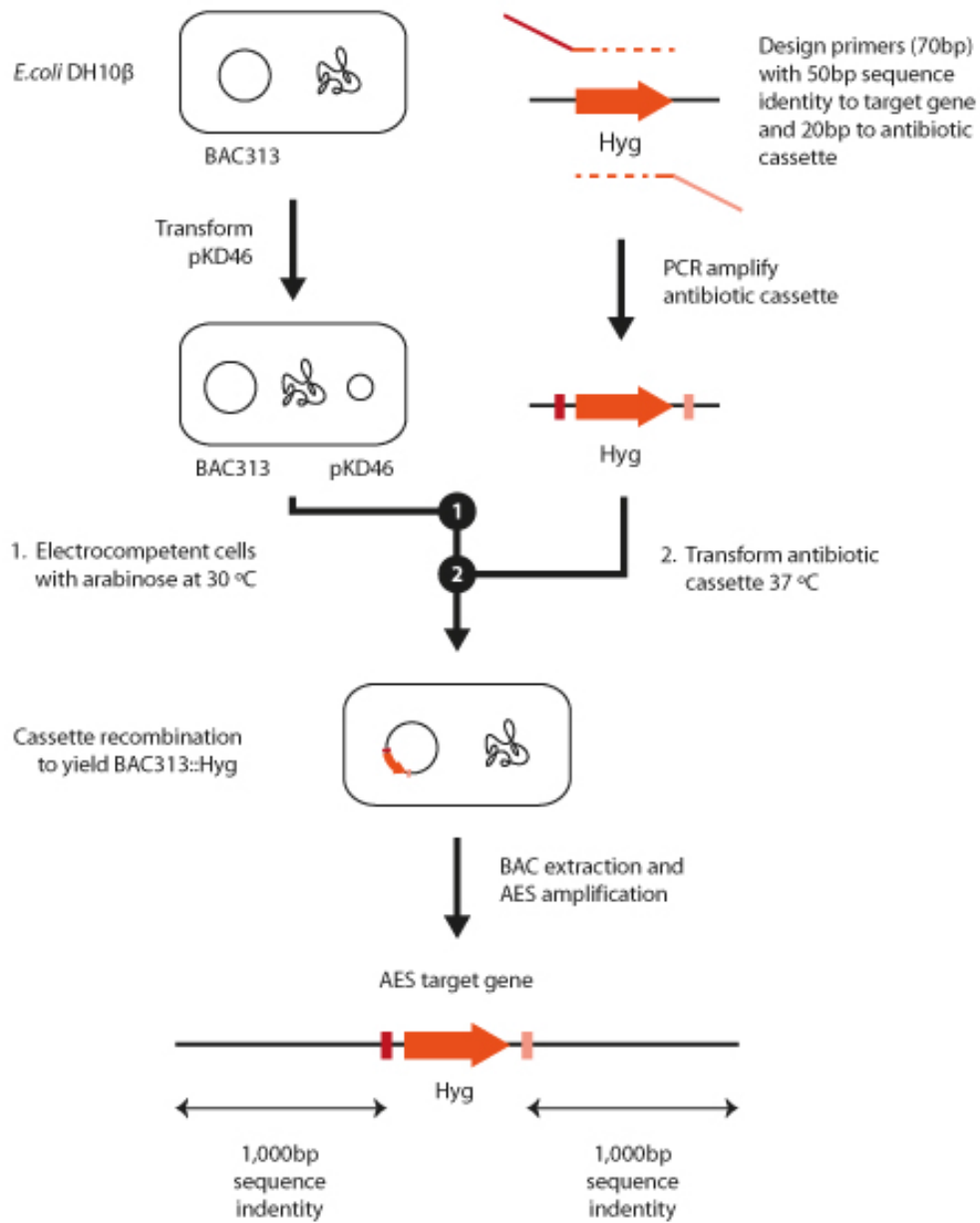
Figure 12. Construction and preparation of AES of the target genes *mmpL4* and *mmpS4* using λ-Red system.

Table 9. Oligonucleotides used for the construction of the *mmpL4-mmpS4* AES.

Oligonucleotide	Sequence 5' → 3'
L4S4-bacFw	CGTGCACCGGATCCGCGGCTTCTTCGGCTCCGAAAA CCGCCCGTCGTACTGATATCTGGATCCACGAAGC
L4S4-bacRv	TTTCGCTGGGTACGGTCGGGGTCCGGGCGGGCCGG GAACGCACCCGCAGCTGGTCTGACAGTTACCAATGC
L4S4aes-Fw	TTTTGCGGCCGCGCAAAGTCGAGGTTCCACTC
L4S4aes-Rv	TTTTTTAATTAACGGGTGTCACCAGGTAGTTC

Once both AESs were achieved, mycobacterial recombineering strains were generated using the plasmid pJV53 (Figure 13).
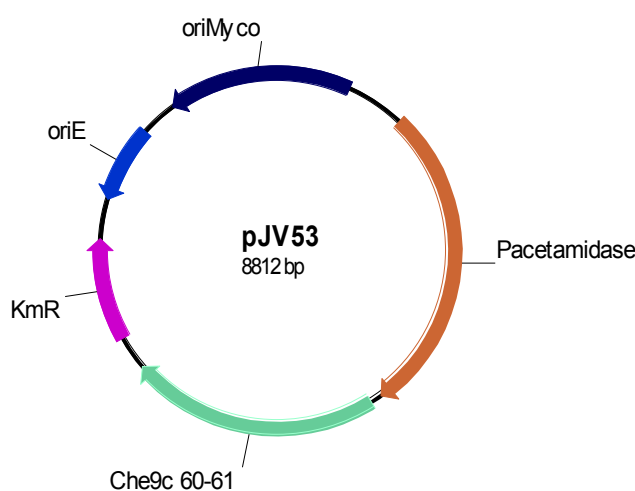
Figure 13. pJV53 and its components. pJV53 plasmid which contains replication origins for *E. coli* and mycobacteria, a Km[R] marker and the c*he9c 60–61* genes expressed under control of the inducible acetamidase promoter.

Mtb H37Rv pJV53 strain was grown to mid-log phase in 7H9T 0.2% succinate. It is necessary to growth the cells in media containing succinate instead of ADC because succinate enhances proper production of the recombination enzymes. Once Mtb H37Rv pJV53 strain was cultured with acetamide to induce expression of Che9c gp60 and gp61 recombinases, competent cells were prepared. This strain was transformed independently with either *mmpL4* AES or *mmpL4-mmpS4* AES that contain regions of 500bp and 1,000bp sequence identity respectively to the locus flanking a Hyg[R] cassette (Figure 14).
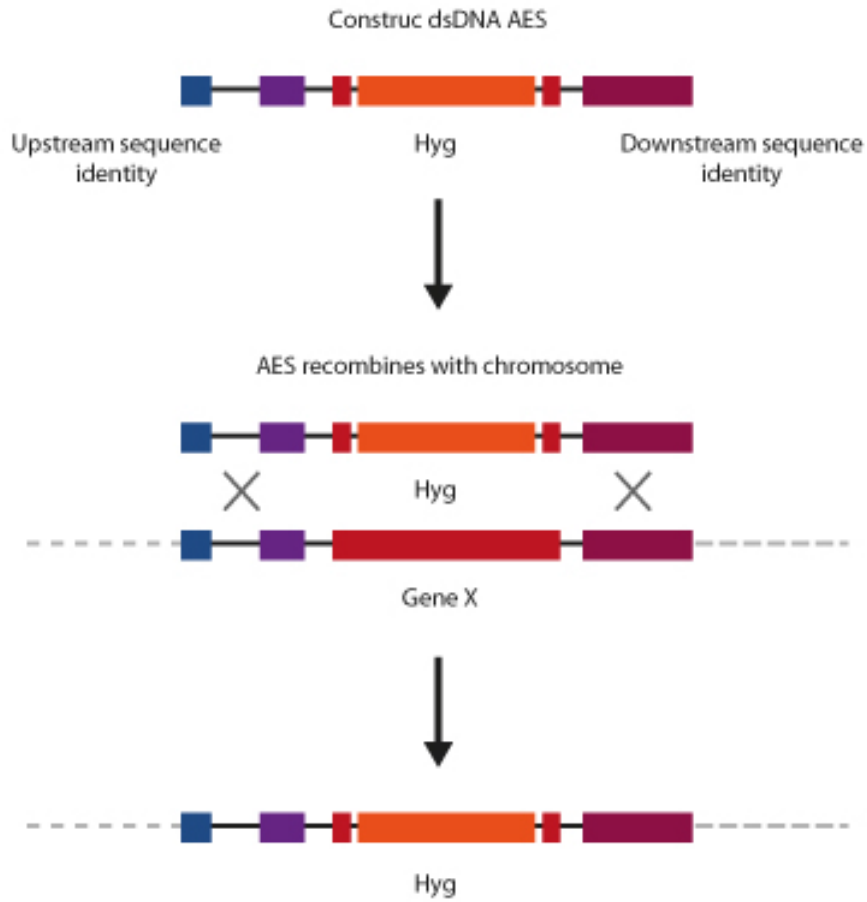
Figure 14. Schematic representation of double crossovers occurred when AES is transformed into the mycobacteria to yield a marked allelic replacement mutant [28].

Hygromycin-resistant recombinant colonies were obtained, and the replacement of the target gene by the AES was verified by Southern Blot and PCR analysis with the oligonucleotides in Table 10.

Table 10. Oligonucleotides used for confirming *M. tuberculosis* knockout mutants deleted in *mmpL4* and in *mmpL4-mmpS4*.

Oligonucleotide	Sequence 5' → 3'
mmpL4KO-Fw	CACTCCAGCGAACGAGG
Hyg-out	TGATCCGGTGGATGACC
mmpL4KO-1f	GCGCGCGGAGTCGTAG
mmpL4KO-1r	GCTGACCGGCATTTTGC
mmpL4S4KO-Fw	AAGCGTGAGTTTGGTCACCT
mmpL4S4KO-Rv	TGCTGATGTCGTAGCTGACC
Hyg-cFw	GCATTGGTAACTGTCAGACCA
Hyg-cRv	GCTTCGTGGATCCAGATATC

Finally, the recombineering expression plasmid pJV53 was removed by growing the cells without selection for Km-resistance for 6 weeks. This resulted in two strains, H37Rv L4KO and H37Rv L4S4KO containing a deletion in *mmpL4* and *mmpL4-mmpS4*, respectively.

3.2.6.2. Specialised transduction

The deletion of the BCG_0489c (*mmpL4*), BCG_0490c (*mmpS4*) and both BCG_0489c and BCG_0490c from *M. bovis* BCG was performed using the method of specialised transduction as described previously by Bardarov *et al* [27]. Approximately 1kb of upstream and downstream flanking sequences of *mmpL4* and *mmpS4* were PCR amplified from *M. bovis* BCG genomic DNA using the primers L4-LL, L4-LR, L4-RL, L4-RR, S4-LL, S4-LR, S4-RL and S4-RR incorporating Van91I and DraIII sites, given in Table 11 and Table 12.

Table 11. Amplified regions of *mmpL4* and *mmpS4 M. bovis* BCG and the primers used in the amplification.

Gene	Upstream PCR (bp)	Downstream PCR (bp)	Upstream primers	Downstream primers
BCG_0489c (*mmpL4*)	1120	1066	L4-LL vs L4-LR	L4-RL vs L4-RR
BCG_0490c (*mmpS4*)	962	1074	S4-LL vs S4-LR	S4-RL vs S4-RR
BCG_0489c- BCG_0490c (*mmpL4-mmpS4*)	962	1066	S4-LL vs S4-LR	L4-RL vs L4-RR

Table 12. Sequence of the primers used to amplify upstream and downstream regions of *mmpL4* and *mmpS4 M. bovis* BCG.

Oligonucleotide	Sequence 5' → 3'	Characteristics
L4-LL	TTTTTTTT<u>CCATAAATTGG</u>AACGCACACCGTGTGATTTG	Van91I site underlined.
L4-LR	TTTTTTTT<u>CCATTTCTTGG</u>GCCTTGCCGTCGTTACTTTG	Van91I site underlined.
L4-RL	TTTTTTTT<u>CACAGAGTG</u>TGTTGGCGGTGGGATCTGAC	DraIII site underlined.
L4-RR	TTTTTTTT<u>CACCTTGTG</u>ACAGATACCGGGCCGGATAG	DraIII site underlined.
S4-LL	TTTTTTTT<u>CCATAAATTGG</u>GGCCAGCAGGATGTCGAATG	Van91I site underlined.
S4-LR	TTTTTTTT<u>CCATTTCTTGG</u>GGGGTCCGAAGATCTCGTAAG	Van91I site underlined.
S4-RL	TTTTTTTT<u>CCATAGATTGG</u>GGCGGTGATGGGAAATATCG	Van91I site underlined.
S4-RR	TTTTTTTT<u>CCATCTTTTGG</u>CGCGGTACATGGTGTAGTAG	Van91I site underlined.

The amplification products were digested with Van91I and DraIII enzymes, the resulting fragments were cloned into Van91I-digested p0004S [27]. Allelic exchange plasmids pΔL4, pΔS4 and pΔL4S4 were selected and propagated following transformation of *E. coli* TOP10 to Hyg[R]. Sequences of inserted DNA fragments were verified (Table 13).

Table 13. Oligonucleotides used to sequence the cloned DNA fragments in pΔL4, pΔS4 and pΔL4S4.

Oligonucleotide	Sequence 5' → 3'
HL	AGGATCCAGGACCTGCCAAT
HR	CTTCACCGATCCGGAGGAAC
OL	CGGCCGATAATACGACTCA
OR	CTGACGCTCAGTCGAACGAA

Allelic exchange plasmids were digested with PacI and ligated to PacI-digested phAE159, a temperature-sensitive phage [27, 118], to yield the recombinant phasmids phΔL4, phΔS4 and phΔL4S4. Ligation products were packaged using MaxPlax™ Lambda Packaging Extracts (Epicentre Biotechnologies) and transduced into *E. coli* HB101 for propagation. Phasmids were

purified and electroporated into *M. smegmatis* mc^{2}155 for phage propagations at the permissive temperature (30°C). The phage propagations were carried out by an agar-layer technique using MP buffer as phage diluent. High titer lysates were prepared from phage propagated in *M. smegmatis* mc^{2}155 (OD$_{600nm}$ = 1.0) grown on 7H9 agar. Phage titers were determined by spotting 10µl of phage diluted in MP buffer onto lawns of *M. smegmatis* mc^{2}155 on 7H9 agar. BCG aliquots prepared for specialised transduction were mixed with high titre recombinant-phage (typically at least 10^9 plaque forming unit/ml) lysates at an MOI of 10:1, and incubated at non-permissive temperature (37ºC) overnight to allow for infection. The mixtures were centrifuged and the pellet resuspended in 3ml 7H9T OADC. After incubating overnight at 37ºC, the recombinant strains with integration of the allelic exchange marker were selected on 7H10 OADC plates containing 75µg/ml Hyg (Figure 15).
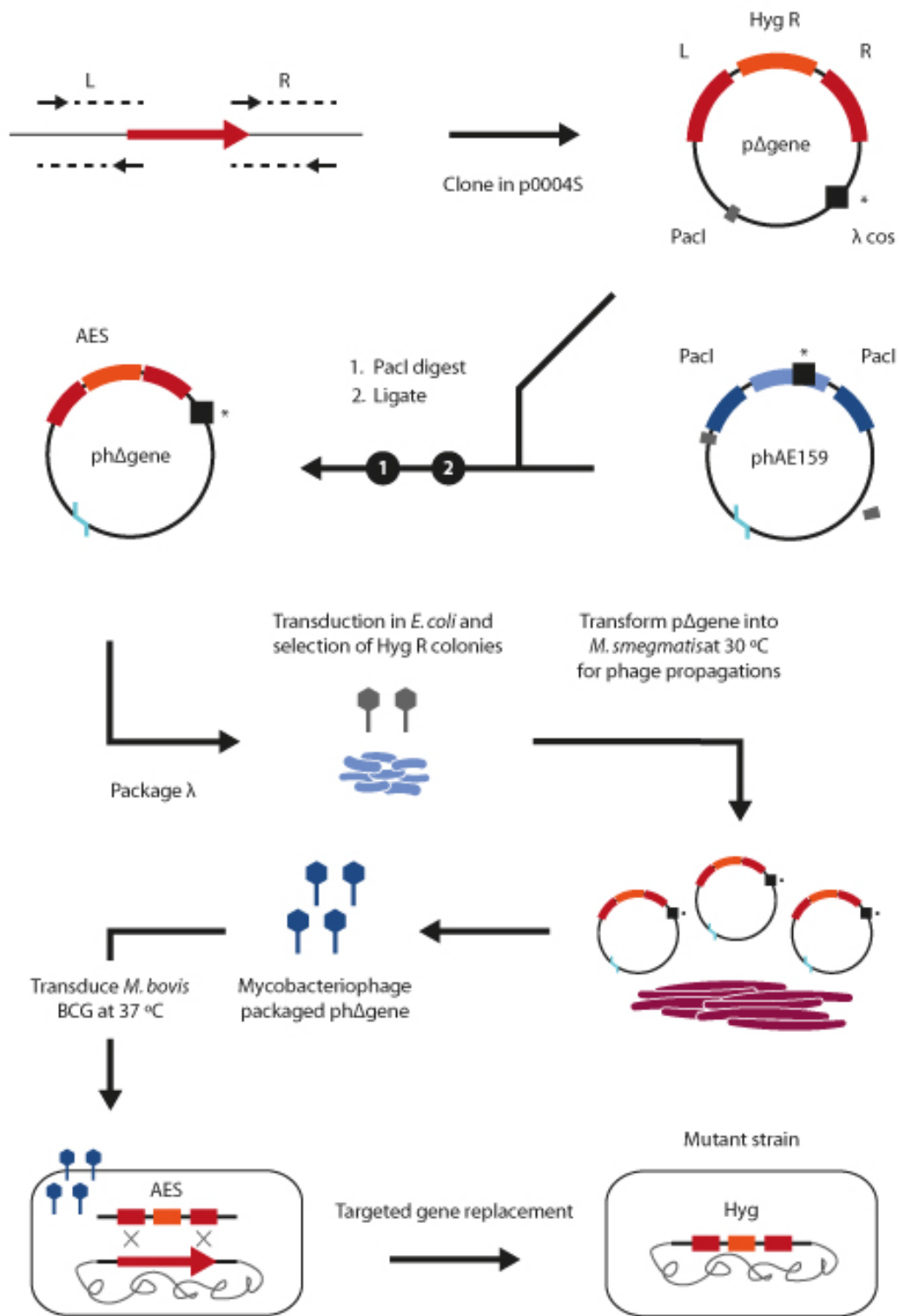
Figure 15. Schematic representation of the process for obtaining knockout mutants by specialised transduction. Adapted from van Kessel [119].

3.2.7. Southern blot

Approximately 3µg of extracted genomic DNA were digested with BamHI. The fragments were separated by electrophoresis through 0.8% agarose gels in Tris-Borate-EDTA (TBE) buffer for 18h at 0.8V/cm. After migration, a standard treatment of the gel was performed. DNA was fixed by UV light for 5min and subjected to a depurination treatment (0.25M HCl for 10min), washing, denaturalization (0.5M NaOH, 1.5M NaCl for 20min) and neutralization (1.5M NaCl, 1M Tris, pH=8.0 for 20min). Hereafter, DNA was vacuum blotted (45-60mbar for 1h 30min) onto a Hybond-N+nylon membrane (Amersham) using 10x SSC buffer (1.5M NaCl, 150mM sodium citrate). Blotted DNA was fixed by UV light for 4min and hybridized with a specific probe. This probe was made by PCR with Taq Gold polymerase (Applied Biosystems) using specific oligonucleotides (Table 14). This PCR product was then purified using GFXTM PCR kit and adjusted to 10ng/µl. After labelling the probe, hybridization patterns were visualized using ECLTM Direct Nucleic Acid Labelling and Detection System (Amersham).

Table 14. Restriction enzymes used for digesting genomic DNA and construction of specific probes for Southern Blot.

M. tuberculosis H37Rv deleted gene	DNA digested with	Probe	
		PCR with oligonucleotides	Size bp
rv0450c (mmpL4)	BamHI	mmpL4-1f vs mmpS4KO-Rv	1046
rv0451c-rv0450c (mmpL4-mmpS4)	BamHI	mmpL4-2f vs mmpL4S4KO-Rv	1175

3.3. Methods for phenotypic characterization

3.3.1. Ethidium Bromide accumulation assay

Mtb strains were grown in 7H9T ADC at 37ºC until an OD_{600nm} of 0.6 to 0.8. Cultures were centrifuged at 4,000rpm for 10 min, the supernatant discarded, the pellet washed in PBS (pH=7.4) and the OD_{600nm} adjusted to 0.8 with PBS with 0.05% Tween-80. Aliquots of 100µl of bacterial suspension were transferred into wells of a 96-well plate containing serial dilutions of ethidium bromide concentrations that ranged from 2-0.125µg/ml.

To determine the effect of chlorpromazine (CPZ) and verapamil (VP) on the accumulation of ethidium bromide, inhibitors were added to a selected concentration of ethidium bromide. Each inhibitor was used at ½ the MIC in order to not compromise the cellular viability. Relative fluorescence was acquired every 51 seconds for 60 minutes at 37ºC, in a SynergyTM HT

Detection Microplate Reader (Biotek® Instruments), using 530/25nm and 590/20nm as excitation and detection wavelengths, respectively.

3.3.2. Susceptibility assays: Minimum Inhibitory Concentration

3.3.2.1. Resazurin Microtiter Assay (REMA)

Serial two-fold dilutions of antibiotics were performed in 7H9G ADC medium, in 96-well microtiter plates, with a final volume of 100μl per well.

Liquid cultures of Mtb strains in logarithmic phase were adjusted to 10^5 CFU/ml in 7H9G ADC. 100μl of this suspension were added to each well and plates were incubated 6 days at 37ºC. 30μl of 0.1mg/ml resazurin solution were then added to each well, and results were observed after 48h of incubation at 37ºC. Resazurin (blue) is an indicator of bacterial growth, since metabolic activity of bacteria reduces it to resofurin (pink).

Minimum Inhibitory Concentration (MIC) is the concentration of antibiotic of the well with the lowest concentration of drug that does not change colour from blue to pink.

3.3.2.2. BacTiter-Glo Microbial Cell Viability Assay

The BacTiter-Glo Microbial Cell Viability Assay (Promega) is a method for determining the number of viable bacterial cells in a sample based on quantitation of the ATP present. It is used when drugs with redox activity interfere with resazurin.

The assay is very similar to REMA described above. In an opaque-walled 96-well-plate, double of the desired concentrations of the antibiotic are added in 100μl of 7H9G ADC. Wells are inoculated by adding 100μl of a culture whose concentration is 10^5 CFU/ml. After 7 days of incubation, 100μl of BacTiter-Glo Reagent was added to each well, incubated 30min at RT, and recorded luminescence (integration time = 1 second per well) in a SynergyTM HT Detection Microplate Reader.

3.3.3. Infection assays

3.3.3.1. Intracellular replication in MH-S cells

Intracellular replication of Mtb strains were tested in MH-S (murine alveolar macrophages) cells. MH-S cells were grown in Dulbecco's modified Eagle medium (DMEM) supplemented with 10% fetal bovine serum (FBS) and 4mM L-glutamine ("complete DMEM" from now).

Infections were performed at a multiplicity of infection (MOI) of 1:1 bacteria per macrophage, with 20,000 MH-S cells per well. After 4h, infection was stopped by removing bacterial suspension and cells were washed three times with 1ml PBS, and finally cultured in 2ml complete DMEM per well to allow intracellular replication. Medium was replaced when needed (typically every 1-2 days) by removing 1.5ml of overlaying DMEM and adding the same volume of fresh complete DMEM.

In order to know the number of intracellular bacteria at the end of time of infection (4h) and days 3, 5 and 7 post-infection, DMEM medium was removed, and 300µl 0.1% triton X-100 were added to each well in order to lyse the cells. 700µl of PBS were added per well and the solution carefully mixed. Several dilutions of this lysate were plated on 7H10 ADC plates and viable bacteria numbers was estimated after 2-3 weeks by counting the number of colonies.

3.3.3.2. Apoptosis induction in MH-S cells

Apoptosis induction of Mtb strains were tested in MH-S (murine alveolar macrophages) cells. MH-S cells were seeded in wells, in complete DMEM. Infections were performed at a multiplicity of infection (MOI) of 5-10 bacteria per macrophage, with 400,000 MH-S cells per well. After 4h, infection was stopped by removing bacterial suspension and cells were washed three times with 1ml PBS, and finally cultured in 6ml complete DMEM per well to allow intracellular replication.

At day 3 post-infection, both supernatant and trypsinized cells were collected together in 15 ml screw-cup tubes. Phosphatidylserine exposure and membrane integrity were analysed by using Annexin-V and 7-actinomycinD (BD Biosciences) and flow cytometry according to manufacturer instructions. Briefly, cells were incubated with Annexin-V and 7AAD in Annexin-binding buffer for 15min. After that, cells were fixed with 4% paraformaldehyde during 30min. PFA Paraformaldehyde solution contained 2.5mM $CaCl_2$.

3.3.4. Ziehl-Neelsen Staining on infected MH-S cells

In parallel with intracellular replication assays, infected MH-S cells were stained by Ziehl-Neelsen method. Infections were performed at an MOI of 1:1 bacteria per macrophage, with 100,000 MH-S cells per well.

MH-S cells were seed on circular glass slide covers of 12mm diameter (Knittel-Gläser) in 24-well cell culture plates, incubated at 37ºC 5% CO_2 for 24h, and then infected as it has been described in infection assay section. Cells were fixed with 500µl of 4% paraformaldehyde for 30min at RT, and washed with 500µl PBS. In order to enable phenol-carbol fuchsin stain to penetrate the waxy mycobacterial cell wall, the slide covers were heated at 60-65ºC for 5min, washed off with water, and covered with an acid alcohol solution (0.5% HCl, 70% ethanol) until they were decolorized. After washing, the slide covers were covered with methylene blue stain

for 5min, washed again, and dried. Finally, slide covers were stuck up-side down on a microscope slide, and examined under a Nikon Eclipse E400 microscope linked to a MOTICAM 2500 digital camera, using the 100x oil immersion objective.

3.3.5. Real-Time Quantitative PCR (qRT-PCR)

Reverse transcription was done from 1µg of RNA using 0.5µg of Random Hexamers (Integrated DNA Technologies) and the SuperScript III (Invitrogen – Life Technologies), performing the reaction at 25ºC for 5min, 50ºC for 2 hours and 70ºC for 15min. Actinomycin D (Sigma) was added to each sample in order to prevent second-strand cDNA synthesis during reverse transcription. cDNA prepared in this way was diluted 1:10 prior to use it to Real Time PCR amplification in the StepOne Plus Real Time PCR System (Applied Biosystems) using Master Mix containing Syber Green (Roche), and the suitable set of primers (Table 15), which were designed using the Primer Express Software (Applied Biosystems). A melting curve was performed for every pair of primers to verify that they produce a single product. PCR amplification was carried out as recommended for the manufacturer (95ºC for 10min; and 40 cycles of 95ºC for 15s, 60ºC for 1min). All the reactions were performed in triplicate, and the levels of mRNA were calculated relative to *sigA* mRNA and the reference strain H37Rv by the ΔΔCt method.

Table 15. Oligonucleotides used in RT-PCR.

Oligonucleotide	Sequence 5' -> 3'	Gene
RTL1-Fw	GCGCCCCCTCAGAAGTTT	*mmpL1*
RTL1-Rv	CGACCAGCAGATGGGAATGT	*mmpL1*
RTL2-Fw	ACCACAACATTTTCAGCCTTTCA	*mmpL2*
RTL2-Rv	CCGCAATCGCCATGAGA	*mmpL2*
RTL3-Fw	CGCCCTGGAGCTGGATT	*mmpL3*
RTL3-Rv	TCGTGGTGGTCAGCAGGAT	*mmpL3*
RTL4-Fw	CGCCCTGCCTGGATACAA	*mmpL4*
RTL4-Rv	GGGTATGAAGTCCGGTAGGTAGTC	*mmpL4*
RTL5-Fw	TGCCACGTTCTGTCTGAGCTT	*mmpL5*
RTL5-Rv	GGCACACCGAGGGTCTGA	*mmpL5*
RTL6-Fw	GCGGCCTGAAATTGTTCCT	*mmpL6*
RTL6-Rv	ATCGCCTTCATGGGAGATGA	*mmpL6*
RTL7-Fw	CGCGGAACCTCAAAAACAAA	*mmpL7*

RTL7-Rv	GGTGTGGATCGTTTCCAGGTATT	*mmpL7*
RTL8-Fw	CGGCTTCCGTCGAGAGTTC	*mmpL8*
RTL8-Rv	GGTTAGACGGGAAATGCTTGTC	*mmpL8*
RTL9-Fw	TGGGTGAAGCACTCGCAAA	*mmpL9*
RTL9-Rv	CGGTGTACTATTCGCCACAATTT	*mmpL9*
RTL10-Fw	CGTCGAACGCATCGTGAA	*mmpL10*
RTL10-Rv	GCGGGTCCTGTCACGTTT	*mmpL10*
RTL11-Fw	ACGCGGGCACCAGTGA	*mmpL11*
RTL11-Rv	GCAGTTTGCCCGGACTGAT	*mmpL11*
RTL12-Fw	GGTCAACGATATCCTCCGTGTT	*mmpL12*
RTL12-Rv	GGCATCCTCGAGTTCGGTATT	*mmpL12*
RTL13a-Fw	TCGAGGTGTTGACCGACAAG	*mmpL13a*
RTL13a-Rv	CGTAACCACGATCAGCATTTTC	*mmpL13a*
RTL13b-Fw	TCGTGGTCCCAGCATTCAT	*mmpL13b*
RTL13b-Rv	CTCGGTGCCCACCAATTC	*mmpL13b*
RTS1-Fw	ACCCGATCATCGCGTTTTAC	*mmpS1*
RTS1-Rv	TGGCGGGCCGAAGAC	*mmpS1*
RTS2-Fw	TCTTCGGTGTTCACGAGCAA	*mmpS2*
RTS2-Rv	GCGGGACGTCGAAATCAG	*mmpS2*
RTS3-Fw	TGTGTACATCCCGTGGTCCAT	*mmpS3*
RTS3-Rv	GAGCCAACGTCGGATTGC	*mmpS3*
RTS4-Fw	GAAAACCGCCCGTCGTACT	*mmpS4*
RTS4-Rv	TTAGGGTTGAATGGTTTGCTGTT	*mmpS4*
RTS5-Fw	AGGCGACGGCACTTCCA	*mmpS5*
RTS5-Rv	GTCCGCTCGTCCTTCACTTC	*mmpS5*
sigA-Fw	CCGATGACGACGAGGAGATC	sigma factor *sigA*
sigA-Rv	CGGAGGCCTTGTCCTTTTC	sigma factor *sigA*

3.3.6. Extraction and analysis of mycobacterial lipids

3.3.6.1. Extraction of free lipids

Mtb strains were grown in 300ml 7H9T ADC at 37ºC for one month. Cultures were centrifuged and bacterial pellets were autoclaved. Afterwards, cell pellets were washed with PBS, and two consecutive extractions with 4ml of petroleum ether (60-80C) were performed; pellets were kept for extraction of non-polar lipids (below). Both supernatants were collected to a new glass tube sealed with a polytetrafluoroethene (Teflon®)-lined screw cap. Solvent was completely evaporated on a heating block (50ºC) under a stream of nitrogen gas and dried free lipids were resuspended in 400µl of chloroform:methanol 2:1.

3.3.6.2. Extraction of non-polar lipids

2ml of methanol: 0.3% NaCl (10:1) were added to the pellets from the protocol above, followed by 2ml of petroleum ether (60-80C). After stirring, the upper layer was transferred to a new glass tube. 2ml of petroleum ether (60-80C) were added to the lower layer in the previous tube, mixed, centrifuged, and the upper layer collected to the previous glass tube; tubes containing the lower layer were kept for extraction of polar lipids (below). The non-polar lipid extracts were dried and resuspended as free lipids.

3.3.6.3. Extraction of polar lipids

2.3ml of chloroform: methanol: 0.3% NaCl in a 9:10:3 ratio were added to the tubes from the procedure above. The mixture was stirred for 1h, and the supernatants were re-extracted twice using 5:10:4 mixture of chloroform: methanol: 0.3% NaCl. Equal volumes of chloroform and 0.3% NaCl were added and the mixture stirred for 5min, after which the organic phase was discarded and the aqueous phase containing the polar lipids was removed, dried and resuspended as free lipids. The remaining pellets were also dried, and kept for the following protocol.

3.3.6.4. Extraction of FAMEs and MAMEs

Dried pellets from the procedure above were then subjected to alkaline hydrolysis using 2 ml 5% tetrabutylammonium hydroxide (TBAH) at 95°C overnight and mixed with 2ml of water, 4ml of dichloromethane, and 500µl of iodomethane for 30min. The upper aqueous phase was discarded after centrifugation and the lower organic phase was washed twice with water and dried. The resultant mixture of fatty acid methyl esters (FAMEs) and mycolic acid methyl esters

(MAMEs) were extracted using diethyl ether, re-dried and resuspended in 400μl of chloroform:methanol 2:1.

3.3.6.5. Thin layer chromatography analysis

Free, non-polar and polar lipid extracts were analysed by two-dimensional thin layer chromatography (2D-TLC) and FAMEs and MAMEs were analysed by one-dimensional thin layer chromatography (1D-TLC). Free and non-polar lipids were analysed using four different solvent systems (A-D) (Table 16), polar lipids by two different systems (D and E) (Table 17), and FAMEs and MAMEs by one single system (F) (Table 18) according to Dobsong *et al* [120]. Approximately 400μg of each lipid sample were spotted on TLC plates (5554 silica gel 60F524, Merck) for 1D and 2D-TLC analysis using following solution systems and allowing plates to dry between each run. Finally, lipids in TLCs were revealed by staining with a solution of 5% molybdophosphoric acid (MPA) in 95% ethanol and heating.

Table 16. Solvent systems for 2D-TLC for free and non-polar lipid analysis.

System	Direction 1	Runs
A	Petroleum ether 60-80/ Ethyl acetate (98:2)	3
B	Petroleum ether 60-80/ Acetone (92:8)	3
C	Chloroform/ Methanol (96:4)	1
D	Chloroform/ Methanol/ Water (100:14:0.8)	1
System	Direction 2	Runs
A	Petroleum ether 60-80/ Acetone (98:2)	1
B	Toluene/ Acetone (95:5)	1
C	Toluene/ Acetone (80:20)	1
D	Chloroform/ Acetone/ Methanol / Water (50:60:2.5:3)	1

Table 17. Solvent systems for 2D-TLC for polar lipid analysis.

System	Direction 1	Runs
D	Chloroform/ Methanol/ Water (100:14:0.8)	1
E	Chloroform/ Methanol/ Water (60:30:6)	1
System	**Direction 2**	**Runs**
D	Chloroform/ Acetone/ Methanol / Water (50:60:2.5:3)	1
E	Chloroform/ Acetic acid (glacial)/ Methanol / Water (40:25:3:6)	1

Table 18. Solvent systems for 1D-TLC FAMEs and MAMEs analysis.

System	Solvents	Runs
F	Petroleum ether/ Acetone (95:5)	1

3.3.7. Protein extraction from mycobacteria

3.3.7.1. Extraction of cellular proteins

2ml of a 7H9T ADC culture of Mtb in log-phase was pelleted by centrifugation (4,000rpm for 5min at RT). The pellet was washed twice with PBS in order to remove BSA, resuspended in 7H9T dextrose NaCl, and then transferred to 10ml of 7H9T dextrose NaCl to grow during 3 weeks. Cells were pelleted by centrifugation (4,000rpm for 10min at RT) and resuspended in PBS. To avoid proteolytic degradation, protease inhibitors (cOmplete Protease Inhibitor Cocktail Tablets – Roche) were added prior to cell lysis. Mycobacterial cells were disrupted by sonication using the BioRuptor (Bio-Rad) for 15min (30s at high power) allowing cooling in an ice-water bath for 30s between pulses. The samples were centrifuged at 4,000rpm for 20min at 4ºC and the supernatant containing whole-cell protein extracts was filtered through a 0.22µm-pore-size low protein binding filter (Millex). Proteins were precipitated with 10% trichloroacetic acid (TCA) final concentration on ice for 1h. After centrifugation at 4,000rpm for 1h at 4ºC, the pelleted proteins were washed with pre-chilled acetone, dried briefly and resuspended in 500µl of 2D buffer (2M thiourea, 7M urea, 2% (w/v) CHAPS). Cellular proteins were quantified using the RC DC protein assay (Bio-Rad) and stored at -80ºC.

3.3.7.2. Extraction of culture filtrate proteins

4ml of a 7H9T ADC culture of Mtb in log-phase was pelleted by centrifugation (4,000rpm for 5min at RT). The pellet was washed twice with PBS in order to remove BSA, resuspended in 7H9T dextrose NaCl, and then transferred to 40ml of 7H9T dextrose NaCl to grow during 3

weeks. Cells were pelleted by centrifugation (4,000rpm for 10min at RT) and resuspended in PBS. The supernatant containing culture proteins was filtered through a 0.22µm-pore-size low protein binding filter. Proteins were precipitated with 10% TCA final concentration on ice for 1h. After centrifugation at 4000rpm for 1h at 4ºC, the pelleted proteins were washed with pre-chilled acetone, dried briefly and resuspended in 100µl of 2D buffer. Culture proteins were quantified using the RC DC protein assay and stored at -80ºC.

3.3.8. Gel electrophoresis of proteins

3.3.8.1. One-dimensional SDS-polyacrylamide gel electrophoresis

10µg of each protein extract were boiled (for 5min) in presence of 3µl of 150mM Tris/HCl pH=7.4, 3% SDS, 0.3mM sodium molybdate, 30mM sodium pyrophosphate, 30mM NaF, 30% glycerol, 30% mercaptoethanol and 0.06% bromophenol blue. Cellular and culture filtrate proteins were separated by electrophoresis through a 5% stacking gel over a 12 % resolving polyacrylamide gel containing 0.1% SDS in running buffer (25mM Tris, 192mM glycine, 3.4mM SDS) at constant amperage of 30mA/gel. PageRuler Plus Prestained Protein Ladder (Thermo Scientific) were used as molecular weight marker. The gels were stained with Coomassie brilliant blue.

3.3.8.2. Two-dimensional SDS-polyacrylamide gel electrophoresis

100µg of each culture filtrate protein sample was dissolved in the necessary quantity of rehydration buffer (2D buffer + 65mM DTT, 0.5% IPG buffer, 0.002% (w/v) bromophenol blue) up to reach 125µl final volume, and loaded onto 7 cm IPG strips (pH 4–7; Amersham Biosciences). Loaded IPG strips were rehydrated overnight at room temperature. Isoelectric focusing (IEF) was performed on Protean IEF cell (Bio-rad) and focused for 10min at 50V, 30min at 300V, 1h at 300V, 90min at 4,000V, and finally for 1h at 4,000 V. Following IEF, individual strips were equilibrated for 15min in 375mM Tris-HCl, 6M urea, 20% (v/v) glycerol, 2% (w/v) sodium dodecyl sulfate (SDS), 2% (w/v) DTT, and in a solution of the same composition that also contained 2.5% (w/v) iodoacetamide. The strips were placed onto a 12% (w/v) SDS polyacrylamide gel and sealed with 0.5% (w/v) agarose. SDS-PAGE electrophoretic separation was carried out for 90min at 100V until the bromophenol blue dye reached the bottom of the gel.

200µg of each cellular protein sample was dissolved in the necessary quantity of rehydration buffer (2D buffer + 65mM DTT, 0.5% IPG buffer, 0.002% (w/v) bromophenol blue) up to reach 450µl final volume, and loaded onto 24 cm IPG strips (pH 3–7; Amersham Biosciences). Loaded IPG strips were rehydrated overnight at room temperature. Isoelectric focusing (IEF) was performed on Protean IEF cell (Bio-rad) and focused for 10min at 50V, 2h at 500V, 1h at 1,000V, and finally for 11h at 10,000V. Following IEF, individual strips were equilibrated for 15

min in 375mM Tris-HCl, 6M urea, 20% (v/v) glycerol, 2% (w/v) sodium dodecyl sulfate (SDS), 2% (w/v) DTT, and in a solution of the same composition that also contained 2.5% (w/v) iodoacetamide. The strips were placed onto a 12% (w/v) SDS polyacrylamide gel and sealed with 0.5% (w/v) agarose. SDS-PAGE electrophoretic separation was carried out for 20h at 2W/gel.

After electrophoresis, gels were stained with colloidal Coomassie Blue G-250 (Fisher Scientific).

3.3.9. Analysis and identification of proteins

Spot scanning was performed using GS-800 Densitometer (Bio-rad) and Quantity One software (Bio-rad). Stained gels were analyzed by using progenesis SameSpots software (Nonlinear Dynamics). Statistically significant changes in protein spots were determined using ANOVA test ($p < 0.05$) followed by a posteriori test, and finally the False Discovery Rate (FDR) procedure ($q < 0.05$).

Protein spots of interest were excised from SDS-PAGE gels using EXQuest Spot Cutter (Bio-rad) and washed with water, ammonium bicarbonate (25mM NH_4HCO_3) and acetonitrile. Next, samples were reduced by incubation with dithiotreitol (10mM) at 60ºC for 45min and alkylated by incubation with iodoacetamide (50mM) at room temperature for 30min. Finally proteins were trypsin digested overnight at 37ºC with a ratio enzyme:protein of 1:10 (Trypsin Gold, Promega). Digestion was stopped by addition of 0.1% TFA and tryptic peptides were extracted sequentially with increasing concentrations of acetonitrile in water. Peptides were concentrated and desalted by passing it through ZipTip C18 columns (Millipore) following the manufacturer's instructions and eluting with 50%ACN/0.1%TFA.

Sample (0.5µl) and matrix (0.7µl saturated solution of *alpha*-Cyano-4-hydroxycinnamic acid (CHCA) in 50% ACN/0.1% TFA) were spotted in duplicate onto an Opti-Tof 384 well insert plate (Applied Biosystems). MALDI-TOF MS was performed using a 4800plus MALDI-TOFTOF (ABSciex) in the reflector mode with accelerating voltage of 20 kV, mass range of 800 to 4000 Da, 1000 shots/spectrum and laser intensity of 3000. MSMS spectra was performed automatically on twenty of most intense precursors, with 1000 shots/spectrum and laser intensity of 4000. Spectra were calibrated externally using a standard protein mixture (4700 Calmix, Applied Biosystems).

Proteins were identified with the search engine Mascot using the SwissProt database (546,439 sequence entries) and UnitProt database (57412064 sequences entries). Search parameters used were: missed cleavage 1, fixed modifications carbamidomethyl (cysteines) and peptide and fragment mass tolerance 0.2Da and 0.3Da, respectively. Individual ions scores >39 were considered a positive hit. To identify the correct protein from a Mascot results list, score and specie had to be considered.

4. Results and Discussion

4.1. Generation of *M. tuberculosis* strains for the study of the efflux pumps MmpL4 and MmpS4

4.1.1. Construction of *M. tuberculosis* knockout mutants

The construction of the Mtb H37Rv knockout mutants deleted in *rv0450c* (H37Rv L4KO) and in both *rv0450c* and *rv0451c* (H37Rv L4S4KO) was carried out following the recombineering method [115].

Electrocompetent cells of Mtb H37Rv strain containing plasmid pJV53 were transformed independently with either 100ng of *mmpL4* AES or *mmpL4-mmpS4* AES. The resulting cells were plated in 7H10 ADC Hyg, and incubated at 37°C until colonies were of sufficient size for subculturing in 7H9T ADC Hyg liquid medium. After 10 to 15 days, genomic DNA was extracted and checked by PCR according to the reactions shown in Table 19.

Table 19. PCRs for confirming *M. tuberculosis* knockout mutants deleted in *mmpL4* and in *mmpL4-mmpS4*.

mmpL4	Size of expected PCR product (bp)	
PCR	**H37Rv wt**	**L4KO**
mmpL4KO-Fw vs Hyg-out	-	1047
mmpL4KO-1f vs mmpL4KO-1r	796	-
mmpL4-mmpS4	Size of expected PCR product (bp)	
PCR	**H37Rv wt**	**L4S4KO**
mmpL4S4KO-Fw vs Hyg-cRv	-	1145
mmpL4S4KO-Rv vs Hyg-cFw	-	1184

Regarding *mmpL4-mmpS4* AES construction, we first used an AES having 500bp of sequence identity at each side of the hygromycin resistant cassette; however, DNA samples from most of the colonies isolates by the procedure above did not resulted in amplification products of the expected size according to Table 19, which were assumed to have originated by illegitimate recombination events. Then, it was necessary to construct a new AES with 1,000bp of sequence identity at each side of the hygromycin resistant cassette; in this case 40% of

candidate colonies were finally confirmed as H37Rv L4S4KO and 15% were H37Rv L4KO since they produced amplification products consistent with the size expected (Table 19).

4.1.2. Confirmation of *M. tuberculosis* knockout mutants by Southern Blot

Southern Blot was the definitive test to validate the knockout mutants. Genomic DNA of H37Rv wt and both knockout mutants (Figure 16 and Figure 17) were digested with BamHI, a restriction enzyme that has little number of recognition sites in the genome, generating fragments of different sizes. Two specific probes were amplified and hybridized in different analysis, revealing the fragments that contained either wild-type or disrupted gene by the Hyg cassette.
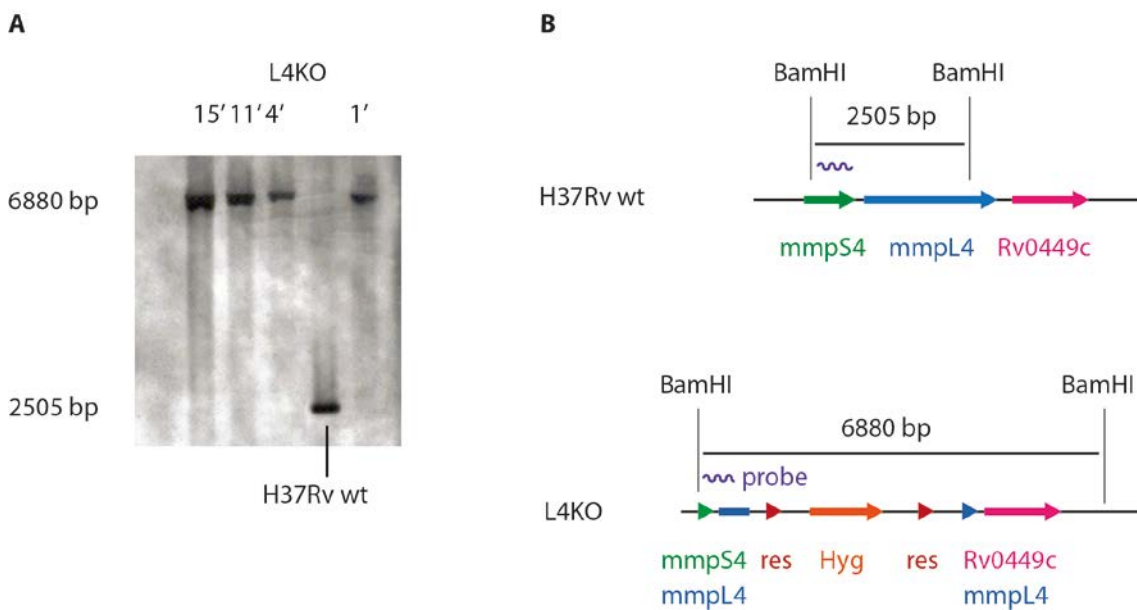
Figure 16. Southern blot analysis of 4 representative H37Rv L4KO strains. (A) DNAs were digested with BamHI and hybridized with a probe of 1046bp containing part of *mmpS4* and *mmpL4* coding sequences (wavy line in panel B). The 2505-bp band for H37Rv wt was replaced by 6880-bp band for L4KO knockout mutants. (B) Schematic representation *rv0449c-mmpS4-mmpL4* operon in the reference strain and in L4KO (not to scale).
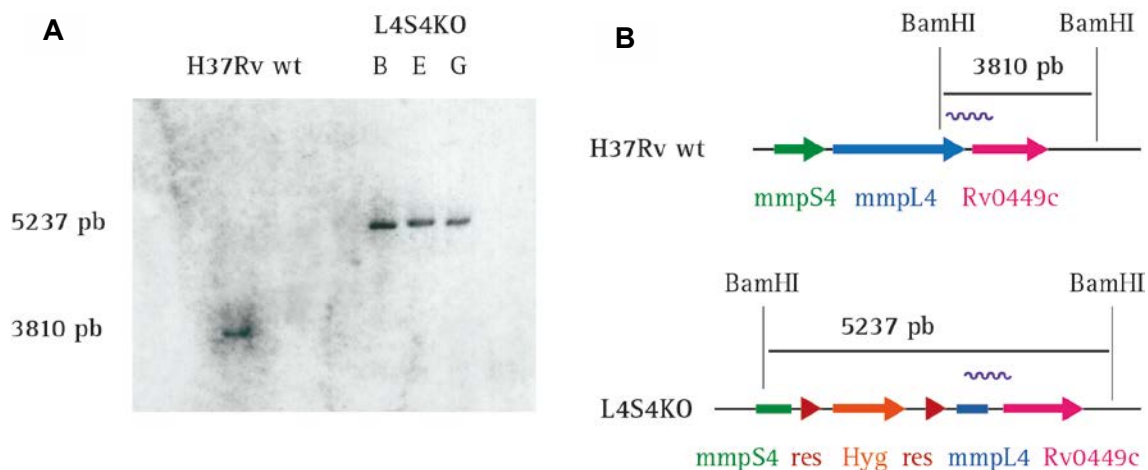
Figure 17. Southern blot analysis of 3 representative H37Rv L4S4KO strains. (A) DNAs were digested with BamHI and hybridized with a probe of 1175bp containing part of *rv0449c* and *mmpL4* coding sequences. The 3810-bp band for H37Rv wt was replaced by 5237-bp band for L4S4KO knockout mutants. (B) Schematic representation *rv0449c-mmpS4-mmpL4* operon in the reference strain and in L4S4KO.

4.1.3. Generation of complemented strains of the *M. tuberculosis* knockout mutants

With the aim of constructing these strains, the integrative plasmid pRBV2 was obtained. This vector has a fragment containing the operon *rv0451c-rv0450c* with its natural promoter detected by RNAseq, in order to keep the physiological expression of these genes.

After transformation of pRBV2 in H37Rv L4KO and L4S4KO, and selection of colonies, the presence of the plasmid was verified by PCR (Table 20).

Table 20. PCRs to verify complemented knockout mutant strains.

Strain	Description	PCR verification	
		Primers	Expected size of PCR product (bp)
H37Rv L4c	H37Rv L4KO complemented with pRBV2	mmpL4-2f vs pMV361B	614
H37Rv L4S4c	H37Rv L4S4KO complemented with pRBV2	mmpL4-2f vs pMV361B	614

4.1.4. Generation of the overexpression strain in *M. tuberculosis*

First, the replicative plasmid pRBZ13 was obtained, and then was transformed in H37Rv wt. After selection of colonies, the presence of the plasmid was verified by PCR (Table 21).

Regarding pRBZ13, it has the same fragment as pRBV2 containing the operon *rv0451c-rv0450c* with its natural promoter. In this case, the increase in the expression of *mmpL4* and *mmpS4* is due to the presence of multiples copies of pRBZ13.

Table 21. PCRs to verify the overexpression strain in *M. tuberculosis*.

| Strain | Description | PCR verification | |
		Primers	Expected size of PCR product (bp)
H37Rv pRBZ13	Overexpression strain for *mmpL4* and *mmpS4*	RP-180 vs mmpL4-2f	657

4.2. *In vitro* phenotypic characterization of *M. tuberculosis* strains

4.2.1. The generated strains were positive for neutral red

Considering that the generated Mtb strains were going to be tested in infection assays, it was necessary to confirm that they had not lost their virulence during genetic manipulations such as electroporation. To this aim, neutral-red staining was performed on all the strains because neutral red fixation is considered a marker of virulence. Besides, neutral-red staining is a fast screening technique for testing integrity of the mycobacterial cell envelope, since it has been proved that a negative neutral-red reaction given by a mycobacterial strain is owing to the lack of more than one type of methyl-branched lipids [121]. Nevertheless, further lipid analyses were needed to assure the integrity of the cell envelope.

Two strains were used as controls: H37Rv, a virulent strain, as positive control; and MTVBAC, an attenuated strain, as negative control. MTBVAC, which has double unmarked *phoP* and *fadD26* deletions, is not able to fix neutral red because the *fadD26* gene is required for PDIM biosynthesis [122]. All strains showed a positive neutral-red reaction (Figure 18), so they were selected for following experiments.
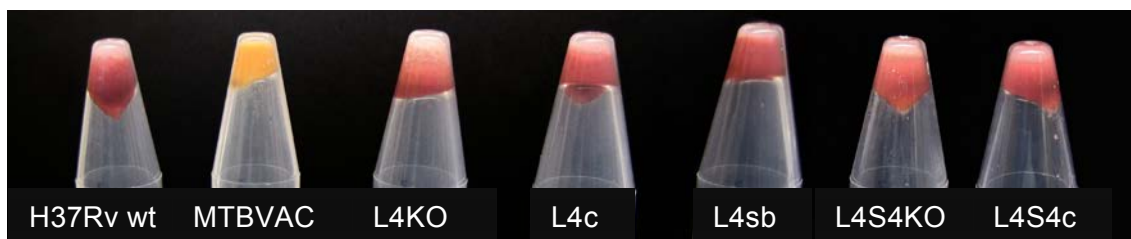
Figure 18. Neutral-red staining of the generated strains in Falcon tubes.

4.2.2. There were not differences in cell morphology between knockout mutant strains and wild-type

After auramine staining, no significant differences were observed in terms of size and shape of bacterial cells (Figure 19) between H37Rv wt and the single mutant H37Rv L4KO or the double mutant H37Rv L4S4KO. Also, the overexpression strain H37Rv L4sb was checked, but there were not differences in cell morphology in comparison to the wild-type strain.
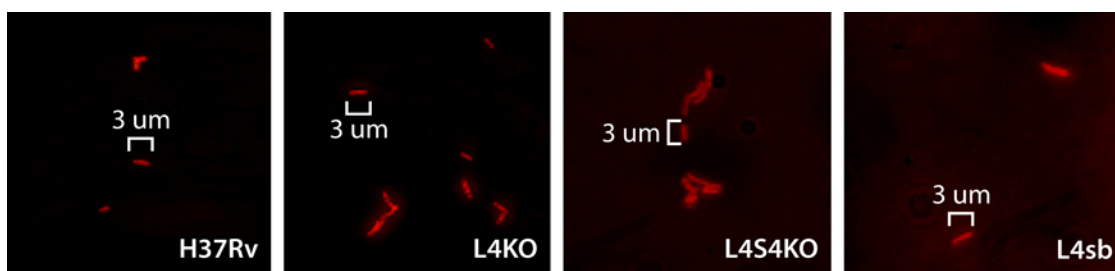
Figure 19. Auramine staining of H37Rv wt, L4KO, L4S4KO, and L4sb bacilli.

4.2.3. Colonies of the overexpression strain L4sb were smaller and smoother than H37Rv wt colonies

H37Rv L4KO and L4S4KO as well as L4sb were plated on 7H10 ADC (Figure 20) in order to check any phenotypic change in colony morphology in comparison with the parental strain H37Rv wt.
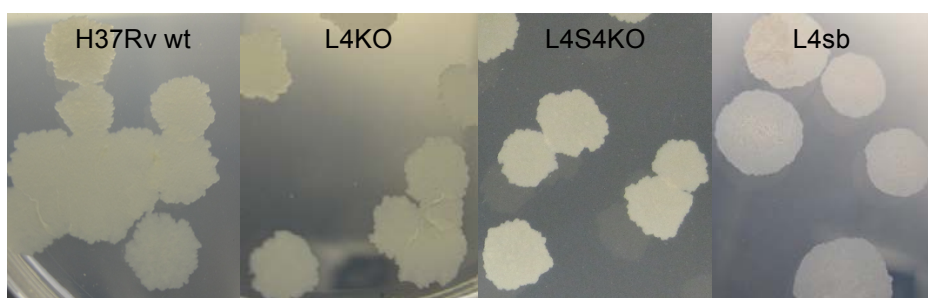
Figure 20. H37Rv, L4KO and L4S4KO colonies on 7H10 ADC.

The colonies of both knockout mutants L4KO and L4S4KO exhibited neither difference in size nor in appearance in relation to the wild-type strain H37Rv. Nevertheless, H37Rv L4sb showed (Figure 20) smooth colony morphology with less ruffled edges and slightly smaller size than H37Rv wt colonies. When the overexpression strain was subcultivated and plated again, two different colony morphologies appeared (Figure 21): small smooth colonies with less ruffled edges equal to the colonies obtained before, and rough colonies with ruffled edges similar to H37Rv wt colonies. Each kind of colony was plated separately and both the smooth and the rough colonies resulted again in a mixture of both morphologies; from the smooth colony the proportion of smooth colonies to roughs was 3/7, and from the rough colony was 5/95.

L4sb   L4sb mixture

Colonies from
smooth L4sb

smooth L4sb   rough L4sb
colony   colony

Colonies from
rough L4sb
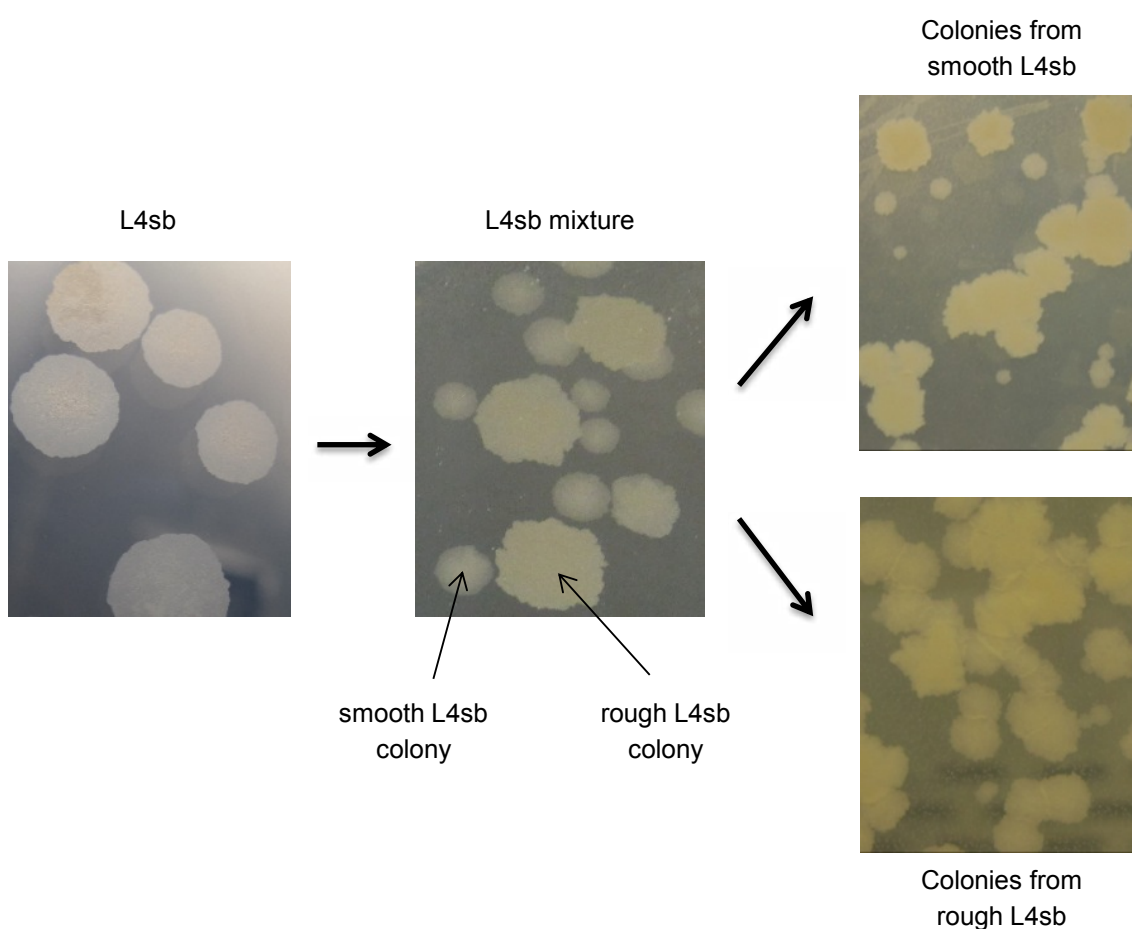
Figure 21. Morphological changes of H37Rv L4sb colonies on 7H10 ADC.

It is likely that these morphological changes undergone by H37Rv L4sb strain could be due to point mutations in genes responsible for architecture and/or composition of the mycobacterial cell wall.

Moreover, H37Rv L4KO, L4S4KO and L4sb were plated on 7H10 ADC with 0.05% Tween-80 (Figure 22) taking H37Rv wt as a reference. It has been demonstrated that Tween-80 is able to alter colony morphology besides preventing mycobacterial clumpling in liquid medium [123-125]. So, the addition of Tween-80 can exhibit a morphological change in the mycobacterial

colony which might pass unnoticed in regular 7H10 ADC plates lacking Tween-80. In these conditions (Figure 22), H37Rv L4sb colonies were even smaller than the colonies obtained in 7H10 ADC (Figure 21), suggesting a marked toxic effect caused by Tween-80. However, no other morphological change could be appreciated in either the overexpression strain or single and double mutant colonies.
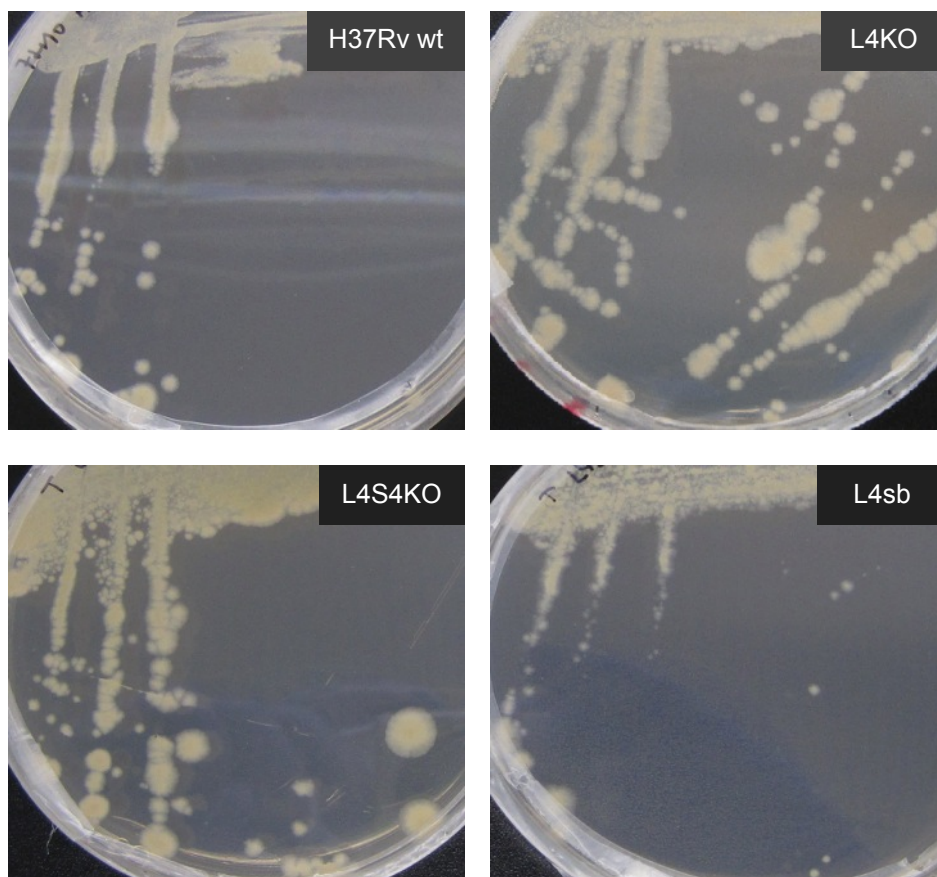
Figure 22. H37Rv L4KO, L4S4KO and L4sb plated on 7H10 ADC with 0.05% Tween-80.

4.2.4. H37Rv wt and the knockout mutants presented similar growth in iron-replete and iron-restricted liquid media

According to Wells *et al* [99], MmpL4/MmpS4 and MmpL5/MmpS5 efflux systems are involved in siderophore export. Specifically, it seems that MmpL4/MmpS4 and MmpL5/MmpS5 take part in the biosynthesis and transport of mycobactins and carboximycobactins. These small molecules capture iron from the medium or the human host, since iron is an essential micronutrient for most forms of life on earth due to its vital role as a redox cofactor of proteins required for critical cellular processes.

In the same study, the growth of the single and double knockout mutants in *mmpS4* and *mmpS5* were checked in iron-replete and iron-deplete media, and it was observed that both proteins are required for normal growth of Mtb under low iron conditions [99]. Therefore, we

decided to examine the growth of H37Rv L4KO and L4S4KO in the same conditions. 7H9T ADC was used as an iron-replete medium; 7H9T ADC 0.1mM 2,2'-dipyridyl (DIP; a ferrous chelator) and 7H9T ADC 0.2mM desferrioxamine (DFO; a ferric chelator) were used as the iron-deplete media.

H37Rv wt, L4KO and L4S4KO cultures were started out with an inoculum of 10^5 CFU/ml and optical densities were measured at regular intervals for 14 days. Triplicate cultures of each strain were grown and standard deviations are shown in Figure 23.
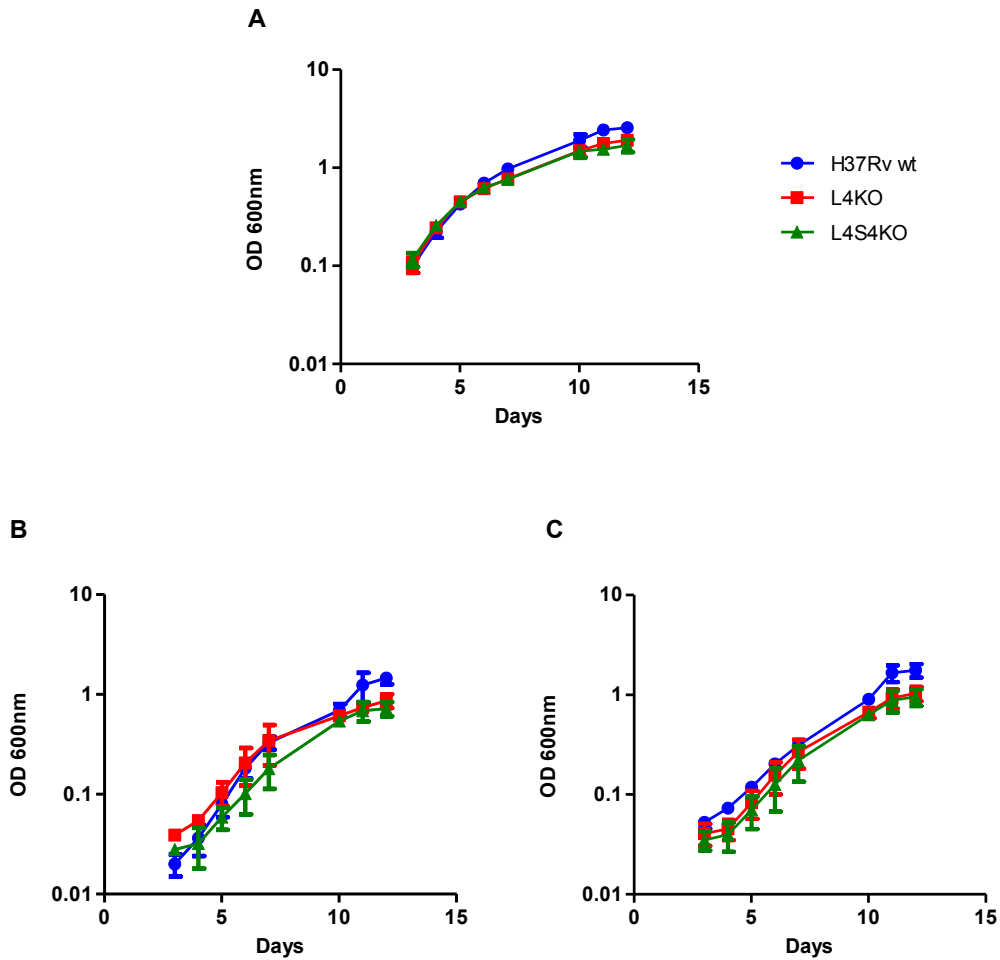
Figure 23. Growth of H37Rv wt, L4KO and L4S4KO in 7H9 media containing different quantities of iron. (A) 7H9T ADC (iron-replete medium), (B) 7H9T ADC DIP (iron-depleted medium), and (C) 7H9T ADC DFO.

There were no significant differences between the growth of the wild-type strain and the single and double knockout mutants neither in iron-replete nor in iron-deplete medium. However, it should be noted that the growth of H37Rv L4KO and L4S4KO was slightly slower than H37Rv wt in both 7H9T ADC and 7H9T ADC DFO in a repetitive and systematic way.

The fact that both H37Rv L4KO and L4S4KO did not exhibit a low-iron growth defect phenotype could be explained because of the presence of MmpL5 and MmpS5. This efflux system might be counteracting the lack of function of MmpL4 and MmpS4 due to their suggested redundant role in siderophore transport.

4.2.5. MmpL4/MmpS4 efflux system does not play a critical role in drug resistance

Drug susceptibility assays were performed with single and double knockout mutants (L4KO, L4S4KO), the overexpression strain (L4sb), along with the parental strain H37Rv. The compounds tested (Table 22) included the most widely used antituberculosis drugs, as well as other drugs known to be efflux substrates for RND proteins from other organisms. Also, the common efflux pump substrate ethidium bromide and the efflux inhibitors chlorpromazine and verapamil were tested (Table 23). Finally, those compounds increasing or decreasing expression of *mmpL4* RNA in the microarray analysis prepared by Boshoff *et al* [126] were also tested (Table 24).

Table 22. MIC values of various antituberculosis medicines and other antibiotics for H37Rv wt, L4KO, L4S4KO, and L4sb obtained by REMA.

Compound	MIC (µg/ml)			
	H37Rv	L4KO	L4S4KO	L4sb
INH	0.5	0.5	0.5	0.5
RIF	0.05	0.05	0.05	0.05
EMB	4-8	4	4	4
SM	0.25	0.25	0.25	0.25
PAS	0.03	0.03	0.03	0.03
VAN	64	64-128	128	64-128
GM	4	4	4	4
SP	2-4	2	4	2-4
AC	2	2	2	2
AK	0.5	0.5	0.5	0.5
TC	1-2	1-2	2	1-2

Inh, isoniazid; Rif, rifampicin; Emb, ethambutol; Sm, streptomycin; PAS, para-aminosalicylic acid; Van, vancomycin; Gm, gentamicin; Sp, spectinomycin; Ac, acriflavine; Ak, amikacine; Tc, tetraciclyne.

Table 23. MIC values of ethidium bromide, chlorpromazine and verapamil for H37Rv wt, L4KO, L4S4KO, and L4sb obtained by REMA.

Compound	MIC (µg/ml)			
	H37Rv	L4KO	L4S4KO	L4sb
EtBr	2	2	1	2
CPZ	16	16	16	8
VP	256	128	256	128

EtBr, ethidium bromide; Cpz, chlorpromazine; Vp, verapamil.

Table 24. MIC values of the selected redox compounds for H37Rv wt, L4KO, L4S4KO, and L4sb obtained by BacTiter-Glo Microbial Cell Viability Assay.

Compound	CIM (µg/ml)			
	H37Rv	L4KO	L4S4KO	L4sb
CLO	0.03	0.016	0.016	0.016
TRC	16	16	16	16
TRZ	4	4	4	4
PA824	50	100	100	50
CAP	1	1	1	1
DCCD	50	50	50	50
H_2O_2	544	544	544	544

Clo, clofazimine; Trc, triclosan; Trz, tioridazine; PA824, pretomanid; Cap, capreomycin; DCCD, diciclohexilcarbodiimida.

None of the strains of our study displayed significant alterations in susceptibility to the compounds tested despite multiple independent experiments. These results suggest that the MmpL4 and MmpS4 proteins do not play a major role in intrinsic Mtb drug resistance, although compensatory effects caused by other different MmpL proteins or any other efflux pump cannot be ruled out.

4.2.6. There were differences in the ethidium bromide accumulation among the strains studied

The ethidium bromide (EtBr) accumulation assay was selected so as to evaluate efflux activity in H37Rv wt and the rest of the strains generated in this study: H37Rv L4KO, L4S4KO, L4c, L4S4c and L4sb. EtBr is a very common efflux pump substrate which emits weak fluorescence

in aqueous solution (external to the cell) and becomes strongly fluorescent when enters the bacterial cells due to its binding to nucleic acids [127].

First, each of the strains was tested (Figure 24) at different EtBr concentrations. The L4KO and L4S4KO mutants showed an increased accumulation of EtBr relative to wild-type H37Rv strain, whereas the overexpression L4sb strain presented noticeable decreased accumulation of EtBr. Nonetheless, complemented strains of both mutants, L4c and L4S4c, exhibited an increased accumulation of EtBr in relation to H37Rv wt in the manner of their respective knockout mutants. All strains tested maintained the detected changes in the accumulation of EtBr at all concentrations tested.

The strong reduction in the accumulation of EtBr exhibited by L4sb suggests that MmpL4/MmpS4 efflux system transports EtBr efficiently. Keeping this in mind, a greater increase in the EtBr accumulation of both knockout mutants would be expected [75]. Since accumulation of EtBr in the knockout mutants is lower than expected, this can be explained by the fact that other Mtb efflux pumps are able to transport EtBr, hence compensating the lack of MmpL4/MmpS4; in addition, their contribution to the global EtBr transport might be bigger than that of the MmpL4/MmpS4 proteins. Moreover, the lack of MmpL4 and MmpL4/MmpS4 membrane proteins in L4KO and L4S4KO respectively, might cause other alterations in the mycobacterial membrane permeability, which may explain the rise in EtBr accumulation.

It should be pointed out that there were significant differences in the transport of EtBr among knockouts and the wild-type strain during EtBr accumulation assays (normally lasting for 60min), which were not appreciated in susceptibility assays (which usually last for 8 days). This suggests that regular MIC determination could not be the most suitable assay for investigating the substrate profile of efflux pumps, so that more sensitive assays are necessary to evaluate the possible transport of the tested compounds by the knockout mutants.
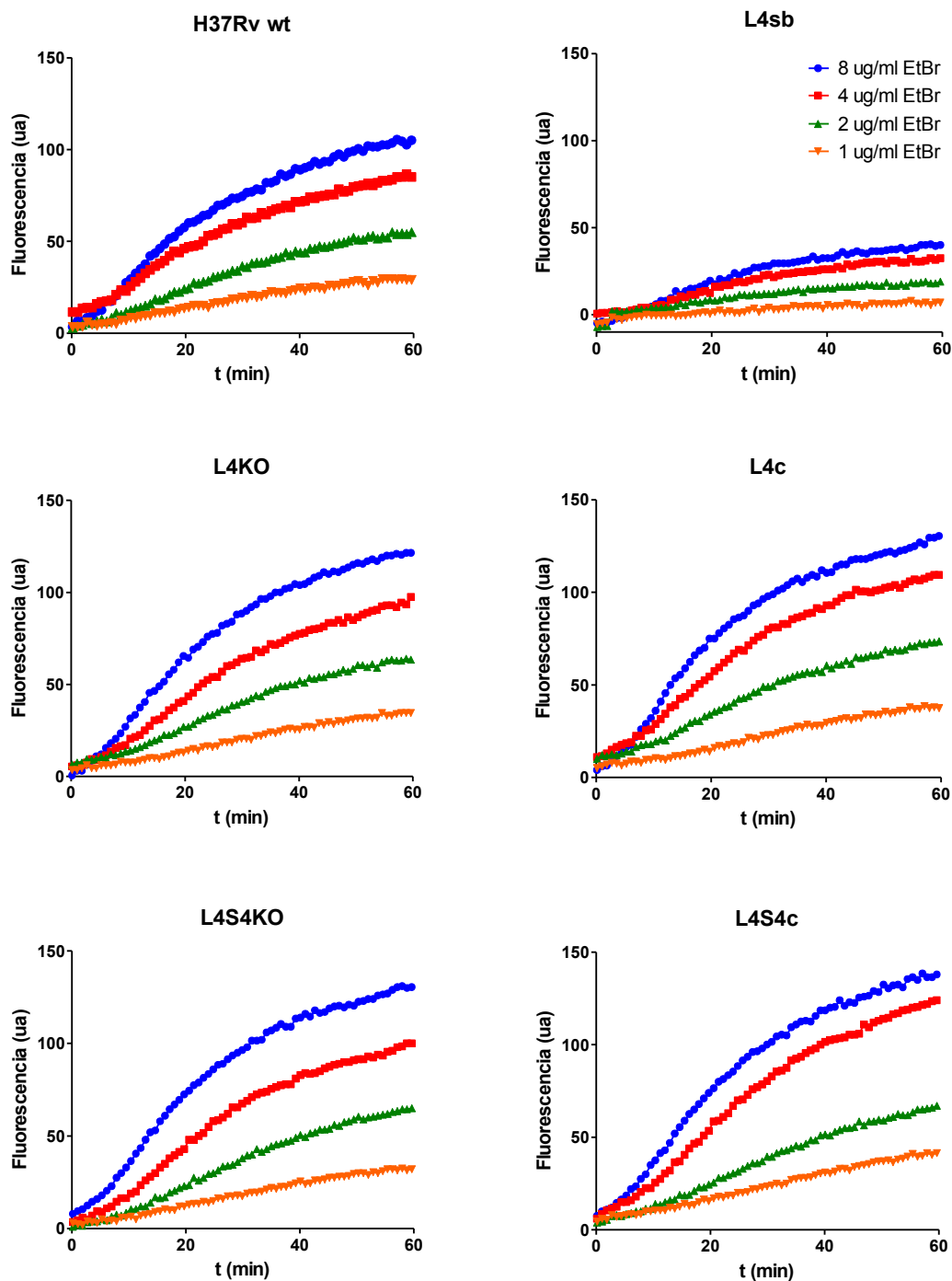
Figure 24. Accumulation of ethidium bromide at 8 µg/ml, 4 µg/ml, 2 µg/ml, and 1 µg/ml by H37Rv wt, L4sb, L4KO, L4c, L4S4KO, and L4S4c. Data were expressed as arbitrary units of fluorescence and obtained from two independent wells in one representative experiment.

Second, we decided to use 1µg/ml EtBr concentration to check the effect of efflux inhibitors (Figure 25), CPZ and VP, in the accumulation of EtBr in each of the strains. Ethidium bromide and efflux inhibitors were used at half of the MIC so as not to compromise cellular viability.

According to the results obtained, VP is the best inhibitor because it caused greater accumulation of EtBr in all the strains tested; this agrees with previous publications in which VP changes notably EtBr accumulation levels on mycobacterial strains [75, 128]. On the contrary, CPZ seems to exert no significant influence in EtBr accumulation, at least for the first 60min after the addition to the mycobacteria.
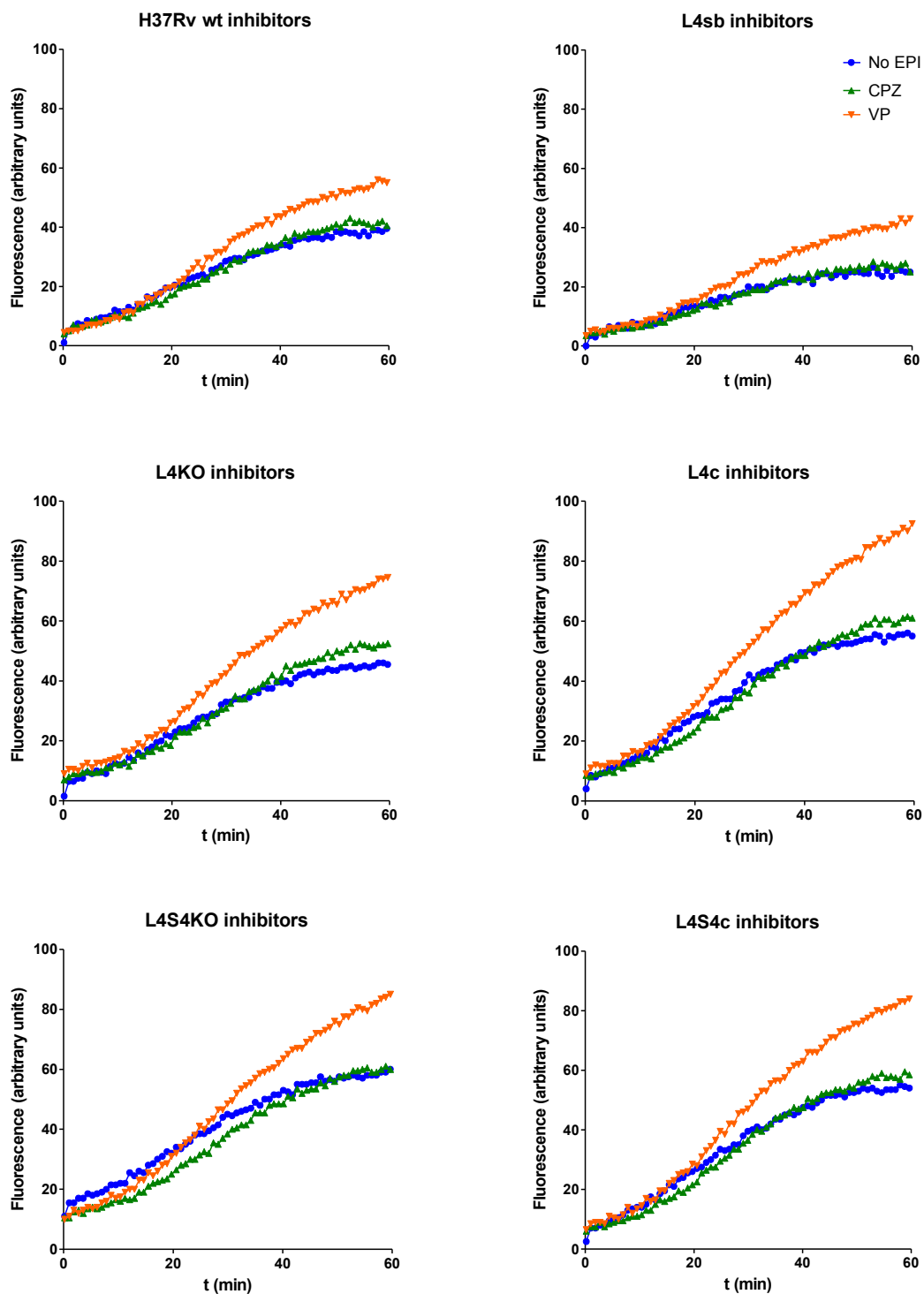
Figure 25. Effect of efflux inhibitors CPZ and VP on the accumulation of EtBr at 1 µg/ml for H37Rv wt, L4sb, L4KO, L4c, L4S4KO, and L4S4c. Data were expressed as arbitrary units of fluorescence and obtained from two independent wells in one representative experiment.

H37Rv L4c and L4S4c showed an increased accumulation of EtBr for each condition compared to H37Rv wt. That is to say, the complemented strains exhibited similar EtBr levels to their respective knockout mutants again, suggesting that the process of complementation could have failed. It is difficult to figure out where the failure might be: mRNA expression, regulation or protein translation. In an alternative explanation, Mtb could be forced to get a compensatory mutation to counteract the lack of MmpL4-MmpS4 because of their important role, which would allow complementation strains to maintain a level of EtBr accumulation similar to wild-type strain; if this were the case, complementation would have little effect, if any. This hypothesis of selection of compensatory mutations could explain the morphological change in L4sb colonies described previously; the overexpression of these important proteins without any regulation may oblige Mtb to acquire mutations quickly to compensate it, resulting in a change in colony morphology.

4.2.7. The overexpression of *mmpL4* and *mmpS4* caused pronounced decrease in intracellular replication of L4sb in MH-S cells

To investigate the role of MmpL4 and MmpS4 in virulence of Mtb, MH-S cells were infected independently with L4KO, L4c, L4S4KO, and L4S4c strains, taking the virulent strain H37Rv and the attenuated strain BCG as controls. Mycobacterial replication (Figure 26) was analysed at 0, 3, 5 and 7 days post-infection. According to the results, both knockout mutants and their complemented strains were able to replicate between 0.5 and 1 logarithm less than H37Rv wt. This decrease could be an effect caused by the slight drop showed in the growth of the strains in liquid medium or because of the own function of MmpL4 and MmpS4. In any case, the decrease in intracellular replication of L4KO and L4S4KO was not significant in comparison with the reference strain.
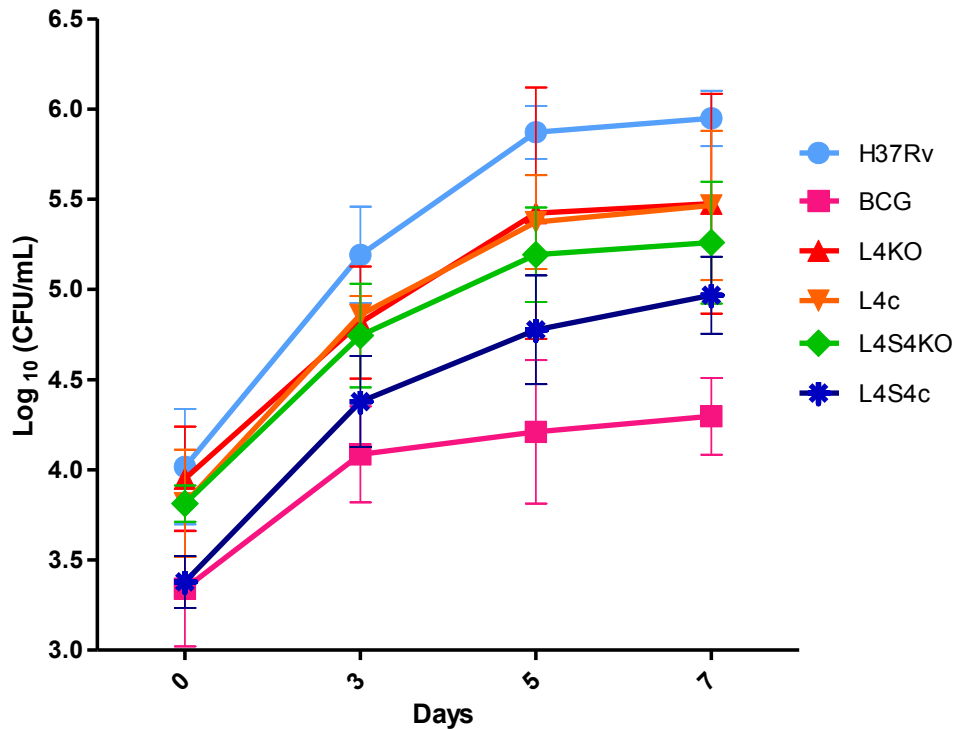
Figure 26. Replication of H37Rv wt, BCG, L4KO, L4c, L4S4KO, and L4S4c in MHS-infected cells. Data were expressed as $Log_{10} \pm$ SD of CFU counts per millilitre and obtained from two independent wells in three independent experiments.

Interestingly, L4sb showed a significant drop of more than 1 logarithm compared to H37Rv wt (Figure 27). We think this fall in L4sb intracellular replication could be produced by a reduction in the bacterial growth rate which was shown in liquid and solid media repeatedly. However, what caused this modification in L4sb growth rate? Our hypothesis is that the overexpression of *mmpL4* and *mmpS4* changed L4sb fitness. Bacterial fitness can be affected by the amount of protein processing, which includes synthesis, maturation, maintenance, and disposal. Specially, membrane proteins damage fitness when overexpressed by membrane piercing, engaging membrane-specific folding pathways, or interfering with other membrane proteins [129]. But it is also true that depending on the role of the membrane protein, growth rate and other characteristics like virulence or drug resistance are affected [70, 75, 130, 131]. Nevertheless, the recently discovered role of MmpL4/MmpS4 in siderophore export does not seem to have effect on bacterial growth when they are overexpressed unlike Mtb siderophore export mutant (double *mmpS4/mmpS5* knockout mutant). This mutant exhibited a growth defect due to impaired iron acquisition and self-poisoning by continuously synthesizing siderophores in order to overcome iron starvation [105].
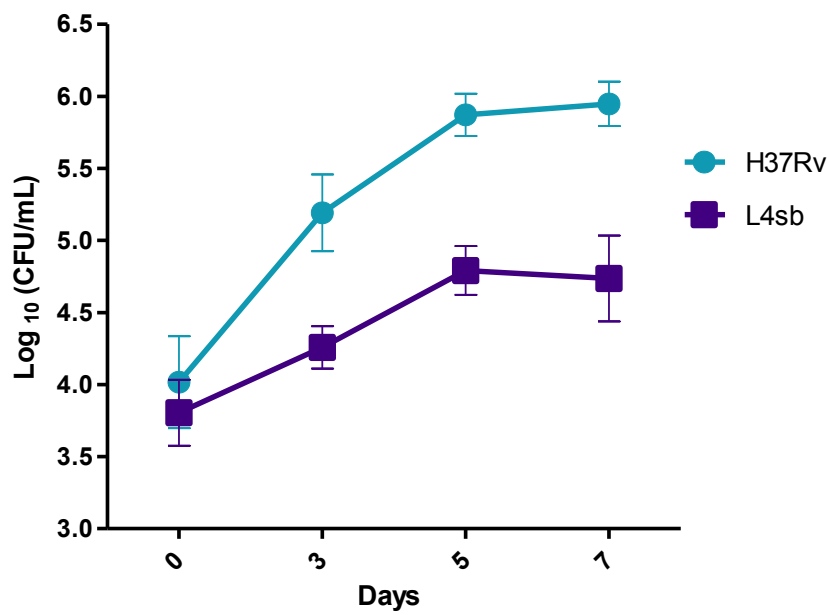
Figure 27. Replication of H37Rv wt and L4sb in MHS-infected cells. Data were expressed as $Log_{10} \pm$ SD of CFU counts per millilitre and obtained from two independent wells in three independent experiments.

In parallel with replication assays, progression of MH-S infection was studied by Ziehl-Neelsen staining (Figure 28). No phenotypical differences were observed among the strains of study: H37Rv wt, L4KO, L4c, L4S4KO, L4S4c, and L4sb.
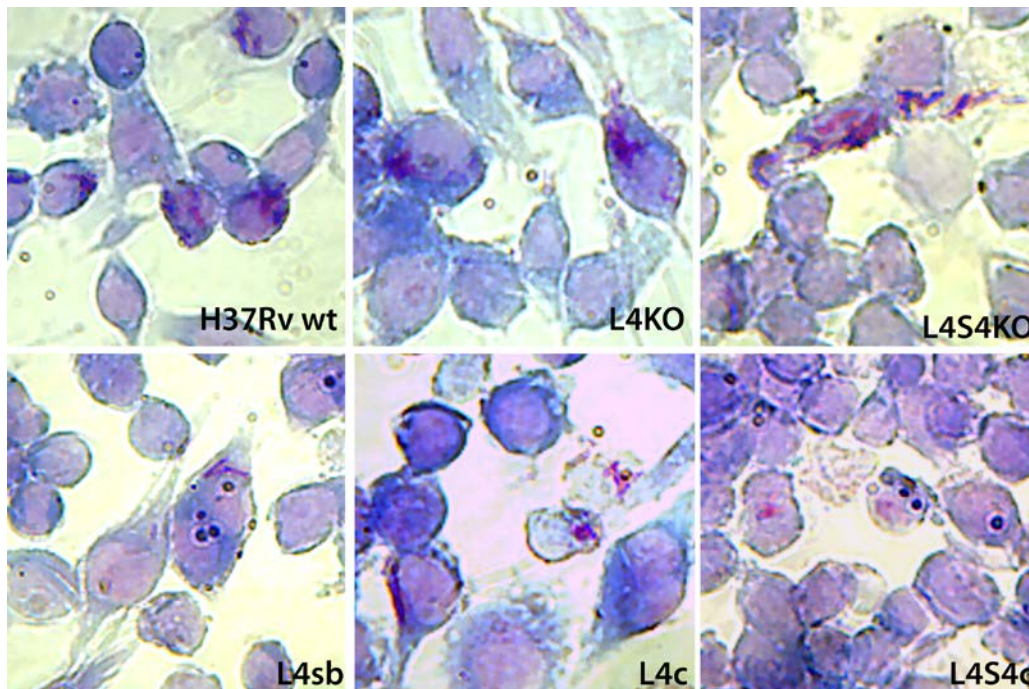
Figure 28. Ziehl-Neelsen staining of infected MH-S at MOI 1:1. Macrophages appear as violet and bacteria appear as fuchsia.

4.2.8. The L4S4KO double knockout mutant and the L4sb overexpression strain were less cytotoxic than the wild-type strain

Apoptotic induction assays were performed in MH-S cells so as to find out mycobacterial cytotoxicity. The strains tested were L4KO, L4S4KO and L4sb. H37Rv wt was the positive control of cytotoxicity and BCG the negative one. Also, non-infected MHS was the negative control of the assay to confirm the basal cell death. Two different MOI were chosen (5:1 and 10:1) in order to be able to see significant differences between controls and the tested strains. After 3 days, cell death was determined by flow cytometry.

With MOI of 5:1 and 10:1, L4S4KO showed a significant drop in cytotoxicity compared to H37Rv wt (Figure 29, green bars); in the case of the L4KO mutant, although exhibited a low decrease compared to the reference H37Rv, this was not significant. It appears that it is necessary the loss of both efflux pump components, i.e. MmpL4 and MmpS4 to exhibit an attenuated phenotype.
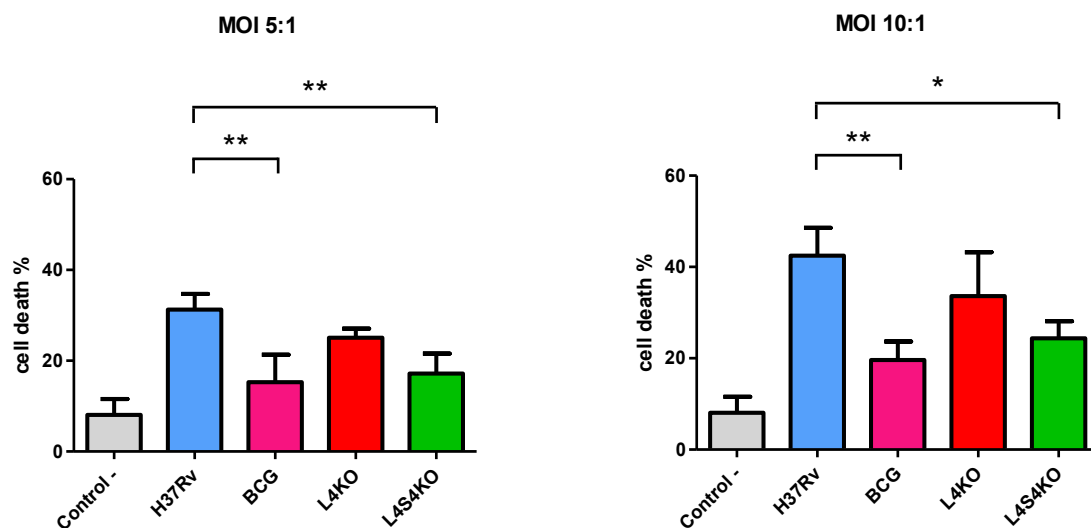
Figure 29. Cell death caused by H37Rv wt, BCG, L4KO and L4S4KO at MOI of 5:1 and 10:1 in MH-S cells. Data were expressed as percentage ± SD of cell death and obtained from three independent experiments.

Nonetheless, there is a possibility that the decrease in cytotoxicity observed in Figure 29 could be due to reduced efficiency of infection of the mutant strain, instead of a real this decrease in cytotoxicity due to the absence of both MmpL4 and MmpS4 proteins. To prove this hypothesis, mycobacteria infecting MH-S cells were recovered 4 hours post-infection and plated (Figure 30). The number of bacilli of H37Rv wt, L4KO and L4S4KO infecting MH-S cells was similar, so all of them had the same ability to infect cells. Then, we confirmed that deletion of *mmpL4/mmpS4* genes results in a lower capability of the bacillus for inducing cell death.
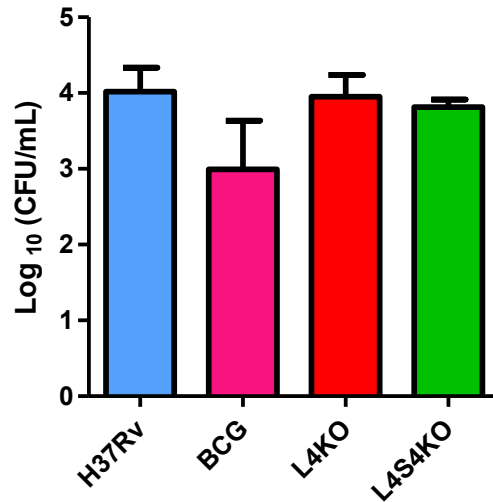
Figure 30. Number of mycobacteria infecting MH-S cells in intracellular replication assays 4 hours post-infection. Data were expressed as $Log_{10} \pm$ SD of CFU counts per millilitre and obtained from two independent wells in three independent experiments.

Regarding the overexpression strain, L4sb manifested significant reduction in cytotoxicity (Figure 31) in comparison to H37Rv wt at MOI 5:1 and 10:1. This marked fall in cytotoxicity could be related to the decrease in intracellular replication that this strain showed in MH-S cells (Figure 27, above); if a strain had intracellular growth impairment, fewer bacteria there would be inside the infected cell, and consequently, less cytotoxicity would produce. It should be pointed out that L4sb caused equal level of cell death at both MOI. This suggests that the decrease in cytotoxicity might be due to the role of MmpL4/MmpS4 rather than the amount of L4sb bacilli.
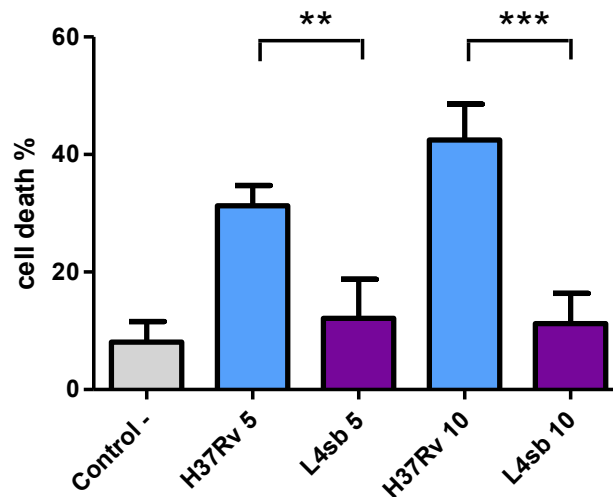
Figure 31. Cell death caused by H37Rv wt and L4sb at MOI of 5:1 and 10:1 in MH-S cells. Data were expressed as percentage ± SD of cell death and obtained from three independent experiments.

4.3. Molecular study of *M. tuberculosis* strains

4.3.1. The loss of *mmpL4* increased the expression of *mmpL5* and *mmpS5* at logarithmic phase

Firstly, the *mmpL4* expression was checked by RT-PCR in the strains of study: H37Rv wt, single mutant L4KO, its complemented strain L4c, and the overexpression strain L4sb. As might be expected, in both logarithmic and stationary phases (Figure 32), there were no amplification signal of *mmpL4* in L4KO, and *mmpL4* expression was detected in L4c at levels similar to those in the reference strain H37Rv. In addition, L4sb showed a 10–fold increase in *mmpL4* expression in stationary phase and almost a 30-fold increase in logarithmic phase of growth, in comparison with H37Rv. These results verified that all strains used for this work showed an expression level of *mmpL4* consistent with their genetic features.
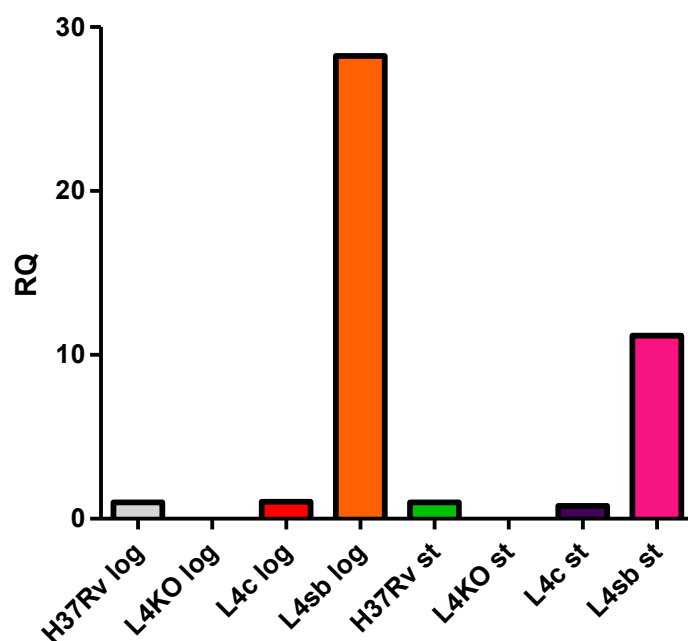
Figure 32. Relative quantification (RQ) of *mmpL4* in H37Rv wt, L4KO, L4c and L4sb strains with respect to H37Rv wt at logarithmic (log) and stationary (st) phases by qRT-PCR. The RNA levels were normalized to the levels of *sigA* mRNA. Result is a representative experiment of three independent experiments.

Then, we decided to test whether the lack of *mmpL4* had an influence on the expression of other *mmpL* and *mmpS* genes. In logarithmic phase (Figure 33, left panel), *mmpL5* and *mmpS5* expression increased about two times, whereas expression levels of the other *mmpL* and *mmpS* genes scarcely changed in L4KO strain. As MmpL5/MmpS5 and MmpL4/MmpS4 efflux systems appear to have a redundant role in siderophore export [99], it is likely that the rise in

transcriptional expression of the *mmpL5* and *mmpS5* might try to compensate for the absence of the other export system.

Although widespread changes were observed in *mmpL* and *mmpS* genes in L4KO at stationary phase, they were slight rises which were not significant. Only *mmpL6*, *mmpL9*, *mmpL10*, and *mmpL13a* expression levels increased up to two times in comparison to H37Rv wild-type. Unfortunately, out of these four proteins, just the role of MmpL10 is known, hence hampering to figure out a putative functional network connecting all these five transporters. Nevertheless, the fact that MmpL10 is involved in translocation of DAT and biosynthesis of PAT may support a similar role of MmpL4 in lipid transport. In fact, it has been demonstrated that MmpL3 transports TMM and take parts in iron metabolism as heme importer. Hence, the hypothesis of MmpL4/MmpS4 involving two different roles in Mtb is plausible. Moreover, this is supported by morphological changes exhibited in L4sb colonies which can be caused by differences in membrane lipid composition.

Concerning the complemented strain of L4KO (namely, L4c), it appears to restore *mmpL5* and *mmpS5* expression levels similar to those of H37Rv wt at logarithmic phase (Figure 33, left panel). However, L4c showed an expression pattern of all other *mmpL* and *mmpS* genes comparable to that of L4KO at stationary phase (Figure 33, right panel). It should be noted that *mmpS4* RNA level in L4c was twice as much as L4KO at logarithmic and stationary phase because the complemented strain had two copies of *mmpS4*.
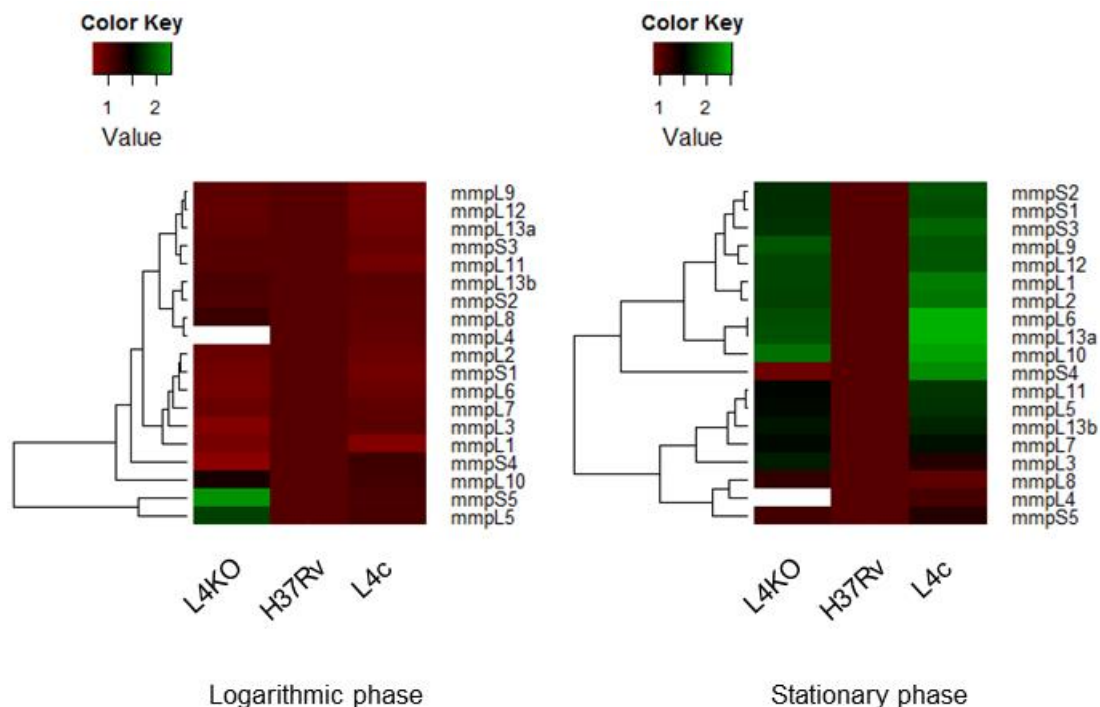
Figure 33. Relative quantification (RQ) of 13 *mmpL* genes and 5 *mmpS* genes in H37Rv wt, L4KO and L4c strains with respect to H37Rv wt at logarithmic and stationary phases by qRT-PCR. The RNA levels of *mmpL* and *mmpS* genes were normalized to the levels of *sigA* mRNA. Results were the means of three

independent experiments. Green and red colours indicate increased or decreased expression, respectively, in comparison with wt strain.

4.3.2. Main lipids of *M. tuberculosis* were not affected by the loss of *mmpL4* and *mmpS4*

There are 13 *mmpL* genes in the genome of Mtb. Currently, the role of 7 of the 13 MmpL transporters is known. As 5 of these 7 MmpL proteins (MmpL3, MmpL7, MmpL8, MmpL10, and MmpL11) are dedicated to biosynthesis and transport of mycobacterial cell wall lipids, we decided to check if MmpL4/MmpS4 efflux system was involved in lipid transport too. Besides, 2 of these 5 MmpL transporters (MmpL3 and MmpL11) also take part in iron uptake mechanism.

Four fractions of lipids were extracted from each strain (H37Rv wt, L4KO, L4c, L4S4KO, L4S4c, and L4sb): free lipids from the envelope, non-polar lipids, polar lipids, and fatty acid methyl esters (FAMEs) and mycolic acid methyl esters (MAMEs).

Each fraction was a mixture of lipids, which were resolved using thin layer chromatography (TLC) and different combinations of solvent systems. Then, TLCs were stained and the patterns of spots obtained from free, non-polar and polar lipid extracts were compared with those got by Bhatt *et al* [132] in order to identify the main lipids of Mtb. Moreover, TLC containing FAMEs and MAMEs was compared to that obtained by Belardinelli *et al* [133]. However, no significant changes were seen in the patterns of lipids from any fraction (Annex I). Possibly, the use of other techniques such as mass spectrometry, which can quantify lipid content more accurately than TLC, could reveal subtle differences between fractions from different strains that could not be detected by using TLC.

4.3.3. The loss of *mmpL4* and *mmpS4* activated lipid metabolism

Finally, we decided to analyse the proteome of H37Rv wt, L4KO, L4c, L4S4KO, L4S4c and L4sb as an alternative approach to investigate whether MmpL4/MmpS4 efflux system was really involved in lipid metabolism.

For this purpose, cellular proteins of each strain of study expressed at stationary phase were separated by 2D-PAGE (two-dimensional polyacrylamide gel electrophoresis). Once the gels were scanned, SameSpots software was utilized for a differential gel analysis. To start with the study, three groups of strains were created: H37Rv vs L4KO vs L4c, H37Rv vs L4S4KO vs L4S4c, and H37Rv vs L4sb. For the first two groups, spot intensity differences were statistically analysed by one-way ANOVA with the post hoc Tukey's test to establish significant differences among group means. For the third group, spot intensity differences were examined by Student's t-test. Afterwards, the False Discovery Rate (FDR) procedure was used to detect false positives derived from multiple testing. Unfortunately, for all the spots with $p < 0.05$ their q value was

>0.05, which means that there were no statistically significant changes in the expression of none of the proteins. Statistical analysis was carried out using the data obtained from 3 different sets of independent biological samples.

However, despite the fact that the overall results were not statistically significant, we considered that there were a few proteins whose abundance changed moderately from one strain to another, and this could be easily identified even by the naked eye, so we speculated whether they might be biologically relevant. Then, we decided to be more demanding and restrictive and select those spots with $p < 0.01$ to be excised and trypsin digested. Five proteins were then identified (Figure 34) with the search engine Mascot using SwissProt and UnitProt databases.
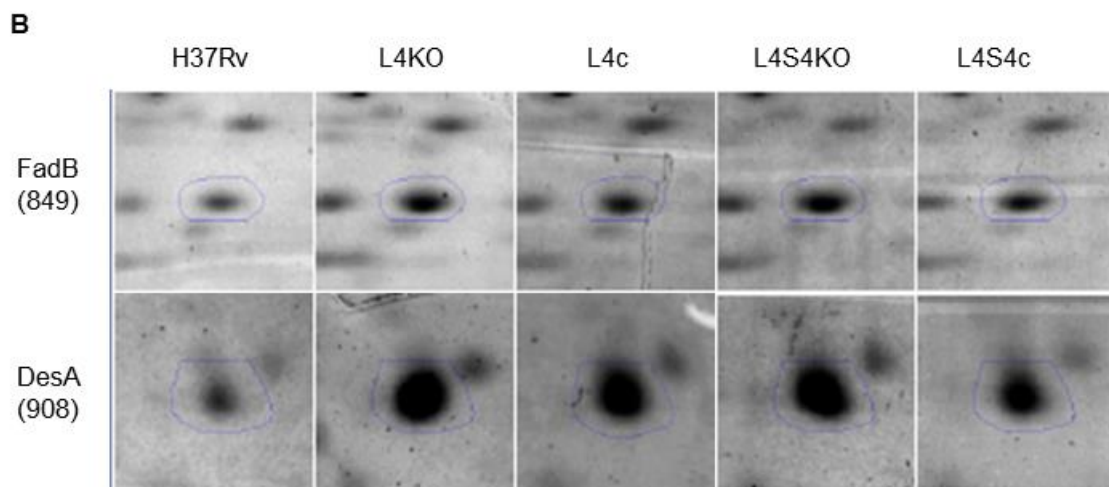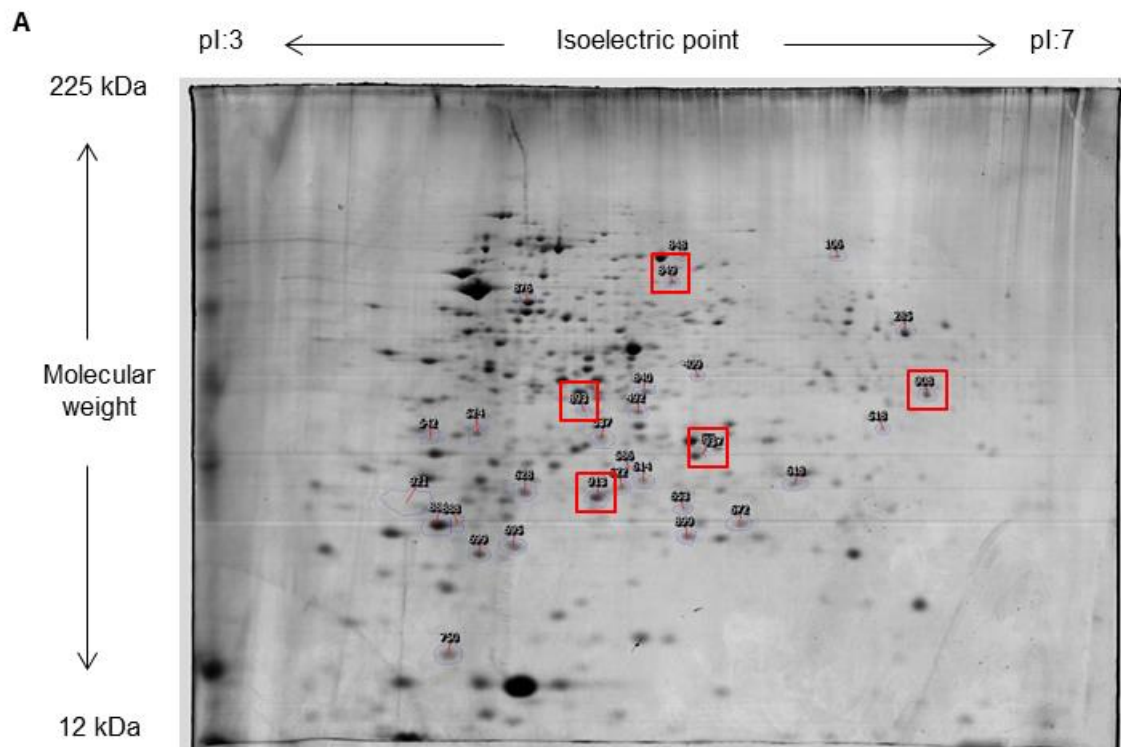
Figure 34. 2D-PAGE analysis of changes in the proteome of *Mycobacterium tuberculosis* strains. (A) Representative Coomassie-stained 2D-PAGE gel image of L4S4c strain showing spots with $p<0.05$ numbered according to pI and Mw. The numbered protein spots marked with squares 849 (FadB), 893 (OpcA), 908 (DesA), 913 (Rv0148), and 937 (SucD) were the differentially abundant proteins with $p<0.01$. (B) 2D-PAGE comparison of up-regulated spots 849 and 908.

The identified proteins were classified according to functional category using TubercuList database [23]. 3 of these 5 proteins (Table 25) were related to intermediary metabolism and respiration, and 2 of them were involved in lipid metabolism.

Table 25. Identified proteins with $p<0.01$.

Spot	Protein name	Gene name	Rv number	Functional category
849	3-hydroxyacyl-CoA dehydrogenase FadB	*fadB*	Rv0860	Lipid metabolism
893	Oxidoreductase OpcA	*opcA*	Rv1446c	Intermediary metabolism and respiration
908	Acyl-[acyl-carrier protein] desaturase DesA1	*desA1*	Rv0824c	Lipid metabolism
913	Probable short-chain type dehydrogenase/reductase	*rv0148*	Rv0148	Intermediary metabolism and respiration
937	Succinyl-CoA synthetase SucD	*sucD*	Rv0952	Intermediary metabolism and respiration

Interestingly, the proteins involved in lipid metabolism increased their expression in both knockouts (and their complemented strains) more than twice (Table 26) with respect to the reference strain. On the other hand, those related to intermediary metabolism and respiration showed slight decrease in their expression in L4S4KO, L4S4c, and L4c compared with H37Rv wt.

Table 26. Fold changes of the identified proteins with p<0.01 in the strains of study.

Spot	Protein name	Rv number	L4KO		L4c		L4S4KO		L4S4c	
			+/-	FC	+/-	FC	+/-	FC	+/-	FC
849	3-hydroxyacyl-CoA dehydrogenase FadB	Rv0860	+	2.4	+	2.1	+	2.7	+	2.1
893	Oxidoreductase OpcA	Rv1446c			-	1.2	-	1.1	-	1.2
908	Acyl-[acyl-carrier protein] desaturase DesA1	Rv0824c	+	2.2	+	1.9	+	2.7	+	2.2
913	Probable short-chain type dehydrogenase/ reductase	Rv0148					-	1.4	-	1.1
937	Succinyl-CoA synthetase SucD	Rv0952			-	1.2				

Abbreviations: FC (Fold change).

+/-: + means this protein was overexpressed in this strain in comparison to the reference strain H37Rv.

   - means this protein was less expressed in this strain than in H37Rv wt.

Regarding L4sb, three proteins (Table 27) only exhibited certain change in their expression (p<0.05) in comparison to H37Rv wt. Again, there were proteins related to the functional categories lipid metabolism, and intermediary metabolism and respiration.

Table 27. Identified proteins with p<0.05 in the overexpression strain L4sb.

Spot	Protein name	Gene name	Rv number	Functional category	+/-	FC
285	Probable 3-ketoacyl-ACP reductase FabG4	*fabG4*	Rv0242c	Lipid metabolism	+	1.3
622	Flavodoxin	*rv0925c*	Rv0925c	Intermediary metabolism and respiration	-	1.3
876	60 kDa chaperonin 1 GroEL1	*groEL1*	Rv3417c	Virulence, detoxification, adaptation	-	1.3

Abbreviations: FC (Fold change).

+/-: + means this protein was overexpressed in this strain in comparison to the reference strain H37Rv.

   - means this protein was less expressed in this strain than in H37Rv wt.

Concerning culture filtrate proteins, it was not possible to carry out the statistical analysis since the number of sets was insufficient.

To sum up, although the statistical analysis revealed that protein expression differences among the strains were not significant, both the fold change and the strains suffering those changes were consistent and sound. For example, in the instance of FadB, this protein showed differential expression in L4KO, L4c, L4S4KO, and L4S4c in comparison to the reference strain. Avoiding the complemented strains due to their apparent lack of complementation, FadB expression increased not only in the single knockout mutant but also in the double. Besides FadB, DesA1 and other spots in the Annex II support the fact that the expression of these proteins has changed owing to the absence of MmpL4 and MmpS4. Consequently, these proteins with altered expression have biological relevance. Interestingly, all the proteins in the functional category of lipid metabolism were related to a specific class of lipid: fatty acids.

In conclusion, taking into account that most of the identified proteins have a connection with fatty acids, we suggest that MmpL4/MmpS4 efflux pump is clearly involved in lipid metabolism.

4.4. Generation of *M. bovis* BCG strains for the study of the efflux pumps MmpL4 and MmpS4

4.4.1. Construction of *M. bovis* knockout mutants

M. bovis BCG has got genes identical to *mmpL4* and *mmpS4*, so we decided to inactivate them as well, in a similar manner to those in *M. tuberculosis*. The reason for constructing *M. bovis* BCG knockout mutants was to carry out lipid analysis complementary to those made with the *M. tuberculosis* mutants (section 4.3.2), including radioactive analyses that are more sensitive and easier to do in a BSL-2 laboratory.

Basically, the construction of *M. bovis* BCG knockout mutants delected in BCG_0489c (BCG L4KO), in BCG_0490c (BCG S4KO), in both BCG_0489c and BCG_0490c (BCG L4S4KO) was performed using the method of specialised transduction developed by Bardarov *et al* [27]. Briefly, phΔL4, phΔS4 and phΔL4S4 recombinant phages were designed to replace *mmpL4*, *mmpS4* and *mmpL4-mmpS4* in *M. bovis* BCG wt, respectively. These temperature sensitive phages included a hygromycin resistance marker interrupting each target genes. Transductants were selected at the non-permissive temperature of 37ºC on selective plates containing 150µg/ml hygromycin.

4.4.2. Generation of the overexpression *M. bovis* BCG L4sb strain

Considering that sequences of *rv0450c* and *rv0451c* are the same as BCG_0489c and BCG_0490c, the replicative plasmid pRBZ13 used to generate Mtb H37Rv L4sb strain was utilized to construct *M. bovis* BCG L4sb strain. After transformation of pRBZ13 in BCG wt, the resulting strain was verified by PCR using RP-180 and mmpL4-2f primers.

4.5. Comparative lipid analysis of *M. bovis* BCG wt and *M. bovis* BCG overexpressing *mmpL4* and *mmpS4*

4.5.1. The overexpression of *mmpL4* and *mmpS4* caused a decrease in PDIM production in *M. bovis* BCG

Three extracts were obtained from both BCG wt and BCG L4sb strains: free lipids from the envelope, non-polar and polar lipids. In order to identify individual lipid components within these extracts, radiolabeled lipids were subjected to 2D-TLC analysis using solvent systems of increasing polarity. Then, TLCs were developed and the patterns of spots obtained from free, non-polar and polar lipid extracts were compared with those got by Pirson *et al* [134] so as to identify the main lipids of *M. bovis* BCG.

Analysis of the free (Figure 35A) and non-polar lipids (Figure 35B) using the least polar TLC system identified the presence of phthiocerol dimycocerosates (PDIMs), and triacyl glycerol (TAG), which were quantified. Interestingly, the amount of PDIMs showed a strong decrease in BCG L4sb in comparison with the reference strain in both extracts. At the same time, several other spots located in the lower part of the TLC increased greatly, and another spot appeared next to one of the PDIM spots in BCG L4sb in the free lipid extract. It should be pointed out that this group of overproduced lipids were located not only inside the bacterium but also in its envelope, suggesting that these lipids were transported across the membrane.

Based on these results, our hypothesis is that MmpL4 and MmpS4 might be involved in the biosynthesis/transport of a precursor of PDIM in BCG. In other words, we believe that the overexpression of MmpL4/MmpS4 efflux system decreases the availability of a precursor of PDIM because this precursor biomolecule would be now more demanded in other pathway to synthesize one or several different lipids, according to the results of the TLCs.
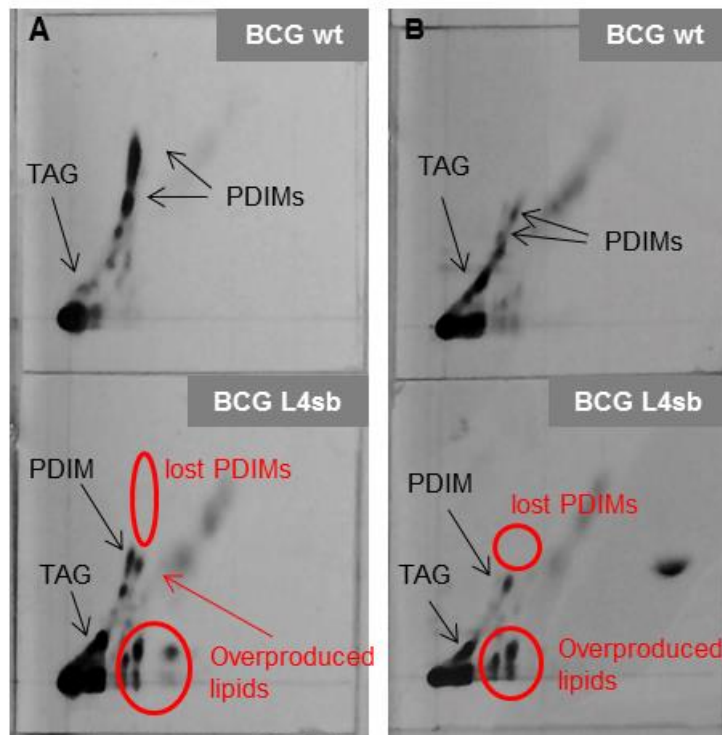
Figure 35. 2D-TLC analysis of lipids from BCG wt and BCG L4sb using system A. (A) Free lipids extract. (B) Non-polar lipids extract.

However, no significant changes were seen neither in the rest of the lipids from free-lipid and non-polar extracts nor in the patterns of lipids from the polar fraction (Annex III).

4.6. Comparative morphological analysis of *M. bovis* BCG wt and *M. bovis* BCG L4sb colonies

4.6.1. BCG L4sb showed slight modification in its colony morphology

Considering morphological changes observed in H37Rv L4sb (section 4.2.3), a culture of BCG L4sb was plated in order to verify if the same changes took place in the BCG strain. The morphology of BCG L4sb was compared with BCG wt and MmpL3 BCG overexpression strain (BCG L3sb) so as to check if the differences were due to an increment of membrane proteins or the effect of MmpL4 and MmpS4 proteins themselves.

Slighter changes in colony morphology appeared in BCG L4sb in comparison with H37Rv L4sb (Figure 36) when they were compared to their respective wild types. The minor morphological changes in BCG L4sb could be explained because BCG wt had already lost several membrane proteins and lipids during the process of attenuation for getting the tuberculosis vaccine, which affected its colony morphology. As a consequence, the overexpression of MmpL4 and MmpS4 could have little effect on its morphology. No differences were observed in BCG L3sb colonies.

Therefore, it is likely that slight changes observed in BCG L4sb were due to the effect of the efflux system MmpL4/MmpS4.

Figure 36. Colonies of *M. bovis* BCG parental (wt), BCG overexpressing *mmpL4* and *mmpS4* (BCG L4sb), and BCG overexpressing *mmpL3* (BCG L3sb) strains on 7H11 plates after incubation at 37ºC for 3 weeks.

4.6.2. BCG L4sb hardly grew on plates with Tween-80 detergent

Interestingly, BCG L4sb had impaired growth when Tween-80 was present in the solid culture medium (Figure 37), whereas BCG wt and BCG L3sb grew without problems in the same medium. Also, H37Rv L4sb showed the same inability to growth on plates containing Tween-80, similarly to BCG L4sb. Thus, overexpression of MmpL4 and MmpS4 in mycobacteria results in increased toxicity of Tween-80. In other words, the MmpL4/MmpS4 efflux system would have an additional role to that in siderophore transport, making mycobacteria more susceptible to Tween-80 detergent.

Figure 37. Colonies of *M. bovis* BCG parental (wt), BCG overexpressing *mmpL4* and *mmpS4* (BCG L4sb), and BCG overexpressing *mmpL3* (BCG L3sb) strains on 7H11 plates with Tween-80 after incubation at 37ºC for 3 weeks.

5. **Future perspectives**

During this PhD thesis, the role of the MmpL4/MmpS4 efflux system in mycobacteria has been investigated, and some interesting insights have been obtained. Simultaneously, new questions have arisen, which will be addressed in the near future.

The morphological changes in colony aspect related to MmpL4/MmpS4 overexpression in *M. tuberculosis* will be further investigated. It is likely that compensatory mutations could be responsible for this alteration, so first, whole genome of smooth and rough variants will be investigated. Once genomic DNAs have been sequenced, the obtained short DNA sequence reads will be aligned to the reference H37Rv wt sequence. Afterwards, single nucleotide polymorphisms (SNPs) in smooth and rough L4sb strains will be searched and analysed their potential involvement with the observed colony morphology changes in the overexpression strains.

In order to confirm the involvement of MmpL4/MmpS4 in lipid metabolism, it will be necessary to check by qRT-PCR the expression levels of those genes encoding proteins related to fatty acids that have been identified by proteomics. For this purpose, new cultures of the strains of study will be grow in Middlebrook 7H9 supplemented with 0.2% dextrose and 0.085% NaCl (the same medium used for protein extraction) so as to extract their RNA at stationary phase. It is important to grow the strains in the same medium in which proteins have been extracted since differences in both media would make impossible to compare the results obtained.

The construction of knock-out mutants BCG L4KO, BCG S4KO, and BCG L4S4KO will be confirmed by PCR and southern blot before analysing their lipid content. In addition, BCG L4sb lipid profile will be analysed by mass spectrometry to discover its likely implication in PDIM production.

6. **Conclusions**

- The MmpL4 and MmpS4 efflux pumps of *M. tuberculosis* are not involved in intrinsic resistance to the drugs and compounds that have been assayed.

- The MmpL4/MmpS4 efflux system is active in transporting ethidium bromide.

- Deletion of MmpL4/MmpS4 efflux system does not result in a growth defect of *M. tuberculosis* in iron-depleted media, concluding that its role in siderophore transport is redundant with that of MmpL5/MmpS5 efflux system.

- The loss of *mmpL4* alters genes related to siderophore export (*mmpL5* and *mmpS5*) and lipid biosynthesis and transport (*mmpL10*) suggesting MmpL4/MmpS4 efflux system probably plays both roles in *M. tuberculosis*.

- The overexpression of the MmpL4/MmpS4 efflux system in *M. tuberculosis* caused a morphological change in its colonies, a decrease in its *in vitro* growth rate, and an alteration in its membrane permeability suggesting that these proteins have an influence in the mycobacterial membrane composition.

- The MmpL4 and MmpS4 efflux pumps are necessary for the complete virulence of *M. tuberculosis* in infecting macrophages.

- Main lipids of *M. tuberculosis* were not affected by the deletion of *mmpL4* and *mmpS4* genes.

- Proteomic data suggests that the lack of MmpL4 and MmpS4 proteins increased the fatty acid metabolism in *M. tuberculosis*.

- The overexpression of MmpL4/MmpS4 efflux system appears to change the PDIM production in *M. bovis*.

Conclusiones

- Las bombas de eflujo MmpL4 y MmpS4 de *M. tuberculosis* no están implicadas en la resistencia intrínseca a los fármacos y compuestos que se han ensayado.

- El sistema de eflujo MmpL4/MmpS4 transporta bromuro de etidio.

- La deleción del sistema de eflujo MmpL4/MmpS4 no produce ningún defecto en el crecimiento de *M. tuberculosis* en medios con escasa concentración de hierro debido a la función redundante que posee este sistema y el sistema de eflujo MmpL5/MmpS5 en el transporte de sideróforos.

- La pérdida de *mmpL4* altera la expresión de genes relacionados con el transporte de sideróforos (*mmpL5* y *mmpS5*) y la biosíntesis y transporte de lípidos (*mmpL10*), sugiriendo que el sistema de eflujo MmpL4/MmpS4 probablemente desempeñe ambas funciones en *M. tuberculosis*.

- La sobreexpresión del sistema de eflujo MmpL4/MmpS4 en *M. tuberculosis* causa cambios en la morfología de sus colonias, disminuye su velocidad de crecimiento *in vitro* y altera la permeabilidad de su membrana, lo cual indica que estas proteínas influyen en la composición de la membrana micobacteriana.

- Las bombas de eflujo MmpL4 y MmpS4 son necesarias para la completa virulencia de *M. tuberculosis* cuando infecta macrófagos.

- Los principales lípidos de *M. tuberculosis* no se ven afectados por la deleción de los genes *mmpL4* y *mmpS4*.

- Los datos de proteómica sugieren que la pérdida de las proteínas MmpL4 y MmpS4 incrementa el metabolismo de ácidos grasos en *M. tuberculosis.*

- La sobreexpresión del sistema de eflujo MmpL4/MmpS4 parece influir en la producción de PDIM en *M. bovis*.

7. References

1. Nerlich, A.G. and S. Losch, *Paleopathology of human tuberculosis and the potential role of climate.* Interdiscip Perspect Infect Dis, 2009. **2009**: p. 437187.
2. Comas, I., et al., *Out-of-Africa migration and Neolithic coexpansion of Mycobacterium tuberculosis with modern humans.* Nat Genet, 2013. **45**(10): p. 1176-82.
3. Supply, P., et al., *Genomic analysis of smooth tubercle bacilli provides insights into ancestry and pathoadaptation of Mycobacterium tuberculosis.* Nat Genet, 2013. **45**(2): p. 172-9.
4. Gagneux, S., *Host-pathogen coevolution in human tuberculosis.* Philos Trans R Soc Lond B Biol Sci, 2012. **367**(1590): p. 850-9.
5. WHO, *Global tuberculosis report 2014. World Health Organization.* 2014.
6. Kernodle, D.S., *Decrease in the effectiveness of Bacille Calmette-Guerin vaccine against pulmonary tuberculosis: a consequence of increased immune suppression by microbial antioxidants, not overattenuation.* Clin Infect Dis, 2010. **51**(2): p. 177-84.
7. CDC. *Diagnosis of Tuberculosis Disease. Centers for Disease Control and Prevention.* 2011; Available from: http://www.cdc.gov/tb/publications/factsheets/testing/diagnosis.htm.
8. Babady, N.E. and N.L. Wengenack, *Clinical Laboratory Diagnostics for Mycobacterium tuberculosis. Chapter 1.*, P.-J. Cardona, Editor. 2012.
9. Clayden, P., et al., *2014 Pipeline Report. HIV, Hepatitis C Virus (HCV), and Tuberculosis (TB) drugs, diagnostics, vaccines, preventive technologies, research toward a cure, and immune-based and gene therapies in development.*, A. Benzacar, Editor. 2014.
10. Zumla, A., P. Nahid, and S.T. Cole, *Advances in the development of new tuberculosis drugs and treatment regimens.* Nat Rev Drug Discov, 2013. **12**(5): p. 388-404.
11. WHO/IUATLD, *Anti-tuberculosis drug resistance in the world. Report nº2. Prevalence and Trends.* 2000. 253.
12. Cohen, K.A., W.R. Bishai, and A.S. Pym, *Molecular basis of drug resistance in Mycobacterium tuberculosis.* Microbiology Spectrum, 2014. **2**(3).
13. Almeida Da Silva, P.E. and J.C. Palomino, *Molecular basis and mechanisms of drug resistance in Mycobacterium tuberculosis: classical and new drugs.* J Antimicrob Chemother, 2011. **66**(7): p. 1417-30.
14. Gandhi, N.R., et al., *Extensively drug-resistant tuberculosis as a cause of death in patients co-infected with tuberculosis and HIV in a rural area of South Africa.* Lancet, 2006. **368**(9547): p. 1575-80.
15. Dheda, K., et al., *Global control of tuberculosis: from extensively drug-resistant to untreatable tuberculosis.* Lancet Respir Med, 2014. **2**(4): p. 321-38.
16. WGONTD. *Working Group on New TB Drugs.* 2015; Available from: http://www.newtbdrugs.org/.
17. Stackebrandt, E., F. A. Riney, and N.L. Ward-Rainey, *Proposal for a New Hierarchic classification System, Actinobacteria classis now.* International Journal of Systematic Bacteriology, 1997. **47**: p. 479-491.
18. Trifiro, S., et al., *Ghost mycobacteria on Gram stain.* J Clin Microbiol, 1990. **28**(1): p. 146-7.
19. Bifani, P., et al., *Molecular characterization of Mycobacterium tuberculosis H37Rv/Ra variants: distinguishing the mycobacterial laboratory strain.* J Clin Microbiol, 2000. **38**(9): p. 3200-4.

20. Cole, S.T., et al., *Deciphering the biology of Mycobacterium tuberculosis from the complete genome sequence.* Nature, 1998. **393**(6685): p. 537-44.

21. Camus, J.C., et al., *Re-annotation of the genome sequence of Mycobacterium tuberculosis H37Rv.* Microbiology, 2002. **148**(Pt 10): p. 2967-73.

22. Lew, J.M., et al., *TubercuList--10 years after.* Tuberculosis (Edinb), 2010. **91**(1): p. 1-7.

23. Cole, S.T. *Tuberculist.* 2013 March 2013; Available from: http://tuberculist.epfl.ch/.

24. Sayes, F., et al., *Strong immunogenicity and cross-reactivity of Mycobacterium tuberculosis ESX-5 type VII secretion: encoded PE-PPE proteins predicts vaccine potential.* Cell Host Microbe, 2012. **11**(4): p. 352-63.

25. Ekiert, D.C. and J.S. Cox, *Structure of a PE-PPE-EspG complex from Mycobacterium tuberculosis reveals molecular specificity of ESX protein secretion.* Proc Natl Acad Sci U S A, 2014. **111**(41): p. 14758-63.

26. Parish, T. and N.G. Stoker, *Use of a flexible cassette method to generate a double unmarked Mycobacterium tuberculosis tlyA plcABC mutant by gene replacement.* Microbiology, 2000. **146 (Pt 8)**: p. 1969-75.

27. Bardarov, S., et al., *Specialized transduction: an efficient method for generating marked and unmarked targeted gene disruptions in Mycobacterium tuberculosis, M. bovis BCG and M. smegmatis.* Microbiology, 2002. **148**(Pt 10): p. 3007-17.

28. van Kessel, J.C. and G.F. Hatfull, *Mycobacterial recombineering.* Methods Mol Biol, 2008. **435**: p. 203-15.

29. Hoffmann, C., et al., *Disclosure of the mycobacterial outer membrane: cryo-electron tomography and vitreous sections reveal the lipid bilayer structure.* Proc Natl Acad Sci U S A, 2008. **105**(10): p. 3963-7.

30. Zuber, B., et al., *Direct visualization of the outer membrane of mycobacteria and corynebacteria in their native state.* J Bacteriol, 2008. **190**(16): p. 5672-80.

31. Groenewald, W., et al., *Differential spontaneous folding of mycolic acids from Mycobacterium tuberculosis.* Chem Phys Lipids, 2014. **180**: p. 15-22.

32. Lemassu, A., et al., *Extracellular and surface-exposed polysaccharides of non-tuberculous mycobacteria.* Microbiology, 1996. **142 (Pt 6)**: p. 1513-20.

33. Sani, M., et al., *Direct visualization by cryo-EM of the mycobacterial capsular layer: a labile structure containing ESX-1-secreted proteins.* PLoS Pathog, 2010. **6**(3): p. e1000794.

34. Ouellet, H., J.B. Johnston, and P.R. de Montellano, *Cholesterol catabolism as a therapeutic target in Mycobacterium tuberculosis.* Trends Microbiol, 2011. **19**(11): p. 530-9.

35. Lopez-Marin, L.M., *Nonprotein structures from mycobacteria: emerging actors for tuberculosis control.* Clin Dev Immunol, 2012. **2012**: p. 917860.

36. Hossain, M.M. and M.N. Norazmi, *Pattern recognition receptors and cytokines in Mycobacterium tuberculosis infection--the double-edged sword?* Biomed Res Int, 2013. **2013**: p. 179174.

37. Killick, K.E., et al., *Receptor-mediated recognition of mycobacterial pathogens.* Cell Microbiol, 2013. **15**(9): p. 1484-95.

38. Ehlers, S. and U.E. Schaible, *The granuloma in tuberculosis: dynamics of a host-pathogen collusion.* Front Immunol, 2013. **3**: p. 411.

39. Guirado, E. and L.S. Schlesinger, *Modeling the Mycobacterium tuberculosis Granuloma - the Critical Battlefield in Host Immunity and Disease.* Front Immunol, 2013. **4**: p. 98.

40. Russell, D.G., et al., *Mycobacterium tuberculosis wears what it eats.* Cell Host Microbe, 2010. **8**(1): p. 68-76.

41. Paulson, T., *Epidemiology: A mortal foe.* Nature, 2013. **502**(7470): p. S2-3.

42. Flannagan, R.S., G. Cosio, and S. Grinstein, *Antimicrobial mechanisms of phagocytes and bacterial evasion strategies.* Nat Rev Microbiol, 2009. **7**(5): p. 355-66.

43. Wang, J. and M.A. Behr, *Building a better bacillus: the emergence of Mycobacterium tuberculosis.* Front Microbiol, 2014. **5**: p. 139.

44. Behar, S.M., M. Divangahi, and H.G. Remold, *Evasion of innate immunity by Mycobacterium tuberculosis: is death an exit strategy?* Nat Rev Microbiol, 2010. **8**(9): p. 668-74.

45. Sun, J., et al., *Mycobacterial nucleoside diphosphate kinase blocks phagosome maturation in murine RAW 264.7 macrophages.* PLoS One, 2010. **5**(1): p. e8769.

46. Russell, D.G., *Mycobacterium tuberculosis and the intimate discourse of a chronic infection.* Immunol Rev, 2011. **240**(1): p. 252-68.

47. Vergne, I., et al., *Mechanism of phagolysosome biogenesis block by viable Mycobacterium tuberculosis.* Proc Natl Acad Sci U S A, 2005. **102**(11): p. 4033-8.

48. Ehrt, S. and D. Schnappinger, *Mycobacterial survival strategies in the phagosome: defence against host stresses.* Cell Microbiol, 2009. **11**(8): p. 1170-8.

49. Forrellad, M.A., et al., *Virulence factors of the Mycobacterium tuberculosis complex.* Virulence, 2012. **4**(1): p. 3-66.

50. McKinney, J.D., et al., *Persistence of Mycobacterium tuberculosis in macrophages and mice requires the glyoxylate shunt enzyme isocitrate lyase.* Nature, 2000. **406**(6797): p. 735-8.

51. Camacho, L.R., et al., *Identification of a virulence gene cluster of Mycobacterium tuberculosis by signature-tagged transposon mutagenesis.* Mol Microbiol, 1999. **34**(2): p. 257-67.

52. Zhang, M., et al., *Expression and characterization of the carboxyl esterase Rv3487c from Mycobacterium tuberculosis.* Protein Expr Purif, 2005. **42**(1): p. 59-66.

53. Raynaud, C., et al., *Phospholipases C are involved in the virulence of Mycobacterium tuberculosis.* Mol Microbiol, 2002. **45**(1): p. 203-17.

54. Bretl, D.J., C. Demetriadou, and T.C. Zahrt, *Adaptation to environmental stimuli within the host: two-component signal transduction systems of Mycobacterium tuberculosis.* Microbiol Mol Biol Rev, 2011. **75**(4): p. 566-82.

55. Parish, T., et al., *Deletion of two-component regulatory systems increases the virulence of Mycobacterium tuberculosis.* Infect Immun, 2003. **71**(3): p. 1134-40.

56. Meher, A.K., et al., *Analysis of complex formation and immune response of CFP-10 and ESAT-6 mutants.* Vaccine, 2007. **25**(32): p. 6098-106.

57. Copenhaver, R.H., et al., *A mutant of Mycobacterium tuberculosis H37Rv that lacks expression of antigen 85A is attenuated in mice but retains vaccinogenic potential.* Infect Immun, 2004. **72**(12): p. 7084-95.

58. Mishra, A.K., et al., *Lipoarabinomannan and related glycoconjugates: structure, biogenesis and role in Mycobacterium tuberculosis physiology and host-pathogen interaction.* FEMS Microbiol Rev, 2011. **35**(6): p. 1126-57.

59. Li, X.Z. and H. Nikaido, *Efflux-mediated drug resistance in bacteria: an update.* Drugs, 2009. **69**(12): p. 1555-623.

60. Kwon, H.H., H. Tomioka, and H. Saito, *Distribution and characterization of beta-lactamases of mycobacteria and related organisms.* Tuber Lung Dis, 1995. **76**(2): p. 141-8.

61. Burian, J., et al., *The mycobacterial antibiotic resistance determinant WhiB7 acts as a transcriptional activator by binding the primary sigma factor SigA (RpoV).* Nucleic Acids Res, 2013. **41**(22): p. 10062-76.

62. Ainsa, J.A., et al., *Molecular cloning and characterization of Tap, a putative multidrug efflux pump present in Mycobacterium fortuitum and Mycobacterium tuberculosis.* J Bacteriol, 1998. **180**(22): p. 5836-43.

63. Rodrigues, L., et al., *Contribution of efflux activity to isoniazid resistance in the Mycobacterium tuberculosis complex.* Infect Genet Evol, 2011. **12**(4): p. 695-700.

64.   Siddiqi, N., et al., *Mycobacterium tuberculosis isolate with a distinct genomic identity overexpresses a tap-like efflux pump.* Infection, 2004. **32**(2): p. 109-11.

65.   Reeves, A.Z., et al., *Aminoglycoside cross-resistance in Mycobacterium tuberculosis due to mutations in the 5' untranslated region of whiB7.* Antimicrob Agents Chemother, 2013. **57**(4): p. 1857-65.

66.   Bianco, M.V., et al., *Role of P27 -P55 operon from Mycobacterium tuberculosis in the resistance to toxic compounds.* BMC Infect Dis, 2011. **11**: p. 195.

67.   Ramon-Garcia, S., et al., *Role of the Mycobacterium tuberculosis P55 efflux pump in intrinsic drug resistance, oxidative stress responses, and growth.* Antimicrob Agents Chemother, 2009. **53**(9): p. 3675-82.

68.   Ramon-Garcia, S., et al., *Contribution of the Rv2333c efflux pump (the Stp protein) from Mycobacterium tuberculosis to intrinsic antibiotic resistance in Mycobacterium bovis BCG.* J Antimicrob Chemother, 2007. **59**(3): p. 544-7.

69.   De Rossi, E., et al., *The multidrug transporters belonging to major facilitator superfamily in Mycobacterium tuberculosis.* Mol Med, 2002. **8**(11): p. 714-24.

70.   Gupta, A.K., et al., *jefA (Rv2459), a drug efflux gene in Mycobacterium tuberculosis confers resistance to isoniazid & ethambutol.* Indian J Med Res, 2010. **132**: p. 176-88.

71.   Wilson, M., et al., *Exploring drug-induced alterations in gene expression in Mycobacterium tuberculosis by microarray hybridization.* Proc Natl Acad Sci U S A, 1999. **96**(22): p. 12833-8.

72.   Choudhuri, B.S., et al., *Overexpression and functional characterization of an ABC (ATP-binding cassette) transporter encoded by the genes drrA and drrB of Mycobacterium tuberculosis.* Biochem J, 2002. **367**(Pt 1): p. 279-85.

73.   Pasca, M.R., et al., *Rv2686c-Rv2687c-Rv2688c, an ABC fluoroquinolone efflux pump in Mycobacterium tuberculosis.* Antimicrob Agents Chemother, 2004. **48**(8): p. 3175-8.

74.   Wang, K., et al., *The expression of ABC efflux pump, Rv1217c-Rv1218c, and its association with multidrug resistance of Mycobacterium tuberculosis in China.* Curr Microbiol, 2012. **66**(3): p. 222-6.

75.   Rodrigues, L., et al., *Role of the Mmr efflux pump in drug resistance in Mycobacterium tuberculosis.* Antimicrob Agents Chemother, 2012. **57**(2): p. 751-7.

76.   Pasca, M.R., et al., *mmpL7 gene of Mycobacterium tuberculosis is responsible for isoniazid efflux in Mycobacterium smegmatis.* Antimicrob Agents Chemother, 2005. **49**(11): p. 4775-7.

77.   Andries, K., et al., *Acquired resistance of Mycobacterium tuberculosis to bedaquiline.* PLoS One, 2014. **9**(7): p. e102135.

78.   Hartkoorn, R.C., S. Uplekar, and S.T. Cole, *Cross-resistance between clofazimine and bedaquiline through upregulation of MmpL5 in Mycobacterium tuberculosis.* Antimicrob Agents Chemother, 2014. **58**(5): p. 2979-81.

79.   Milano, A., et al., *Azole resistance in Mycobacterium tuberculosis is mediated by the MmpS5-MmpL5 efflux system.* Tuberculosis (Edinb), 2009. **89**(1): p. 84-90.

80.   Szumowski, J.D., et al., *Antimicrobial efflux pumps and Mycobacterium tuberculosis drug tolerance: evolutionary considerations.* Curr Top Microbiol Immunol, 2012. **374**: p. 81-108.

81.   Adams, K.N., et al., *Drug tolerance in replicating mycobacteria mediated by a macrophage-induced efflux mechanism.* Cell, 2011. **145**(1): p. 39-53.

82.   Kalscheuer, R., et al., *Trehalose-recycling ABC transporter LpqY-SugA-SugB-SugC is essential for virulence of Mycobacterium tuberculosis.* Proc Natl Acad Sci U S A, 2010. **107**(50): p. 21761-6.

83.   Pandey, A.K. and C.M. Sassetti, *Mycobacterial persistence requires the utilization of host cholesterol.* Proc Natl Acad Sci U S A, 2008. **105**(11): p. 4376-80.

84.   Miner, M.D., et al., *Role of cholesterol in Mycobacterium tuberculosis infection.* Indian J Exp Biol, 2009. **47**(6): p. 407-11.

85.   Forrellad, M.A., et al., *Role of the Mce1 transporter in the lipid homeostasis of Mycobacterium tuberculosis.* Tuberculosis (Edinb), 2014. **94**(2): p. 170-7.

86.   Marjanovic, O., A.T. Iavarone, and L.W. Riley, *Sulfolipid accumulation in Mycobacterium tuberculosis disrupted in the mce2 operon.* J Microbiol, 2011. **49**(3): p. 441-7.

87.   Paulsen, I.T. *TransportDB*. 2013 08/07/13; Available from: http://www.membranetransport.org/.

88.   Lamichhane, G., S. Tyagi, and W.R. Bishai, *Designer arrays for defined mutant analysis to detect genes essential for survival of Mycobacterium tuberculosis in mouse lungs.* Infect Immun, 2005. **73**(4): p. 2533-40.

89.   Converse, S.E., et al., *MmpL8 is required for sulfolipid-1 biosynthesis and Mycobacterium tuberculosis virulence.* Proc Natl Acad Sci U S A, 2003. **100**(10): p. 6121-6.

90.   Domenech, P., M.B. Reed, and C.E. Barry, 3rd, *Contribution of the Mycobacterium tuberculosis MmpL protein family to virulence and drug resistance.* Infect Immun, 2005. **73**(6): p. 3492-501.

91.   Alvarez-Ortega, C., J. Olivares, and J.L. Martinez, *RND multidrug efflux pumps: what are they good for?* Front Microbiol, 2013. **4**: p. 7.

92.   Tahlan, K., et al., *SQ109 targets MmpL3, a membrane transporter of trehalose monomycolate involved in mycolic acid donation to the cell wall core of Mycobacterium tuberculosis.* Antimicrob Agents Chemother, 2012. **56**(4): p. 1797-809.

93.   Grzegorzewicz, A.E., et al., *Inhibition of mycolic acid transport across the Mycobacterium tuberculosis plasma membrane.* Nat Chem Biol, 2012. **8**(4): p. 334-41.

94.   Camacho, L.R., et al., *Analysis of the phthiocerol dimycocerosate locus of Mycobacterium tuberculosis. Evidence that this lipid is involved in the cell wall permeability barrier.* J Biol Chem, 2001. **276**(23): p. 19845-54.

95.   Jain, M. and J.S. Cox, *Interaction between polyketide synthase and transporter suggests coupled synthesis and export of virulence lipid in M. tuberculosis.* PLoS Pathog, 2005. **1**(1): p. e2.

96.   Domenech, P., et al., *The role of MmpL8 in sulfatide biogenesis and virulence of Mycobacterium tuberculosis.* J Biol Chem, 2004. **279**(20): p. 21257-65.

97.   Rodriguez, J.E., et al., *Transcription of genes involved in sulfolipid and polyacyltrehalose biosynthesis of Mycobacterium tuberculosis in experimental latent tuberculosis infection.* PLoS One, 2013. **8**(3): p. e58378.

98.   Pacheco, S.A., et al., *MmpL11 protein transports mycolic acid-containing lipids to the mycobacterial cell wall and contributes to biofilm formation in Mycobacterium smegmatis.* J Biol Chem, 2013. **288**(33): p. 24213-22.

99.   Wells, R.M., et al., *Discovery of a siderophore export system essential for virulence of Mycobacterium tuberculosis.* PLoS Pathog, 2013. **9**(1): p. e1003120.

100.   Owens, C.P., et al., *The Mycobacterium tuberculosis secreted protein Rv0203 transfers heme to membrane proteins MmpL3 and MmpL11.* J Biol Chem, 2013. **288**(30): p. 21714-28.

101.   Tullius, M.V., et al., *Discovery and characterization of a unique mycobacterial heme acquisition system.* Proc Natl Acad Sci U S A, 2011. **108**(12): p. 5051-6.

102.   Bigi, F., et al., *The knockout of the lprG-Rv1410 operon produces strong attenuation of Mycobacterium tuberculosis.* Microbes Infect, 2004. **6**(2): p. 182-7.

103.   Silva, P.E., et al., *Characterization of P55, a multidrug efflux pump in Mycobacterium bovis and Mycobacterium tuberculosis.* Antimicrob Agents Chemother, 2001. **45**(3): p. 800-4.

104.   Nikaido, H., *Structure and mechanism of RND-type multidrug efflux pumps.* Adv Enzymol Relat Areas Mol Biol, 2011. **77**: p. 1-60.

105.	Jones, C.M., et al., *Self-poisoning of Mycobacterium tuberculosis by interrupting siderophore recycling.* Proc Natl Acad Sci U S A, 2014. **111**(5): p. 1945-50.

106.	Recht, J., et al., *Genetic analysis of sliding motility in Mycobacterium smegmatis.* J Bacteriol, 2000. **182**(15): p. 4348-51.

107.	Sonden, B., et al., *Gap, a mycobacterial specific integral membrane protein, is required for glycolipid transport to the cell surface.* Mol Microbiol, 2005. **58**(2): p. 426-40.

108.	Deshayes, C., et al., *MmpS4 promotes glycopeptidolipids biosynthesis and export in Mycobacterium smegmatis.* Mol Microbiol, 2010. **78**(4): p. 989-1003.

109.	Nessar, R., et al., *Deletion of the mmpL4b gene in the Mycobacterium abscessus glycopeptidolipid biosynthetic pathway results in loss of surface colonization capability, but enhanced ability to replicate in human macrophages and stimulate their innate immune response.* Microbiology, 2011. **157**(Pt 4): p. 1187-95.

110.	Soto, C.Y., et al., *Simple and rapid differentiation of Mycobacterium tuberculosis H37Ra from M. tuberculosis clinical isolates through two cytochemical tests using neutral red and nile blue stains.* J Clin Microbiol, 2002. **40**(8): p. 3021-4.

111.	van Soolingen, D., et al., *DNA fingerprinting of Mycobacterium tuberculosis.* Methods Enzymol, 1994. **235**: p. 196-205.

112.	Brosch, R., et al., *Use of a Mycobacterium tuberculosis H37Rv bacterial artificial chromosome library for genome mapping, sequencing, and comparative genomics.* Infect Immun, 1998. **66**(5): p. 2221-9.

113.	Birnboim, H.C. and J. Doly, *A rapid alkaline extraction procedure for screening recombinant plasmid DNA.* Nucleic Acids Res, 1979. **7**(6): p. 1513-23.

114.	Wards, B.J. and D.M. Collins, *Electroporation at elevated temperatures substantially improves transformation efficiency of slow-growing mycobacteria.* FEMS Microbiol Lett, 1996. **145**(1): p. 101-5.

115.	Davis, G. and K.J. Kayser, *Methods in molecular biology - Chromosomal mutagenesis*, ed. J.M. Walker. 2008.

116.	Datsenko, K.A. and B.L. Wanner, *One-step inactivation of chromosomal genes in Escherichia coli K-12 using PCR products.* Proc Natl Acad Sci U S A, 2000. **97**(12): p. 6640-5.

117.	*Institut Pasteur - Unité de Génétique Moléculaire Bactérienne. Bacterial Artificial Chromosome Libraries of Mycobacterium tuberculosis H37Rv and M. bovis BCG Pasteur.* 2000.

118.	Lee, S., et al., *Bxz1, a new generalized transducing phage for mycobacteria.* FEMS Microbiol Lett, 2004. **241**(2): p. 271-6.

119.	van Kessel, J.C., *Recombineering in mycobacteria using mycobacteriophage proteins.* Biological Sciences, 2008. **Doctor of Philosophy**: p. 264.

120.	Dobsong, G., et al., *Systematic analysis of complex mycobacterial lipids.* Chemical Methods in Bacterial Systematic, 1985.

121.	Cardona, P.J., et al., *Neutral-red reaction is related to virulence and cell wall methyl-branched lipids in Mycobacterium tuberculosis.* Microbes Infect, 2006. **8**(1): p. 183-90.

122.	Simeone, R., et al., *Delineation of the roles of FadD22, FadD26 and FadD29 in the biosynthesis of phthiocerol dimycocerosates and related compounds in Mycobacterium tuberculosis.* FEBS J, 2010. **277**(12): p. 2715-25.

123.	Dao, D.N., et al., *Mycolic acid modification by the mmaA4 gene of M. tuberculosis modulates IL-12 production.* PLoS Pathog, 2008. **4**(6): p. e1000081.

124.	Piddock, L.J., K.J. Williams, and V. Ricci, *Accumulation of rifampicin by Mycobacterium aurum, Mycobacterium smegmatis and Mycobacterium tuberculosis.* J Antimicrob Chemother, 2000. **45**(2): p. 159-65.

125.	van Boxtel, R.M., R.S. Lambrecht, and M.T. Collins, *Effect of polyoxyethylene sorbate compounds (Tweens) on colonial morphology, growth, and ultrastructure of Mycobacterium paratuberculosis.* APMIS, 1990. **98**(10): p. 901-8.

126.   Boshoff, H.I., et al., *The transcriptional responses of Mycobacterium tuberculosis to inhibitors of metabolism: novel insights into drug mechanisms of action.* J Biol Chem, 2004. **279**(38): p. 40174-84.

127.   Paixao, L., et al., *Fluorometric determination of ethidium bromide efflux kinetics in Escherichia coli.* J Biol Eng, 2009. **3**: p. 18.

128.   Coelho, T., et al., *Enhancement of antibiotic activity by efflux inhibitors against multidrug resistant Mycobacterium tuberculosis clinical isolates from Brazil.* Front Microbiol, 2015. **6**: p. 330.

129.   Tomala, K. and R. Korona, *Evaluating the fitness cost of protein expression in Saccharomyces cerevisiae.* Genome Biol Evol, 2013. **5**(11): p. 2051-60.

130.   Cosson, P., et al., *Pseudomonas aeruginosa virulence analyzed in a Dictyostelium discoideum host system.* J Bacteriol, 2002. **184**(11): p. 3027-33.

131.   Warner, D.M., et al., *Regulation of the MtrC-MtrD-MtrE efflux-pump system modulates the in vivo fitness of Neisseria gonorrhoeae.* J Infect Dis, 2007. **196**(12): p. 1804-12.

132.   Bhatt, A., et al., *Deletion of kasB in Mycobacterium tuberculosis causes loss of acid-fastness and subclinical latent tuberculosis in immunocompetent mice.* Proc Natl Acad Sci U S A, 2007. **104**(12): p. 5157-62.

133.   Belardinelli, J.M. and H.R. Morbidoni, *Mutations in the essential FAS II beta-hydroxyacyl ACP dehydratase complex confer resistance to thiacetazone in Mycobacterium tuberculosis and Mycobacterium kansasii.* Mol Microbiol, 2012. **86**(3): p. 568-79.

134.   Pirson, C., et al., *Differential effects of Mycobacterium bovis--derived polar and apolar lipid fractions on bovine innate immune cells.* Vet Res, 2012. **43**: p. 54.

Annex I

Results of TLC analysis of free lipids, non-polar and polar lipids, and FAMEs and MAMEs from H37Rv wt, L4KO, L4c, L4S4KO, L4S4c, and L4sb in different solvent systems.

Table 1-AI. Summary of solvent systems for TLC lipid analysis.

System	Direction 1	Runs
A	Petroleum ether 60-80/ Ethyl acetate (98:2)	3
B	Petroleum ether 60-80/ Acetone (92:8)	3
C	Chloroform/ Methanol (96:4)	1
D	Chloroform/ Methanol/ Water (100:14:0.8)	1
E	Chloroform/ Methanol/ Water (60:30:6)	1
F	Petroleum ether/ Acetone (95:5)	1
System	**Direction 2**	**Runs**
A	Petroleum ether 60-80/ Acetone (98:2)	1
B	Toluene/ Acetone (95:5)	1
C	Toluene/ Acetone (80:20)	1
D	Chloroform/ Acetone/ Methanol / Water (50:60:2.5:3)	1
E	Chloroform/ Acetic acid (glacial)/ Methanol / Water (40:25:3:6)	1

Figure 1-AI. 2D-TLC analysis of free lipids from H37Rv, L4KO, L4c, L4S4KO, L4S4c, and L4sb using solvent systems A.

Figure 2-AI. 2D-TLC analysis of free lipids from H37Rv, L4KO, L4c, L4S4KO, L4S4c, and L4sb using solvent systems B.

Figure 3-AI. 2D-TLC analysis of <u>free lipids</u> from H37Rv, L4KO, L4c, L4S4KO, L4S4c, and L4sb using solvent <u>systems C</u>.
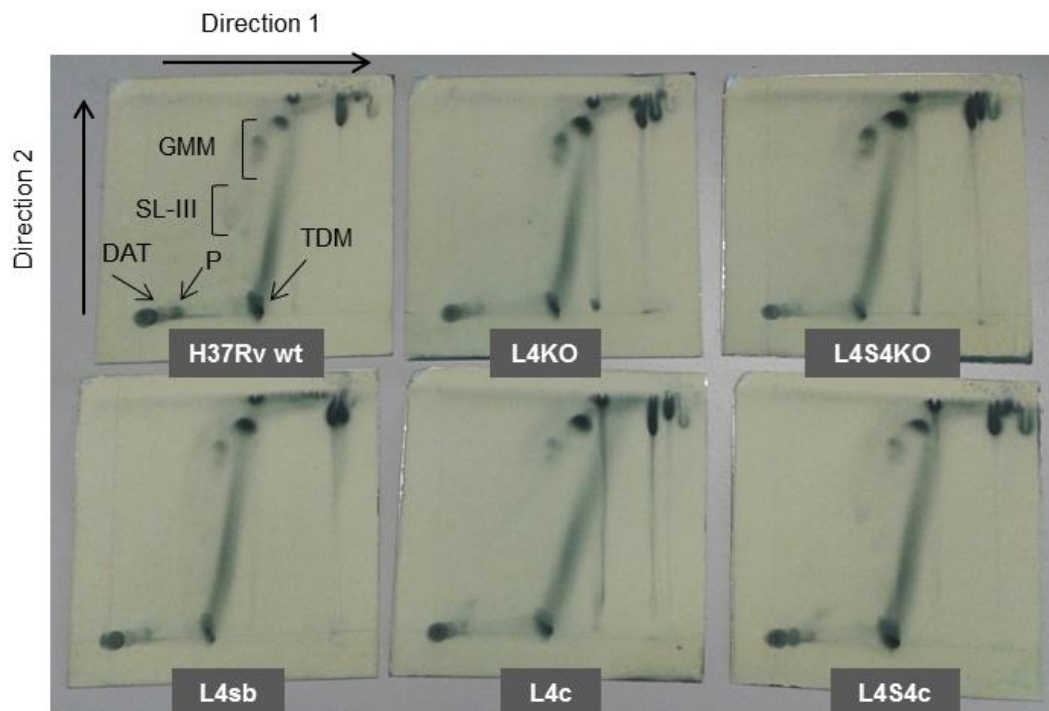
Figure 4-AI. 2D-TLC analysis of *free lipids* from H37Rv, L4KO, L4c, L4S4KO, L4S4c, and L4sb using solvent <u>systems D</u>.
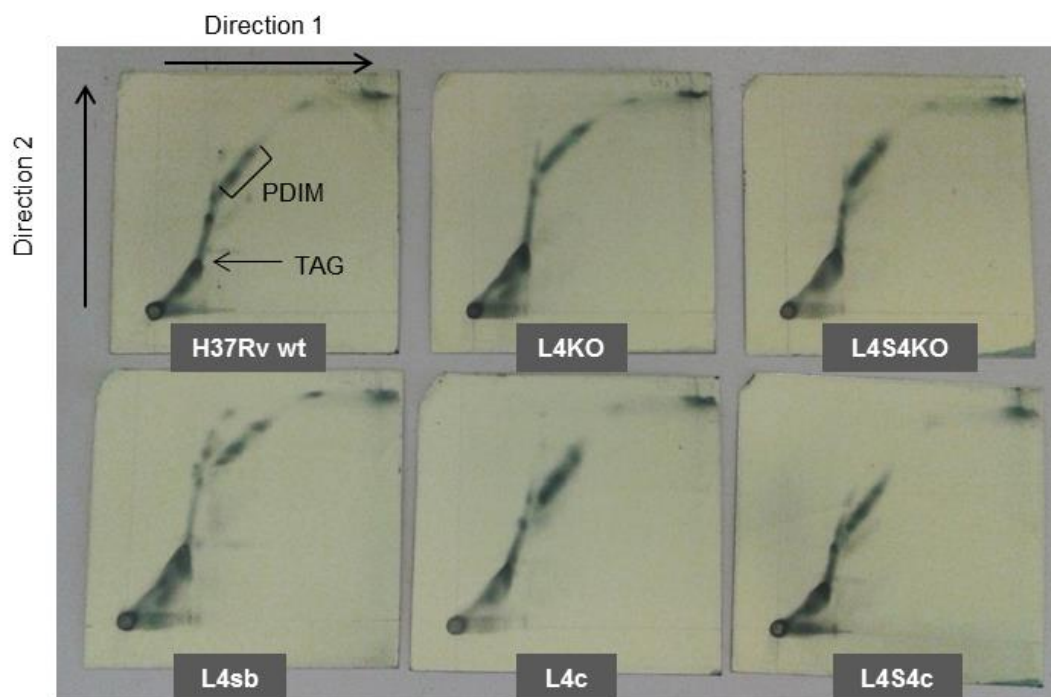
Figure 5-AI. 2D-TLC analysis of non-polar lipids from H37Rv, L4KO, L4c, L4S4KO, L4S4c, and L4sb using solvent systems A.

Figure 6-AI. 2D-TLC analysis of non-polar lipids from H37Rv, L4KO, L4c, L4S4KO, L4S4c, and L4sb using solvent systems B.
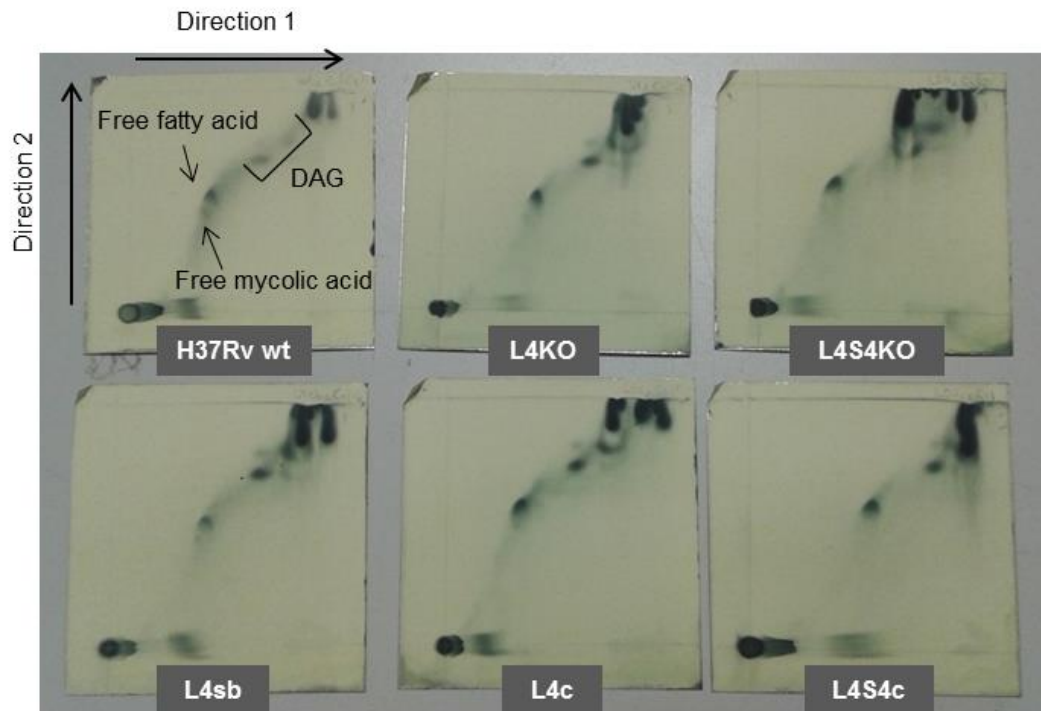
Figure 7-AI. 2D-TLC analysis of non-polar lipids from H37Rv, L4KO, L4c, L4S4KO, L4S4c, and L4sb using solvent systems C.
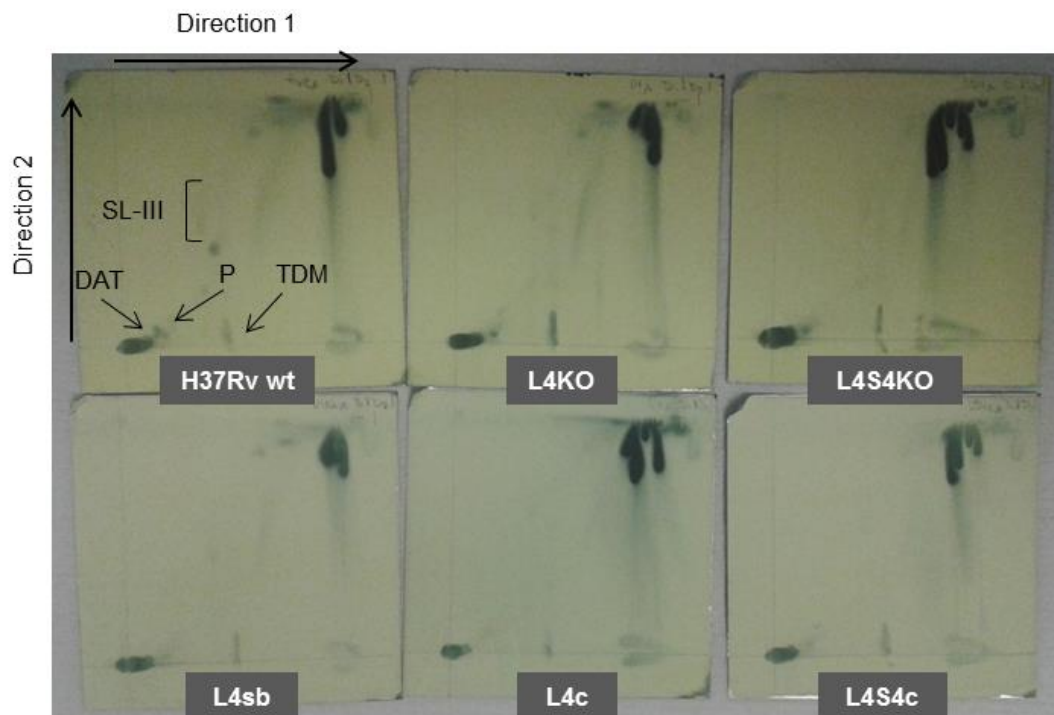
Figure 8-AI. 2D-TLC analysis of non-polar lipids from H37Rv, L4KO, L4c, L4S4KO, L4S4c, and L4sb using solvent systems D.
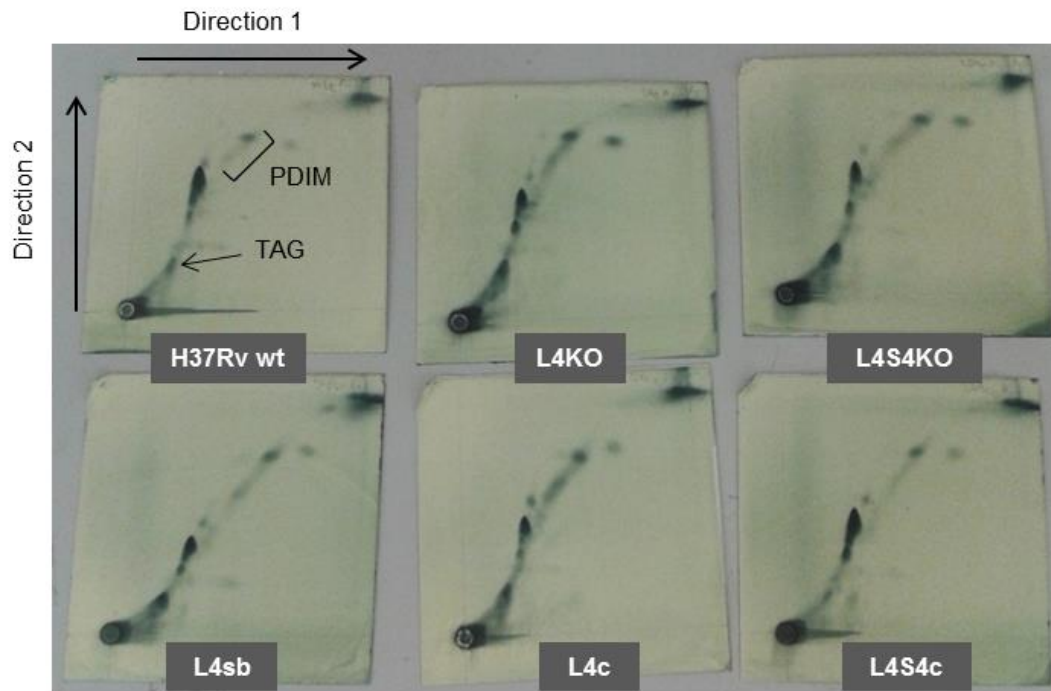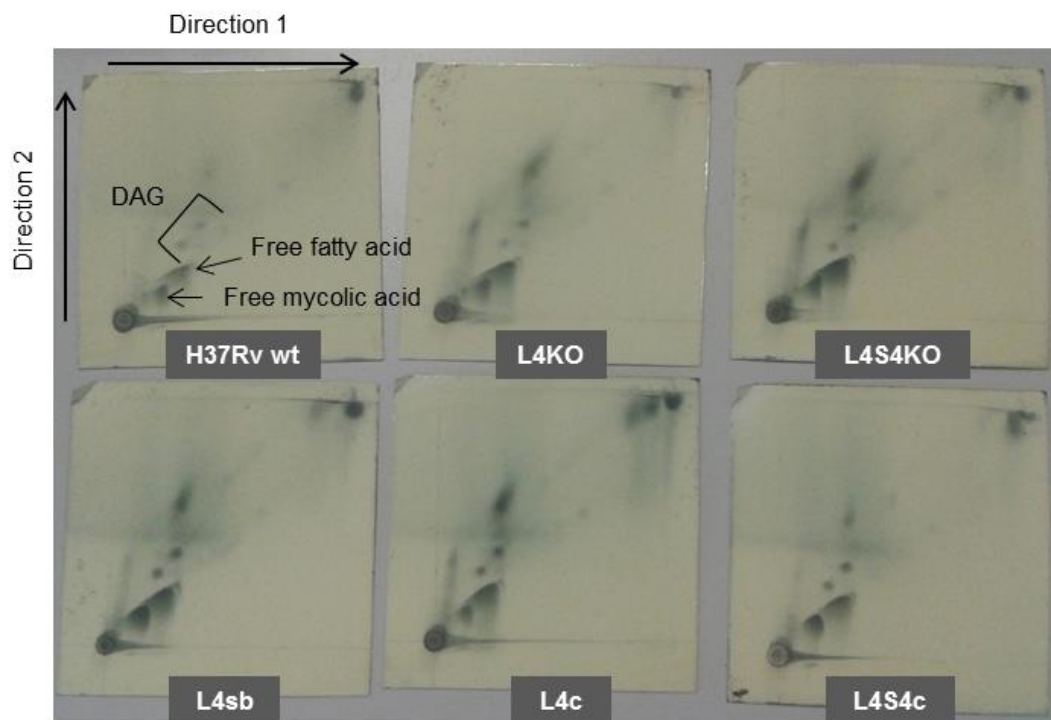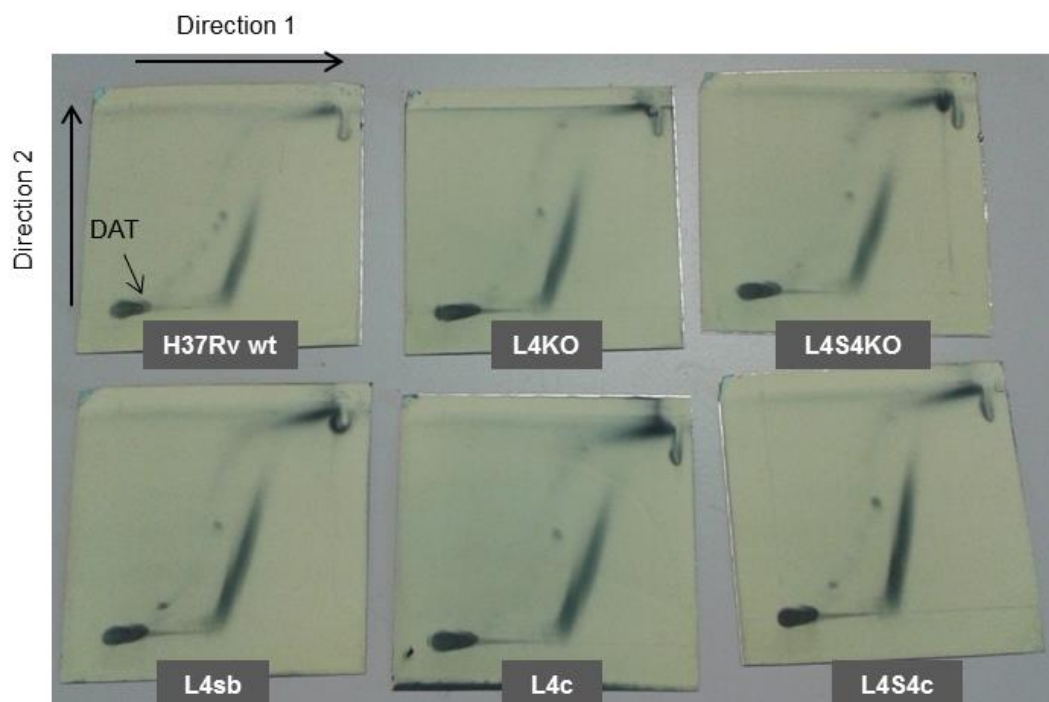
Figure 9-AI. 2D-TLC analysis of polar lipids from H37Rv, L4KO, L4c, L4S4KO, L4S4c, and L4sb using solvent systems D.
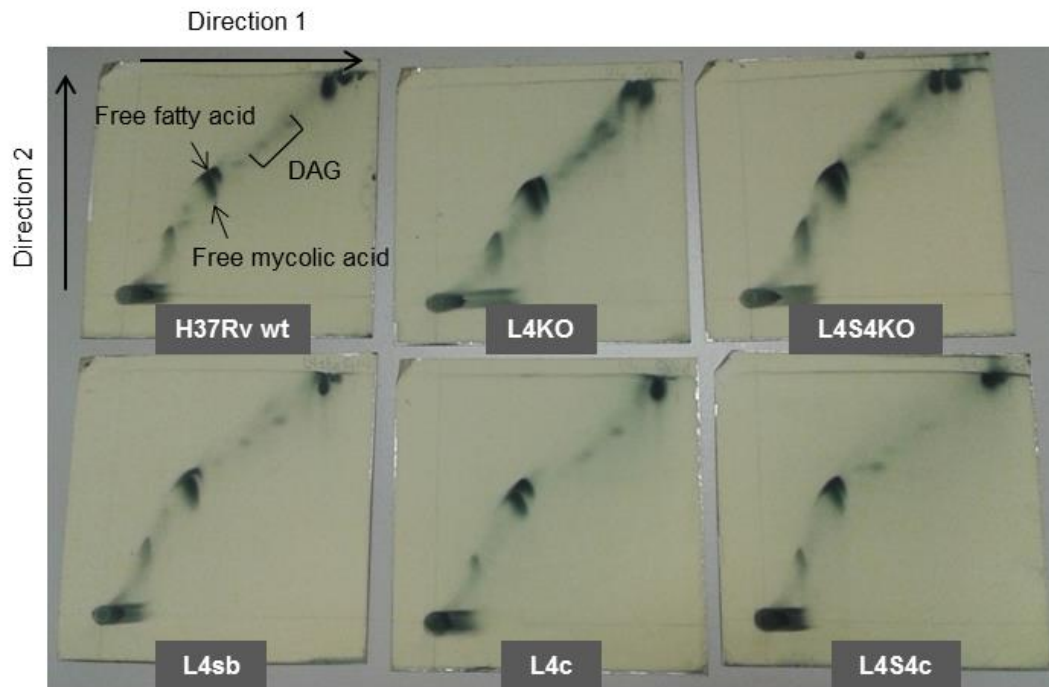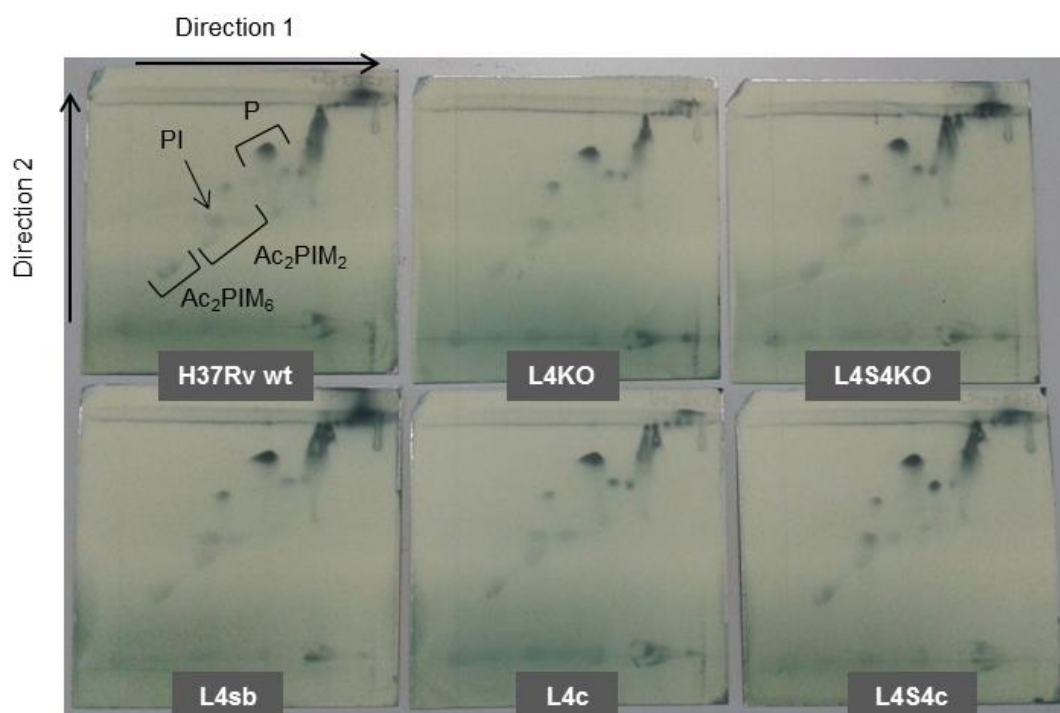

Figure 10-AI. 2D-TLC analysis of polar lipids from H37Rv, L4KO, L4c, L4S4KO, L4S4c, and L4sb using solvent systems E.
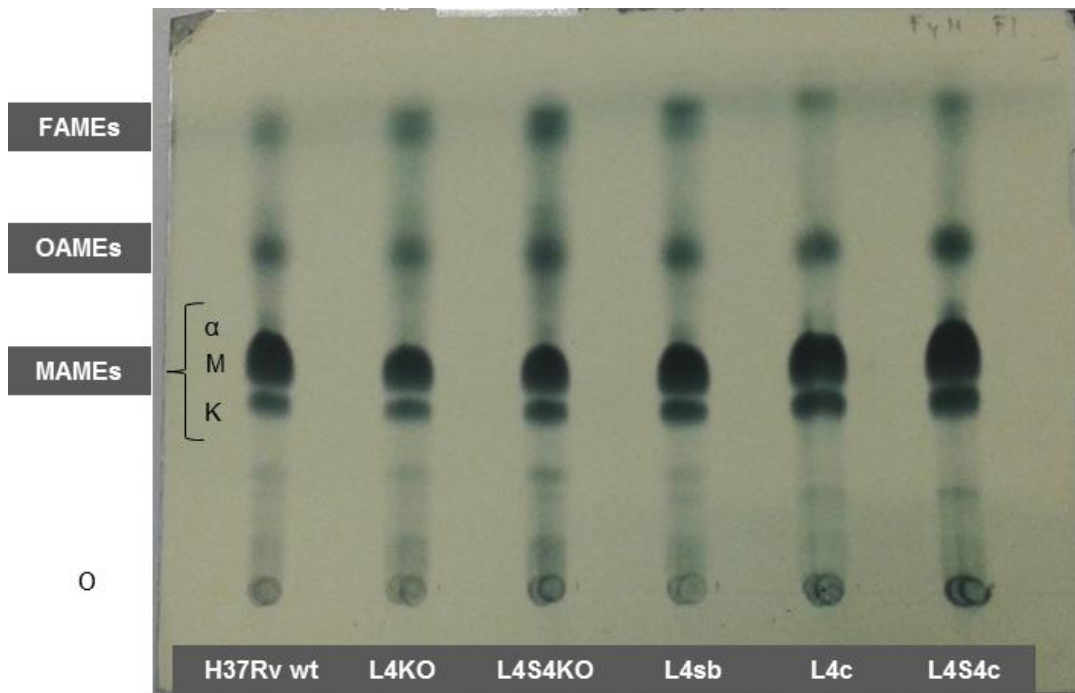
Figure 11-AI. TLC analysis of FAMEs and MAMEs from H37Rv, L4KO, L4c, L4S4KO, L4S4c, and L4sb using solvent system F.

Annex II

Table 1-AII. Variation in the expression of the proteins with p<0.05 in L4KO, L4c, L4S4KO, and L4S4c in comparison with H37Rv wt.

Spot number	Protein name	Rv number	L4KO		L4c		L4S4KO		L4S4c	
			+/-	FC	+/-	FC	+/-	FC	+/-	FC
409	Probable ribonucleotide transport ATP-binding protein ABC transporter Mkl	Rv0655	+	1.9			+	1.8	+	1.8
492	Quinone oxidoreductase Qor	Rv1454c	-	1.3	-	1.3	-	1.3	-	1.3
524	Hypothetical protein	Rv1794	-	1.4						
618	NADH-dependent enoyl-ACP reductase InhA	Rv1484					+	1.5		
653	Probable short-chain type dehydrogenase/reductase	Rv0927c							-	1.4
695	Adenylate kinase Adk	Rv0733	-	1.4			-	1.5		
750	Conserved protein TB16.3	Rv2185c			-	1.4				
848	Biotin carboxyl carrier protein AccA3	Rv3285			+	2.5				
849	3-hydroxyacyl-CoA dehydrogenase FadB	Rv0860	+	2.4	+	2.1	+	2.7	+	2.1
886	Uncharacterized protein	Rv2557	-	1.3	-	1.2	-	1.3	-	1.3
893	Putative OXPP cycle protein OpcA	Rv1446c			-	1.2	-	1.1	-	1.2
899	Enoyl-CoA hydratase EchA3	Rv0632c					-	1.8		
908	Acyl-[acyl-carrier protein] desaturase DesA1	Rv0824c	+	2.2	+	1.9	+	2.7	+	2.2
913	Probable short-chain type dehydrogenase/reductase	Rv0148					-	1.4	-	1.1
937	Succinyl-CoA synthetase (alpha chain) SucD	Rv0952			-	1.2				

Abbreviations: FC (Fold change).

+/-: + means this protein was overexpressed in this strain in comparison to the reference strain H37Rv.

- means this protein was less expressed in this strain than in H37Rv wt.

Even though the statistical analysis revealed that none of the spots were statistically significant, we believed that those proteins with p<0.05 and fold change >1.5 should be studied more thoroughly since they might be biologically relevant.

These proteins were classified (Table 2-AII) according to functional category using TubercuList database. The most relevant finding was that 72% of these proteins were related to lipid metabolism. In addition, 14% of them were involved in intermediary metabolism and respiration and 14% in cell wall and cell processes. Interestingly, all the proteins in lipid metabolism category were associated with fatty acids. Nevertheless, it was not possible to link them to any specific pathway.

Table 2-AII. Functional classification and description of the selected cellular proteins differentially expressed in *Mycobacterium tuberculosis* strains.

Rv number	Protein name	Gene name	Functional category	Biological function
Rv0655	Probable ribonucleotide transport ATP-binding protein ABC transporter Mkl	*mkl*	Cell wall and cell processes	Thought to be involved in active transport of ribonucleotide across the membrane
Rv1484	NADH-dependent enoyl-ACP reductase InhA	*inhA*	Lipid metabolism	Involved in mycolic acid biosynthesis, second reductive step in fatty acid biosynthesis, and in the resistance against isoniazid and ethionamide
Rv0733	Adenylate kinase Adk	*adk*	Intermediary metabolism and respiration	Essential in intracellular nucleotide metabolism
Rv3285	Biotin carboxyl carrier protein AccA3	*accA3*	Lipid metabolism	Involved in the first step of long-chain fatty acid synthesis
Rv0860	3-hydroxyacyl-CoA dehydrogenase FadB	*fadB*	Lipid metabolism	Involved in fatty acid degradation (probably in fatty acid beta-oxidation cycle)
Rv0632c	Enoyl-CoA hydratase EchA3	*echA3*	Lipid metabolism	Could possibly oxidize fatty acids using specific components
Rv0824c	Acyl-[acyl-carrier protein] desaturase DesA1	*desA1*	Lipid metabolism	Catalyzes the principal conversion of saturated fatty acids to unsaturated fatty acids

Regarding protein expression (Table 3-AII), as it was shown in other experiments, the complemented strains did not behave as they were supposed; protein expression levels were

not always similar to the wild-type. It should be pointed out that three of the proteins involved in lipid metabolism (AccA3, FadB, and DesA1) exhibited the highest rise in their expression compared to the reference strain. Furthermore, there were a larger number of proteins whose expression changed in L4S4KO than L4KO.

Table 3-AII. Selected cellular proteins differentially expressed in *Mycobacterium tuberculosis* knockout mutants L4KO and L4S4KO and their complemented strains.

Spot number	Protein name	Rv number	L4KO		L4c		L4S4KO		L4S4c	
			+/-	FC	+/-	FC	+/-	FC	+/-	FC
409	Probable ribonucleotide transport ATP-binding protein ABC transporter Mkl	Rv0655	+	1.9			+	1.8	+	1.8
618	NADH-dependent enoyl-ACP reductase InhA	Rv1484					+	1.5		
695	Adenylate kinase Adk	Rv0733	-	1.4			-	1.5		
848	Biotin carboxyl carrier protein AccA3	Rv3285			+	2.5				
849	3-hydroxyacyl-CoA dehydrogenase FadB	Rv0860	+	2.4	+	2.1	+	2.7	+	2.1
899	Enoyl-CoA hydratase EchA3	Rv0632c					-	1.8		
908	Acyl-[acyl-carrier protein] desaturase DesA1	Rv0824c	+	2.2	+	1.9	+	2.7	+	2.2

Abbreviations: FC (Fold change).

+/-: + means this protein was overexpressed in this strain in comparison to the reference strain H37Rv.

- means this protein was less expressed in this strain than in H37Rv wt.

Annex III

Results of TLC analysis of free lipids, non-polar and polar lipids, from BCG wt and BCG L4sb in different solvent systems.

Table 1-AIII. Summary of solvent systems for TLC lipid analysis.

System	Direction 1	Runs
B	Petroleum ether 60-80/ Acetone (92:8)	3
C	Chloroform/ Methanol (96:4)	1
D	Chloroform/ Methanol/ Water (100:14:0.8)	1
E	Chloroform/ Methanol/ Water (60:30:6)	1
System	Direction 2	Runs
B	Toluene/ Acetone (95:5)	1
C	Toluene/ Acetone (80:20)	1
D	Chloroform/ Acetone/ Methanol / Water (50:60:2.5:3)	1
E	Chloroform/ Acetic acid (glacial)/ Methanol / Water (40:25:3:6)	1
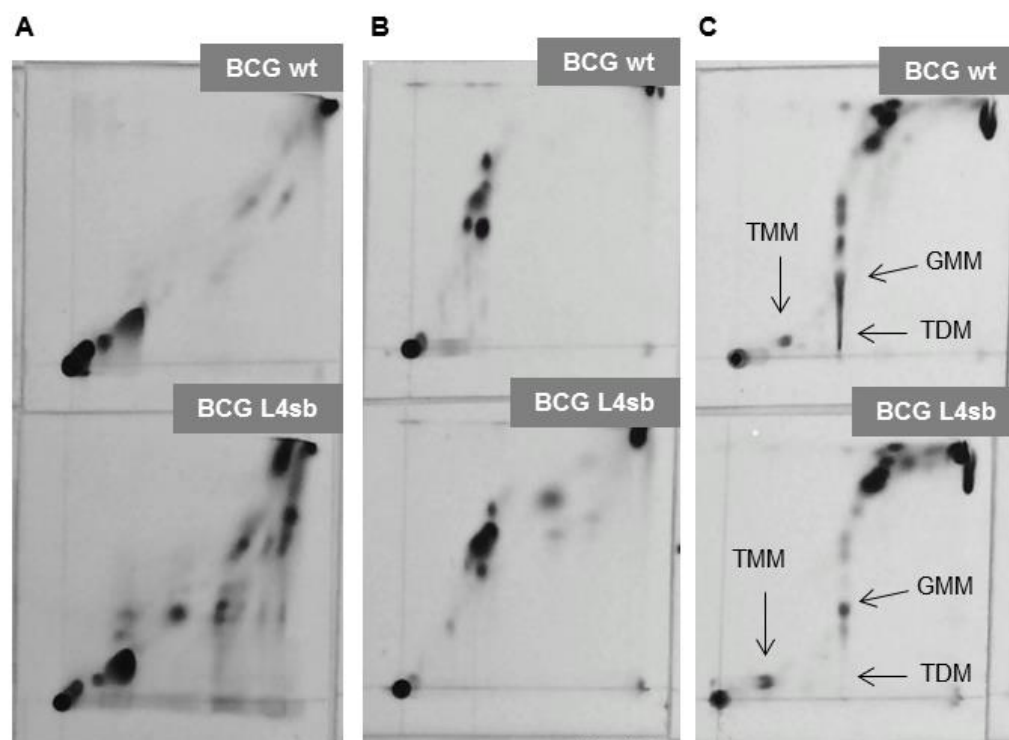
Figure 1-AIII. 2D-TLC analysis of free lipids from BCG wt and BCG L4sb. (A) Solvent systems B. (B) Solvent systems C. (C) Solvent systems D.
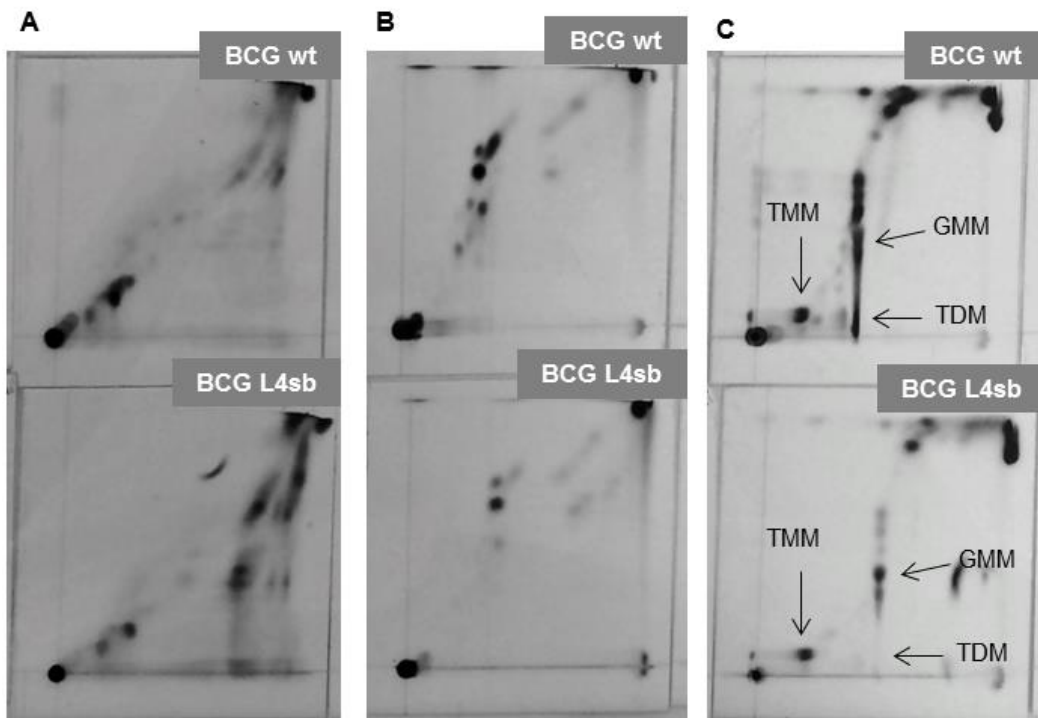
Figure 2-AIII. 2D-TLC analysis of non-polar lipids from BCG wt and BCG L4sb. (A) Solvent systems B. (B) Solvent systems C. (C) Solvent systems D.
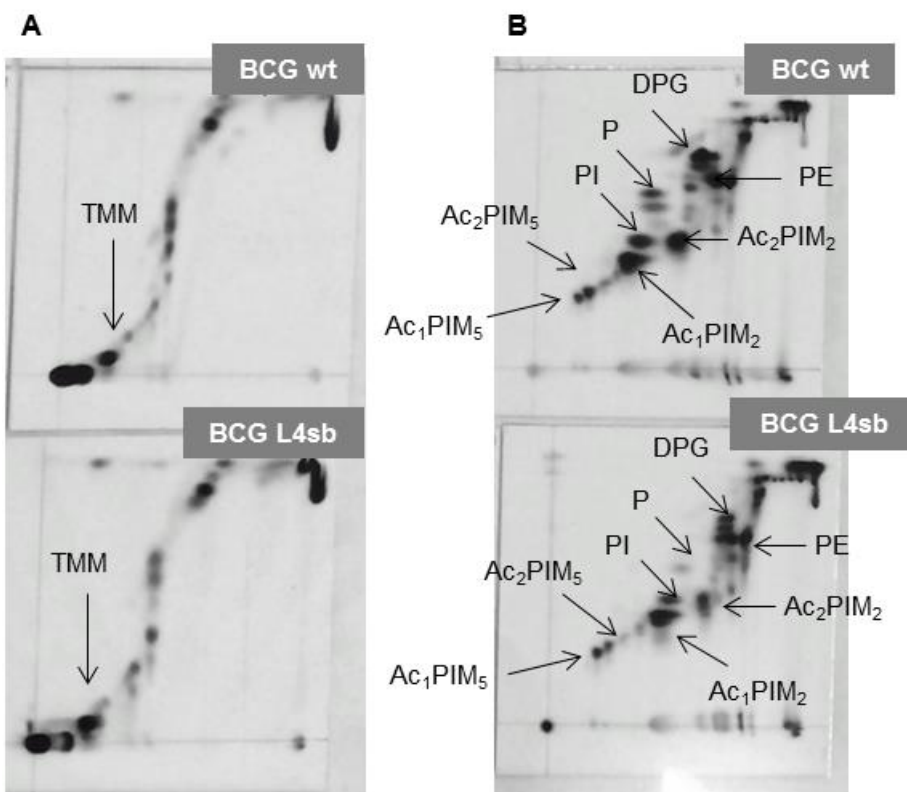
Figure 3-AIII. 2D-TLC analysis of polar lipids from BCG wt and BCG L4sb. (A) Solvent systems D. (B) Solvent systems E.

Annex IV

During my PhD thesis, I contributed to the construction of the Mmr knockout mutant of *M. tuberculosis* using the recombineering method, which is the routine procedure to generate knockouts in our laboratory. In addition, I took part in obtaining its complemented strain MmrKO::pCRS5, and the overexpression strain H37Rv::pCVZ2.

Role of the Mmr Efflux Pump in Drug Resistance in *Mycobacterium tuberculosis*

Liliana Rodrigues, Cristina Villellas, Rebeca Bailo, Miguel Viveiros, José A. Aínsa

Role of the Mmr Efflux Pump in Drug Resistance in *Mycobacterium tuberculosis*

Liliana Rodrigues,[a,b] Cristina Villellas,[a,b] Rebeca Bailo,[a,b] Miguel Viveiros,[c] José A. Aínsa[a,b]

Grupo de Genética de Micobacterias, Departamento de Microbiología, Medicina Preventiva y Salud Pública, Facultad de Medicina, Universidad de Zaragoza, Zaragoza, Spain[a]; Centro de Investigación Biomédica en Red de Enfermedades Respiratorias (CIBERES), Spain[b]; Grupo de Micobactérias, Unidade de Microbiologia Médica, Instituto de Higiene e Medicina Tropical, Universidade Nova de Lisboa (IHMT/UNL), Lisbon, Portugal[c]

Efflux pumps are membrane proteins capable of actively transporting a broad range of substrates from the cytoplasm to the exterior of the cell. Increased efflux activity in response to drug treatment may be the first step in the development of bacterial drug resistance. Previous studies showed that the efflux pump Mmr was significantly overexpressed in strains exposed to isoniazid. In the work to be described, we constructed mutants lacking or overexpressing Mmr in order to clarify the role of this efflux pump in the development of resistance to isoniazid and other drugs in *M. tuberculosis*. The *mmr* knockout mutant showed an increased susceptibility to ethidium bromide, tetraphenylphosphonium, and cetyltrimethylammonium bromide (CTAB). Overexpression of *mmr* caused a decreased susceptibility to ethidium bromide, acriflavine, and safranin O that was obliterated in the presence of the efflux inhibitors verapamil and carbonyl cyanide *m*-chlorophenylhydrazone. Isoniazid susceptibility was not affected by the absence or overexpression of *mmr*. The fluorometric method allowed the detection of a decreased efflux of ethidium bromide in the knockout mutant, whereas the overexpressed strain showed increased efflux of this dye. This increased efflux activity was inhibited in the presence of efflux inhibitors. Under our experimental conditions, we have found that efflux pump Mmr is mainly involved in the susceptibility to quaternary compounds such as ethidium bromide and disinfectants such as CTAB. The contribution of this efflux pump to isoniazid resistance in *Mycobacterium tuberculosis* still needs to be further elucidated.

The World Health Organization (WHO) goal to reduce the global burden of tuberculosis by 2015 (1, 2) faces many challenges, namely, the dissemination of severe cases of drug resistance that reduce the therapeutic efficacy of the available antituberculous drugs. These drug-resistant forms of tuberculosis are known as multidrug and extensively drug-resistant tuberculosis (MDRTB and XDRTB, respectively), with the former defined to be resistance to at least the first-line drugs isoniazid and rifampin and the latter defined to be MDRTB plus resistance to fluoroquinolones and to at least one of the three injectable second-line drugs (kanamycin, amikacin, and capreomycin). Thus, there is a great effort to understand the mechanisms of drug resistance, as well as to develop new drugs and new therapeutic approaches.

Clinically relevant drug resistance in *Mycobacterium tuberculosis* occurs mainly by the acquisition of spontaneous chromosomal mutations that alter the drug target or the prodrug-activating enzymes, followed by the selection of drug-resistant mutants that may occur in the case of exposure to monotherapy or lower antibiotic doses due to inadequate prescription, poor patient compliance, and patient pharmacokinetic variability (3–5). However, these mutations are not found in many low-level-resistant isolates, suggesting that other mechanisms of resistance may also be involved, such as mechanisms involving the permeability barrier provided by the cell wall and the activity of efflux systems.

Bacterial efflux pumps are membrane proteins that are capable of actively transporting a broad range of substrates, including drugs, from the cytoplasm to the exterior of the cell. They are involved in physiological processes, such as cell wall division, maintenance of the pH homeostasis, and secretion of intracellular metabolites (6–8). Increased expression of efflux pump genes confers a low-level-resistant phenotype, and it has been suggested that under these conditions, bacteria have greater

chances of acquiring a chromosomal mutation(s) conferring higher levels of drug resistance (6, 9). A strategy to prevent this chain of events would be the inhibition of efflux pumps, which, in addition, would restore the effectiveness of antimicrobials that are subject to efflux (10–12).

In *M. tuberculosis*, several efflux pumps have been described, but their contribution to clinical drug resistance remains to be completely clarified (13, 14). One of these pumps is Mmr (Rv3065) of the small multidrug resistance (SMR) family of transporters. Previous studies involving Mmr were performed in the heterologous host *Mycobacterium smegmatis* and showed that it was involved in the extrusion of several compounds such as tetraphenylphosphonium, ethidium bromide (EtBr), erythromycin, and acriflavine (15, 16). A recent study has shown that Mmr appears to be involved in the efflux of compounds of the pyrrole class in *M. tuberculosis* (17).

In previous works, we and other authors observed that *mmr* was one of the efflux pump genes that was significantly overexpressed in a number of *M. tuberculosis* strains exposed to high levels of isoniazid (9, 18, 19), which suggested that Mmr could be associated with resistance to isoniazid. In the study to be described, we constructed *M. tuberculosis* mutants lacking or over-

TABLE 1 Strains and plasmids used in this study

Strain or plasmid	Description	Source or reference
M. tuberculosis		
H37Rv (ATCC 25618)	Wild type	Laboratory collection
H37Rv::pLAM12	Control strain	20
H37Rv::pJV53	Recombineering strain	20
MmrKO	H37Rv knockout for *mmr*	This study
MmrKO::pCRS5	Strain MmrKO containing pCRS5	This study
H37Rv::pCVZ2	Strain H37Rv containing pCVZ2	This study
Plasmids		
pLAM12	Replicative plasmid with a kanamycin resistance gene and an acetamidase expression cassette	20
pJV53	Carrying genes for gp60 and gp61 (encoding recombineering enzymes) from mycobacteriophage Che9c cloned into pLAM12, under the control of the acetamidase promoter	20
pYUB854	*E. coli* vector containing the Hyg^r cassette flanked by multiple-cloning sites and γδ *res* sites, *oriE*, and a λ*cos* packaging site	20, 21
pMmr	pYUB854 containing the DNA regions flanking *mmr*	This study
pCRS5	Integrative plasmid, *mmr* cloned into pMV361 (22)	This study
pCVZ2	Replicative plasmid, *mmr* cloned into pSUM36 (23)	This study

expressing Mmr in order to clarify the role of this efflux pump in the development of resistance to isoniazid and other drugs.

MATERIALS AND METHODS

Bacteria and growth conditions. The strains and plasmids used in this study are listed in Table 1. *M. tuberculosis* was grown at 37°C in Middlebrook 7H9 broth (Difco, Detroit, MI) supplemented with 10% (vol/vol) Middlebrook albumin-dextrose-catalase (ADC; Difco) and 0.05% (vol/vol) Tween 80 or on Middlebrook 7H10 (Difco) agar plates supplemented with 10% (vol/vol) ADC and 0.05% (vol/vol) Tween 80. *Escherichia coli* HB101 was grown at 37°C Luria Bertani (LB) broth or on LB agar plates. Plasmids were maintained in *E. coli* with appropriate antibiotics for selection (50 μg/ml of hygromycin, 20 μg/ml of kanamycin). For the selection of resistance markers in mycobacteria, hygromycin or kanamycin was added to the culture medium at final concentrations of 50 μg/ml and 20 μg/ml, respectively.

DNA manipulation. DNA manipulations were carried out by standard techniques (24). Mycobacterial genomic DNA was isolated as described previously (25). Southern blotting was done with an enhanced chemiluminescence direct nucleic acid labeling and detection system (Amersham Biosciences), according to the manufacturer's instructions. A DNA probe specific for the *mmr* gene was generated by PCR, based upon an Rv3065 gene sequence from GenBank (accession number NC_000962; region 3430387 to 3430710); primer sequences are available upon request.

E. coli and *M. tuberculosis* were transformed by electroporation with a Gene Pulser apparatus (Bio-Rad Laboratories Inc., Richmond, CA). Briefly, *E. coli* competent cells were prepared according to standard protocols (24) and transformed by adding DNA to 40-μl aliquots of cells while incubating on ice. Cells were transferred to chilled 0.2-cm cuvettes (Bio-Rad) and transformed using a Bio-Rad Gene Pulser set at 2.5 kV, 200 Ω, and 25 μF. Cells were recovered in 1 ml LB broth for 1 h at 37°C and plated on selective medium. *M. tuberculosis* electrocompetent cells were prepared as previously described (21). Briefly, the culture was centrifuged at 2,880 × *g* for 10 min and the supernatant was discarded. The pellet was resuspended in 1/2 volume of sterile 10% glycerol, and the centrifugation step was repeated. The cells were resuspended in 1/4 volume of sterile 10% glycerol. This process was repeated until in the last step the cells were resuspended in 1/25 volume of sterile 10% glycerol. *M. tuberculosis* competent cells were transformed by electroporation using a Gene Pulser set at 2.5 kV, 1,000 Ω, and 25 μF. Cells were recovered in 1 ml 7H9 broth for 24 h (for the overexpression and complementation mutants) or 72 h (for the knockout [KO] mutant) at 37°C and plated on selective medium.

Strain construction. (i) Inactivation. The construction of an *M. tuberculosis mmr* knockout mutant was performed by allelic exchange, as previously described (20, 21). This method is based on the use of an *M. tuberculosis* recombineering strain transformed with a plasmid that contains mycobacteriophage Che9c-encoded recombination proteins gp60 and gp61. Expression of these proteins in *M. tuberculosis* increases the recombination frequency of the bacteria, allowing the recovery of gene replacement mutants following electroporation of linear DNA molecules containing segments homologous to the chromosomal DNA (20, 21).

Primers were designed to amplify upstream and downstream DNA regions flanking the *mmr* gene (576 and 996 bp, respectively). The PCR products were cloned into pYUB854 flanking a hygromycin resistance cassette. The vector obtained, pMmr, was linearized by double digestion with AvrII and HindIII or amplified by PCR in order to obtain the allelic exchange substrate (AES) (Fig. 1A).

H37Rv::pJV53 (recombineering strain) was grown at 37°C in Middlebrook 7H9 supplemented with 0.05% Tween 80, 20 μg/ml kanamycin, and 0.2% succinate. Once the cells reached an optical density at 600 nm (OD$_{600}$) of 0.5 to 0.6, acetamide was added to a final concentration of 0.2% and the culture was grown at 37°C overnight. On the following day, electrocompetent cells were prepared and transformed with 100 ng of the AES by electroporation. The transformations were recovered by incubation at 37°C in 7H9 supplemented with ADC and Tween 80 for 72 h. The entire reaction mixture was plated on 7H10 agar plates containing kanamycin, hygromycin, and ADC and incubated at 37°C for 3 to 4 weeks, until colonies (potential *mmr* knockout mutants) developed. Colonies were inoculated into 7H9 broth containing kanamycin, hygromycin, and ADC and incubated at 37°C until visible growth was obtained (approximately 10 to 20 days). The presence of an inactivated copy of the *mmr* gene was tested by PCR and Southern blot analysis of each recombinant colony obtained. The mutant strain, namely, *M. tuberculosis* H37Rv MmrKO, was grown in medium lacking kanamycin until it lost the replicating plasmid pJV53.

As controls, recombineering-deficient strain *M. tuberculosis* H37Rv::pLAM12 was also transformed with AES and no colony was recovered, and *M. tuberculosis* H37Rv::pJV53 was used as a negative control for PCR and hybridization analysis.

(ii) Integrative plasmid for complementation. *M. tuberculosis* H37Rv MmrKO was complemented by introducing the integrative plasmid pCRS5, a derivative of vector pMV361 (22) carrying a 1,177-bp DNA fragment containing the *mmr* gene, resulting in *M. tuberculosis* H37Rv MmrKO::pCRS5 (Fig. 1B).
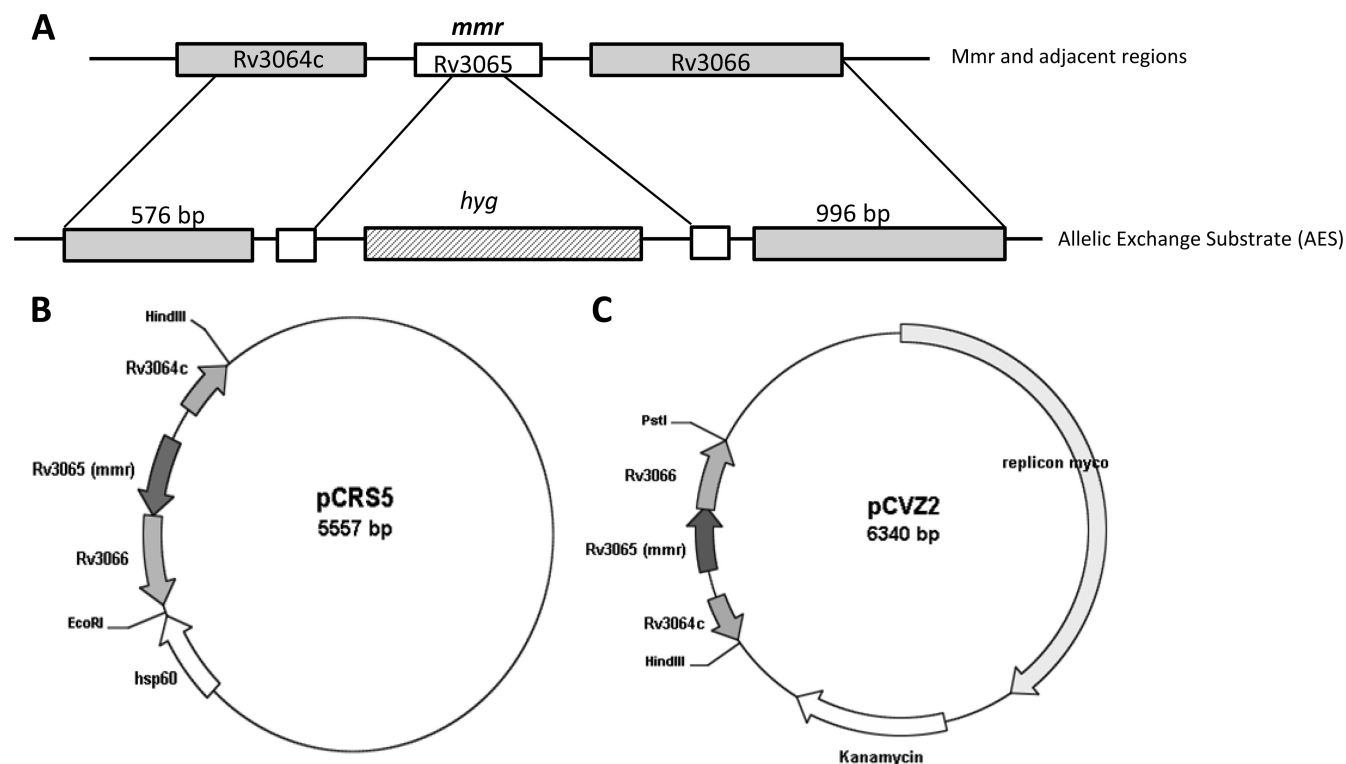
FIG 1 (A) Replacement of the *M. tuberculosis mmr* gene. An allelic exchange substrate (AES) for replacement of *mmr* (Rv3065) was generated by cloning 576-bp upstream and 996-bp downstream regions on either side of the *hyg* resistance cassette of pYUB854. The AES was obtained by PCR or restriction digestion of this segment; (B) integrative plasmid pCRS5 that contains a copy of *mmr* and that was used to complement the Mmr knockout mutant; (C) replicative plasmid pCVZ2 used to overexpress *mmr* in H37Rv.

(iii) Replicative plasmid for overexpression. An 1,177-bp DNA fragment containing the *mmr* gene was cloned into the pSUM36 vector (23) using restriction enzymes HindIII and PstI, yielding plasmid pCVZ2. Plasmid pCVZ2 was electroporated into *M. tuberculosis* H37Rv, resulting in *M. tuberculosis* H37Rv::pCVZ2 (Fig. 1C).

Neutral red staining. Neutral red staining was used to ensure that the constructed strains keep free lipids of the cell wall, such as the virulence factor phthiocerol dimycocerosates (PDIMs). Neutral red staining was performed in a test tube, as described previously (26). Briefly, mycobacterial strains were grown at 37°C on Middlebrook 7H10 medium supplemented with 10% ADC and kanamycin (20 µg/ml) or hygromycin B (50 µg/ml) when required. Bacterial cells were placed in 15-ml screw-cap tubes containing 4 ml of methanol-H_2O (1:1) and incubated at 37°C for 1 h. After centrifugation at 2,880 × *g* for 10 min, the methanol was removed and 4 ml of barbital buffer (1% sodium barbital in 5% NaCl, pH 9.8) and 150 µl of neutral red were added. The results were evaluated after 1 h and 24 h of incubation at 37°C.

Drug susceptibility assays. (i) Determination of MICs. The determination of the MICs for antibiotics, efflux inhibitors, dyes, and biocides against *M. tuberculosis* H37Rv and Mmr mutant strains was performed by the resazurin microtiter assay, as previously described (27). Ciprofloxacin, ethambutol, erythromycin, kanamycin, isoniazid, rifampin, acriflavine, ethidium bromide, safranin O, tetraphenylphosphonium, cetyltrimethylammonium bromide (CTAB), carbonyl cyanide *m*-chlorophenylhydrazone (CCCP), chlorpromazine, and verapamil were purchased from Sigma-Aldrich (Madrid, Spain) and used in the MIC determination. Briefly, mycobacterial strains were grown at 37°C in Middlebrook 7H9 broth supplemented with 10% ADC and 0.05% Tween 80 until an OD_{600} of 0.8. Mycobacterial cultures were diluted in 7H9 supplemented with ADC and 0.5% glycerol in order to obtain a final concentration of 10^5 CFU/ml. The number of CFU corresponding to aliquots of the inoculum

was routinely calculated in order to ensure a constant number of bacterial cells from experiment to experiment. Aliquots of 100 µl were transferred to each well of a 96-well plate that contained 100 µl of each compound at concentrations prepared from 2-fold serial dilutions in 7H9-ADC medium. The inoculated plates were incubated for 6 days at 37°C and for an additional 2 days after the addition of the redox indicator (30 µl of a resazurin solution at 0.1 mg/ml). A change from blue to pink indicates reduction of resazurin and therefore bacterial growth. Thus, the MIC was defined as the lowest concentration of compound that prevented this color change. The MICs of ethidium bromide, tetraphenylphosphonium, acriflavine, safranin O, and CTAB in the presence of the efflux inhibitors chlorpromazine, verapamil, and CCCP were also determined to evaluate the contribution of efflux activity to *M. tuberculosis* susceptibility to these drugs.

(ii) Determination of isoniazid susceptibility on solid medium. To determine if there was any difference between the wild type and the knockout mutant when grown in solid medium in the presence of isoniazid, aliquots of 10 µl of 10-fold serial dilutions of 10^7-CFU/ml exponential-phase cultures were spotted onto 7H10-ADC medium containing concentrations of isoniazid ranging from 0.25 to 0.03 µg/ml. The plates were incubated at 37°C until growth was observed. The assay was performed in duplicate. The results were recorded by the observation of the growth of spots of wild-type and knockout mutant bacterial cells in the isoniazid-containing plates. The highest concentration of isoniazid and the highest dilution that resulted in bacterial growth were recorded for both wild-type and knockout strains and compared. We expected that growth of bacteria at higher isoniazid concentrations than the wild type would correlate with increased ability to tolerate isoniazid.

(iii) Rate of killing. The rate of killing by isoniazid in *M. tuberculosis* H37Rv and the MmrKO mutant was determined as previously described (28). Isoniazid was diluted in 10 ml of Middlebrook 7H9 supplemented

with 10% ADC to give 2×, 4×, and 8× MIC. A drug-free control was included. Mycobacterial cultures at exponential phase were adjusted to an OD_{600} of 0.2, and 100 μl was added to each tube containing the isoniazid dilutions. On days 0, 1, 2, 4, 8, and 16, 100-μl aliquots were taken for counting of the numbers of CFU and inoculated in Middlebrook 7H10-ADC medium. The plates were incubated at 37°C until growth was observed. The assay was performed in duplicate.

(iv) Growth competition assay. The *M. tuberculosis* wild-type strain H37Rv and the MmrKO strain were used for growth competition testing in the presence of isoniazid. Briefly, three flasks containing 10 ml of Middlebrook 7H9-ADC with isoniazid at 0.25 μg/ml (1/2 MIC) were inoculated independently with H37Rv, MmrKO, and both strains, ensuring that the cell density in each flask was 10^5 CFU/ml. The three flasks were incubated at 37°C. The three cultures were serially diluted and plated in duplicate on drug-free Middlebrook 7H10-ADC medium on days 0, 2, 7, and 14. In parallel, the culture containing both the wild-type strain H37Rv and the MmrKO strain was serially diluted and plated in duplicate on 7H10-ADC medium with 50 μg/ml of hygromycin. The number of MmrKO cells in the competition assay was determined from the number of colonies grown in hygromycin-containing plates; the number of H37Rv cells in the competition assay was calculated from the number of colonies in the drug-free plates minus the number of MmrKO cells.

Detection of ethidium bromide efflux by fluorometry. The detection of ethidium bromide efflux on a real-time basis by the *M. tuberculosis* strains was performed using a fluorometric method previously described (29), but with some adaptations for use in a 96-well plate fluorometer. Briefly, *M. tuberculosis* strains were grown in 7H9-ADC medium at 37°C until an OD_{600} of 0.6 to 0.8. Cultures were centrifuged at 2,880 × *g* for 10 min, the supernatant was discarded, the pellet was washed in phosphate-buffered saline (PBS; pH 7.4), and the OD_{600} was adjusted to 0.8 with PBS with 0.05% Tween 80. Aliquots of 100 μl of bacterial suspension were transferred into wells of a 96-well plate containing serial dilutions of ethidium bromide at concentrations that ranged from 2 to 0.125 μg/ml. To determine the effect of chlorpromazine, CCCP, and verapamil on the accumulation of ethidium bromide, 10 μl of each compound was added to the corresponding well of the 96-well plate. Each inhibitor was used at 1/2 the MIC in order to not compromise the cellular viability. Relative fluorescence was acquired every 51 s for 60 min at 37°C in a Synergy HT detection microplate reader (Biotek Instruments), using 530/25 nm and 590/20 nm as excitation and detection wavelengths, respectively. For a better comparison of ethidium bromide accumulation experiments, for each assay we determined the relative final fluorescence (RFF) at the last time point (minute 60) of the assay in comparison with reference conditions by using the formula $(RF_{assay} - RF_{ref})/RF_{ref}$, where RF_{assay} is the relative fluorescence at the last time point of the ethidium bromide accumulation assay and RF_{ref} is the relative fluorescence at the last time point of the ethidium bromide accumulation assay under the reference conditions (30, 31).

When assaying different strains and mutants, the reference condition was the assay of reference strain H37Rv, whereas when assaying the effect of efflux inhibitors, the reference condition was the assay in the absence of any efflux inhibitor. In both cases, high RFF values indicated that cells accumulated more ethidium bromide under the tested conditions than under the reference conditions and vice versa for negative RFF values. RFF values correlated with the contribution of the Mmr efflux pump to the extrusion of this ethidium bromide or the degree of efflux inhibition. The experiments were repeated three times, and the RFF values presented are the averages of three independent assays.

RESULTS AND DISCUSSION

It is widely accepted that many bacterial pathogens activate efflux pumps in response to drug treatment, providing the bacterial cells with a way of adaptation to a hostile environment. This enables the bacteria to survive under such conditions, facilitating the acquisition of mutations that will confer higher and stable levels of

TABLE 2 MICs of several antimicrobial drugs against *M. tuberculosis* H37Rv and Mmr mutant strains[d]

Compound	MIC (μg/ml) for *M. tuberculosis* strain:			
	H37Rv	MmrKO[a]	MmrKO::pCRS5[b]	H37Rv::pCVZ2[c]
Antibiotics				
Isoniazid	0.25	0.25	0.25	0.25
Rifampin	0.06	0.06	0.06	0.06
Ethambutol	1.25	1.25	1.25	1.25
Kanamycin	0.15	0.07	>5[d]	>5[d]
Ciprofloxacin	0.25	0.25	0.25	0.25
Erythromycin	25	25	25	25
Efflux inhibitors				
Chlorpromazine	5	5	5	5
Verapamil	150	150	150	150
CCCP[e]	1.5	1.5	1.5	1.5
Dyes				
Ethidium bromide	2	1	2	4
Tetraphenylphosphonium	12.5	3.1	12.5	12.5
Acriflavine	3.1	3.1	3.1	6.2
Safranin O	1	0.5	1	2
CTAB[e] biocide	12.5	6.2	12.5	12.5

[a] *M. tuberculosis* H37Rv with *mmr* gene inactivated.
[b] MmrKO complemented with integrative vector pCRS5.
[c] *M. tuberculosis* H37Rv containing replicative plasmid pCVZ2.
[d] Increase of the MIC is due to the kanamycin resistance selection marker present in these strains.
[e] CCCP, carbonyl cyanide m-chlorophenylhydrazone; CTAB, cetyltrimethylammonium bromide.

drug resistance (6, 12, 32). Therefore, efflux pumps are becoming attractive for drug discovery programs, with the goal to evaluate if potential new antituberculous compounds may be subject to efflux or to identify efflux inhibitors of currently used antituberculous drugs. This is particularly relevant in a time when MDRTB and XDRTB continue to escalate and fewer alternatives are left to treat the severe forms of drug-resistant tuberculosis.

In this work, we studied the Mmr efflux pump of *M. tuberculosis*. The basis for this study was provided by previous studies that showed overexpression of *mmr* in *M. tuberculosis* strains that had been induced to isoniazid resistance by exposure to this drug for a prolonged period of time (9, 19). Although the *mmr* gene was significantly overexpressed among other overexpressed efflux pump genes present in the *M. tuberculosis* genome, a possible association between the Mmr efflux pump and isoniazid resistance was suggested (9, 19). In order to clarify the role of Mmr in the development of isoniazid resistance, as well as in the resistance to other drugs that are substrates of efflux pumps, we constructed an MmrKO mutant in the H37Rv reference strain using a recombineering method (20) and studied the drug susceptibility profile of this mutant (MmrKO), its complemented counterpart (MmrKO::pCRS5), and an H37Rv derivative strain overexpressing the *mmr* gene from a replicative plasmid (H37Rv::pCVZ2).

We determined the MICs of several compounds against the wild-type strain *M. tuberculosis* H37Rv and the Mmr mutants (Table 2). For the selected group of antibiotics, only a minor decrease in the MIC of kanamycin was observed in the knockout mutant. The remaining antibiotics presented consistent MICs that were not affected by either the inactivation or overexpression of *mmr*. In the particular case of isoniazid, no difference in the MICs was observed between the strains (MIC, 0.25 μg/ml for wild type and

TABLE 3 Effect of efflux inhibitors on the MICs of potential substrates of Mmr efflux pump

M. tuberculosis strain	MIC (μg/ml)[d]																			
	Ethidium bromide				Tetraphenylphosphonium				Acriflavine				Safranin O				CTAB			
	No inhibitor	CCCP	CPZ	VP	No inhibitor	CCCP	CPZ	VP	No inhibitor	CCCP	CPZ	VP	No inhibitor	CCCP	CPZ	VP	No inhibitor	CCCP	CPZ	VP
H37Rv[a]	2	2	2	**0.5**	12.5	**3.1**	12.5	12.5	3	1.5	3	3	1	0.5	1	0.5	12.5	**3.1**	12.5	12.5
MmrKO[a]	1	1	1	**0.13**	3.1	3.1	1.5	1.5	3	1.5	3	1.5	0.5	0.5	0.25	0.5	6.25	3.1	6.25	6.25
MmrKO::pCRS5[b]	2	2	2	1	12.5	**3.1**	12.5	12.5	3	1.5	3	3	1	0.5	1	0.5	12.5	**3.1**	12.5	12.5
H37Rv::pCVZ2[c]	4	2	4	**1**	12.5	6.2	12.5	12.5	6	**0.18**	6	6	2	**0.06**	2	2	12.5	**0.4**	12.5	12.5

[a] *M. tuberculosis* H37Rv with *mmr* gene inactivated.
[b] MmrKO complemented with pCRS5.
[c] *M. tuberculosis* H37Rv containing pCVZ2.
[d] CCCP, carbonyl cyanide *m*-chlorophenylhydrazone; CPZ, chlorpromazine; CTAB, cetyltrimethylammonium bromide; VP, verapamil. Data in bold represent at least a 4-fold reduction, considered to denote a significant MIC reduction in the presence of an efflux inhibitor.

all Mmr mutants). This was an unexpected result, since in previous studies we found overexpression of Mmr after exposure to isoniazid (9, 18, 19), strongly suggesting that this particular efflux pump could be directly related to the transport of this drug. However, we speculated that the determination of the MIC of isoniazid by 2-fold microdilution assay was possibly not sensitive enough for detecting phenotypic differences between wild type and strains with an *mmr* gene deleted or strains overexpressing the *mmr* gene.

Therefore, other approaches were used in order to clarify if the inactivation of *mmr* had an effect, even subtle, on the susceptibility to isoniazid. No difference between the wild type and the knockout mutant was observed when grown in solid medium with isoniazid; both strains grew at a dilution of 10^{-4} until a concentration of 0.06 μg/ml, and no growth was observed at 0.12 and 0.25 μg/ml of isoniazid (data not shown). The rate of killing by inhibitory concentrations of isoniazid was also determined, but no difference between the wild type and knockout strain was observed (data not shown).

Moreover, the growth competition assay showed no difference between the wild-type and mutant strains when simultaneously grown in the presence of isoniazid, with both presenting 10^6 CFU/ml after 7 days of exposure to isoniazid (data not shown).

Therefore, we can hypothesize that Mmr responds to treatment with isoniazid. Although this efflux pump would not directly transport this drug, it could instead transport any other bacterial metabolite either derived from isoniazid itself or generated in response to isoniazid-induced damage. This indicates that the *mmr* overexpression observed in the isoniazid-induced strains (9, 19) may be due to a general stress response caused by the prolonged exposure to this drug. In this case, the *M. tuberculosis* efflux pump systems would present an increased activity in order to extrude any noxious compounds that formed as a direct result of the mechanism of action of isoniazid. This confirms that isoniazid susceptibility was not affected by the inactivation of *mmr* and that the overexpression results observed in the previous studies may be due to a general response to stress rather than a result of isoniazid being a substrate of Mmr. In fact, a recent study that used a computational approach combined with gene expression data and an interactome network has suggested that the SOS response is upregulated under isoniazid treatment (33). This may affect several cellular processes, namely, the regulation of efflux pumps, and be a trigger for drug resistance. It is also possible that Mmr

could be involved in the transport of a cell wall component(s) and that overexpression of this efflux pump would occur to compensate for the cell wall damage caused by isoniazid, which targets InhA, an NADH-dependent enoyl acyl carrier protein reductase involved in the synthesis of mycolic acids (3, 4).

Concerning the other compounds tested, the MmrKO mutant showed an increased susceptibility to ethidium bromide, tetraphenylphosphonium, safranin O, and CTAB. In the particular case of ethidium bromide, the MIC was restored to the wild-type value (2 μg/ml) in the complemented strain MmrKO::pCRS5, whereas the H37Rv strain overexpressing *mmr* (H37Rv::pCVZ2) presented an increased MIC (4 μg/ml). This strain also showed an increased MIC for safranin O and acriflavine, although there was no change for the latter in the knockout mutant. These data confirm that the *mmr* gene cloned in either the integrative plasmid pCRS5 or the replicative plasmid pCVZ2 is being expressed and produces a fully functional Mmr protein. To confirm that this phenotype was in fact due to efflux activity and not to any other indirect mechanism, MICs were determined in the presence of efflux inhibitors (Table 3). Most cases of MIC reduction were obtained with CCCP, followed by verapamil. CCCP drastically reduced by more than 30 times the MICs of acriflavine, safranin O, and CTAB for the *mmr*-overexpressing strain. Since CCCP is a proton gradient uncoupler, these results demonstrate the increased dependency of this efflux pump on the proton motive force, as predicted for efflux pumps of the SMR family of transporters. An MIC reduction was observed for ethidium bromide in all strains in the presence of verapamil, and CCCP caused only a slight reduction (1 dilution) in the strain overexpressing the *mmr* gene. There was a significant reduction of the MIC of ethidium bromide (8 times) in the presence of verapamil for the knockout mutant, which suggests that other efflux pumps that extrude ethidium bromide may be active in this strain and are affected by verapamil. Chlorpromazine promoted a slight reduction of the MIC of tetraphenylphosphonium and safranin O in the knockout mutant.

Following the results obtained for the MIC determination, ethidium bromide was selected as a substrate for detecting efflux activity in *M. tuberculosis* H37Rv and its Mmr mutants. The MmrKO mutant showed a 62% maximum increased accumulation of ethidium bromide at 1 μg/ml relative to wild-type strain H37Rv, whereas overexpressed strain H37Rv::pCVZ2 showed a consistent decreased accumulation of ethidium bromide at all concentrations tested (Table 4; Fig. 2). These results are in agree-

TABLE 4 RFF based on the accumulation of ethidium bromide for each mutant strain compared to that for wild-type strain H37Rv[a]

Strain	RFF at the following ethidium bromide concn (μg/ml):				
	0.125	0.25	0.5	1	2
MmrKO	0.07	0.47	0.53	0.62	0.55
MmrKO::pCRS5	− 0.21	−0.16	−0.20	−0.25	−0.11
H37Rv:pCVZ2	−0.20	−0.20	−0.38	−0.53	−0.58

[a] The values correspond to the last point of measurement at 60 min, when fluorescence had reached a steady state. Data correspond to the averages of three independent assays.

ment with the MIC obtained for ethidium bromide for each strain and further support the possibility that the Mmr efflux activity contributes directly to the susceptibility of *M. tuberculosis* to this compound and that the absence of Mmr decreases the efflux of quaternary compounds in *M. tuberculosis*. The effect of efflux inhibitors on the accumulation of ethidium bromide was also tested in all strains using ethidium bromide at 1/2 the MIC (Fig. 3; Table 5). In general, the accumulation of ethidium bromide by wild-type, knockout mutant, and overexpressing strains in the presence of efflux inhibitors (Fig. 3; Table 5) paralleled that of the same strains in the absence of efflux inhibitors (Fig. 2; Table 4). The inhibitor that promoted higher ethidium bromide accumulation for all strains was verapamil, which is in agreement with the MIC results described above (compare the results with the MICs of ethidium bromide in the presence and absence of an inhibitor; Table 3) and with previous studies (19, 34). Surprisingly, despite not having an effect on the MIC of ethidium bromide (Table 3), chlorpromazine caused an increased accumulation of ethidium bromide in the wild-type and overexpressing strains (Fig. 3).

This work was carried out in *M. tuberculosis*, the natural host of the Mmr efflux pump, and the results largely support those of the previous studies performed in the heterologous host *M. smegmatis* that reported Mmr to be an efflux pump associated with susceptibility to a variety of compounds, such as ethidium bromide, tetraphenylphosphonium, and safranin O (15, 16). Our findings have been corroborated by the use of ethidium bromide, coupled

FIG 3 Effect of efflux inhibitors on the accumulation of ethidium bromide for *M. tuberculosis* H37Rv (A), H37Rv MmrKO (B), and H37Rv::pCVZ2 (C). Ethidium bromide and efflux inhibitors were used at 1/2 the MIC to not compromise cellular viability. CCCP, carbonyl cyanide *m*-chlorophenylhydrazone; CPZ, chlorpromazine; EPI, efflux pump inhibitor; VP, verapamil.
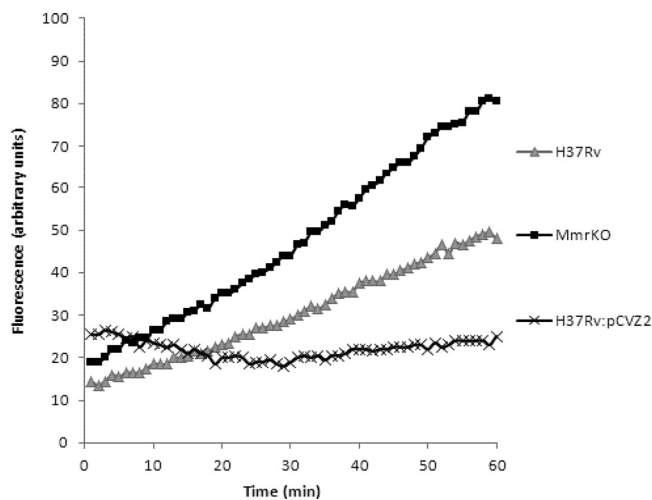

FIG 2 Accumulation of ethidium bromide at 1 μg/ml by *M. tuberculosis* H37Rv, H37Rv MmrKO (H37Rv with the *mmr* gene inactivated), and H37Rv::pCVZ2 (H37Rv containing pCVZ2).

with the use of real-time monitoring of its efflux by a fluorometric system, which was a good marker for the study of the efflux activity of Mmr and may be used to evaluate the activity of potential efflux inhibitors. In addition, this work has shown that Mmr has an effect on susceptibility to CTAB, a widely used disinfectant, demonstrating the role of efflux systems, in particular, Mmr, in *M. tuberculosis* tolerance to this class of compounds. In this case, the use of efflux inhibitors would prevent the development of this tolerance. In conclusion, the study of the Mmr efflux pump may be used as proof of concept for the demonstration of efflux activity in *M. tuberculosis*, and the strategy employed may be

TABLE 5 RFF based on the accumulation of ethidium bromide for H37Rv and each mutant strain in the presence of efflux inhibitors compared with that for the untreated control (without inhibitor)[a]

	RFF for the following efflux inhibitor:		
Strain	CCCP	CPZ	VP
H37Rv	0.17	1.60	2.05
MmrKO	0.21	−0.05	0.46
MmrKO::pCRS5	0.08	0.53	0.61
H37Rv::pCVZ2	1.42	1.05	1.9

[a] The values correspond to the last point of measurement at 60 min, when fluorescence had reached a steady state. Data correspond to the averages of three independent assays.

used to characterize other efflux pumps of *M. tuberculosis* and other mycobacteria.

REFERENCES

1. **Stop TB Partnership.** 2010. The global plan to stop TB 2011–2015. World Health Organization, Geneva, Switzerland.
2. **World Health Organization.** 2012. Global tuberculosis report 2012. World Health Organization, Geneva, Switzerland.
3. **Almeida Da Silva PE, Palomino JC.** 2011. Molecular basis and mechanisms of drug resistance in *Mycobacterium tuberculosis*: classical and new drugs. J. Antimicrob. Chemother. **66**:1417–1430.
4. **Ramaswamy S, Musser JM.** 1998. Molecular genetic basis of antimicrobial agent resistance in *Mycobacterium tuberculosis*: 1998 update. Tuber. Lung Dis. **79**:3–29.
5. **Srivastava S, Pasipanodya JG, Meek C, Leff R, Gumbo T.** 2011. Multidrug-resistant tuberculosis not due to noncompliance but to between-patient pharmacokinetic variability. J. Infect. Dis. **204**:1951–1959.
6. **Piddock LJ.** 2006. Clinically relevant chromosomally encoded multidrug resistance efflux pumps in bacteria. Clin. Microbiol. Rev. **19**:382–402.
7. **Ramón-García S, Martín C, Thompson CJ, Aínsa JA.** 2009. Role of the *Mycobacterium tuberculosis* P55 efflux pump in intrinsic drug resistance, oxidative stress responses, and growth. Antimicrob. Agents Chemother. **53**:3675–3682.
8. **Ramón-García S, Mick V, Dainese E, Martín C, Thompson CJ, De Rossi E, Manganelli R, Aínsa JA.** 2012. Functional and genetic characterization of the tap efflux pump in *Mycobacterium bovis* BCG. Antimicrob. Agents Chemother. **56**:2074–2083.
9. **Machado D, Couto I, Perdigão J, Rodrigues L, Portugal I, Baptista P, Veigas B, Amaral L, Viveiros M.** 2012. Contribution of efflux to the emergence of isoniazid and multidrug resistance in *Mycobacterium tuberculosis*. PLoS One **7**:e34538. doi:10.1371/journal.pone.0034538.
10. **Amaral L, Viveiros M, Kristiansen JE.** 2006. "Non-antibiotics": alternative therapy for the management of MDRTB and MRSA in economically disadvantaged countries. Curr. Drug Targets **7**:887–891.
11. **Rodrigues L, Aínsa JA, Amaral L, Viveiros M.** 2011. Inhibition of drug efflux in mycobacteria with phenothiazines and other putative efflux inhibitors. Recent Pat. Antiinfect. Drug Discov. **6**:118–127.
12. **Viveiros M, Martins M, Rodrigues L, Machado D, Couto I, Ainsa J, Amaral L.** 2012. Inhibitors of mycobacterial efflux pumps as potential boosters for TB drugs. Expert Rev. Anti Infect. Ther. **10**:983–998.
13. **De Rossi E, Aínsa JA, Riccardi G.** 2006. Role of mycobacterial efflux transporters in drug resistance: an unresolved question. FEMS Microbiol. Rev. **30**:36–52.
14. **Louw GE, Warren RM, Gey van Pittius NC, McEvoy CR, Van Helden PD, Victor TC.** 2009. A balancing act: efflux/influx in mycobacterial drug resistance. Antimicrob. Agents Chemother. **53**:3181–3189.
15. **De Rossi E, Branzoni M, Cantoni R, Milano A, Riccardi G, Ciferri O.** 1998. *mmr*, a *Mycobacterium tuberculosis* gene conferring resistance to small cationic dyes and inhibitors. J. Bacteriol. **180**:6068–6071.
16. **Li XZ, Zhang L, Nikaido H.** 2004. Efflux pump-mediated intrinsic drug resistance in *Mycobacterium smeg*matis. Antimicrob. Agents Chemother. **48**:2415–2423.
17. **Balganesh M, Dinesh N, Sharma S, Kuruppath S, Nair AV, Sharma U.** 2012. Efflux pumps of *Mycobacterium tuberculosis* play a significant role in antituberculosis activity of potential drug candidates. Antimicrob. Agents Chemother. **56**:2643–2651.
18. **Gupta AK, Katoch VM, Chauhan DS, Sharma R, Singh M, Venkatesan K, Sharma VD.** 2010. Microarray analysis of efflux pump genes in multidrug-resistant *Mycobacterium tuberculosis* during stress induced by common anti-tuberculous drugs. Microb. Drug Resist. **16**:21–28.
19. **Rodrigues L, Machado D, Couto I, Amaral L, Viveiros M.** 2012. Contribution of efflux activity to isoniazid resistance in the *Mycobacterium tuberculosis* complex. Infect. Genet. Evol. **12**:695–700.
20. **van Kessel JC, Hatfull GF.** 2007. Recombineering in *Mycobacterium tuberculosis*. Nat. Methods **4**:147–152.
21. **van Kessel JC, Hatfull GF.** 2008. Mycobacterial recombineering. Methods Mol. Biol. **435**:203–215.
22. **Stover CK, de LA Cruz VF, Fuerst TR, Burlein JE, Benson LA, Bennett LT, Gansal GP, Young JF, Lee MH, Hatfull GF, Snapper SB, Barletts RG, Jacobs WR, Jr, Bloom BR.** 1991. New use of BCG for recombinant vaccines. Nature **351**:456–460.
23. **Aínsa JA, Martín C, Cabeza M, De la Cruz F, Mendiola MV.** 1996. Construction of a family of *Mycobacterium/Escherichia coli* shuttle vectors derived from pAL5000 and pACYC184: their use for cloning an antibiotic-resistance gene from *Mycobacterium fortuitum*. Gene **176**:23–26.
24. **Sambrook J, Russell DW.** 2001. Molecular cloning: a laboratory manual, 3rd ed. Cold Spring Harbor Laboratory Press, Cold Spring Harbor, NY.
25. **Parish T, Stoker NG.** 1998. Mycobacterial protocols. In Parish T, Stoker NG (ed), Methods in molecular biology, vol 101. Humana Press, Totowa, NJ.
26. **Soto CY, Andreu N, Gibert I, Luquin M.** 2002. Simple and rapid differentiation of *Mycobacterium tuberculosis* H37Ra from *M. tuberculosis* clinical isolates through two cytochemical tests using neutral red and Nile blue stains. J. Clin. Microbiol. **40**:3021–3024.
27. **Palomino JC, Martin A, Camacho M, Guerra H, Swings J, Portaels F.** 2002. Resazurin microtiter assay plate: simple and inexpensive method for detection of drug resistance in *Mycobacterium tuberculosis*. Antimicrob. Agents Chemother. **46**:2720–2722.
28. **Reddy VM, Dubuisson T, Einck L, Wallis RS, Jakubiec W, Ladukto L, Campbell S, Nacy CA.** 2012. SQ109 and PNU-100480 interact to kill *Mycobacterium tuberculosis in vitro*. J. Antimicrob. Chemother. **67**:1163–1166.
29. **Rodrigues L, Wagner D, Viveiros M, Sampaio D, Couto I, Vavra M, Kern WV, Amaral L.** 2008. Thioridazine and chlorpromazine inhibition of ethidium bromide efflux in *Mycobacterium avium* and *Mycobacterium smegmatis*. J. Antimicrob. Chemother. **6**:1076–1082.
30. **Machado L, Spengler G, Evaristo M, Handzlik J, Molnár J, Viveiros M, Kiec-Kononowicz K, Amaral L.** 2011. Biological activity of twenty-three hydantoin derivatives on intrinsic efflux pump system of *Salmonella enterica* serovar Enteritidis NCTC 13349. In Vivo **25**:769–772.
31. **Paixão L, Rodrigues L, Couto I, Martins M, Fernandes P, de Carvalho CC, Monteiro GA, Sansonetty F, Amaral L, Viveiros M.** 2009. Fluorometric determination of ethidium bromide efflux kinetics in *Escherichia coli*. J. Biol. Eng. **3**:18. doi:10.2174/187221209787259910.
32. **da Silva PE, Von Groll A, Martin A, Palomino JC.** 2011. Efflux as a mechanism for drug resistance in *Mycobacterium tuberculosis*. FEMS Immunol. Med. Microbiol. **63**:1–9.
33. **Chen LC, Yeh HY, Yeh CY, Arias CR, Soo VW.** 2012. Identifying co-targets to fight drug resistance based on a random walk model. BMC Syst. Biol. **6**:5. doi:10.1186/1752-0509-6-5.
34. **Rodrigues L, Ramos J, Couto I, Amaral L, Viveiros M.** 2011. Ethidium bromide transport across *Mycobacterium smegmatis* cell-wall: correlation with antibiotic resistance. BMC Microbiol. **11**:35. doi:10.1186/1471-2180-11-35.

Annex V

Lipid Transport in *Mycobacterium tuberculosis* and its Implications in Virulence and Drug Development.

Bailo R, Bhatt A, Aínsa JA.

Annex V

Commentary

Lipid transport in *Mycobacterium tuberculosis* and its implications in virulence and drug development

Rebeca Bailo [a], Apoorva Bhatt [b], José A. Aínsa [a,*]

[a] Departamento de Microbiología, Facultad de Medicina, Universidad de Zaragoza and Instituto de Investigación Sanitaria Aragón (IIS Aragón), c/Domingo Miral s/n, 50009-Zaragoza, and Ciber de Enfermedades Respiratorias (CIBERES), Instituto de Salud Carlos III, Spain
[b] School of Biosciences, College of Life and Environmental Sciences, University of Birmingham, Edgbaston, Birmingham B15 2TT, United Kingdom

ABSTRACT

Tuberculosis is still a major health problem worldwide and one of the main causes of death by a single infectious agent. Only few drugs are really effective to treat tuberculosis, hence, the emergence of multiple, extensively, and totally drug resistant bacilli compromises the already difficult antituberculosis treatments. Given the persistent global burden of tuberculosis, it is crucial to understand the underlying mechanisms required for the pathogenicity of *Mycobacterium tuberculosis* (Mtb), the causal agent of tuberculosis, in order to pave the way for developing better drugs and strategies to treat and prevent tuberculosis.

The exclusive mycobacterial cell wall lipids such as trehalose monomycolate and dimycolate (TMM, TDM), phthiocerol dimycocerosate (PDIM), sulpholipid-1 (SL-1), diacyl trehalose (DAT), and pentacyl trehalose (PAT), among others, are known to play an important role in pathogenesis; thus, proteins responsible for their transport are potential virulence factors. MmpL and MmpS proteins mediate transport of important cell wall lipids across the mycobacterial membrane. In Mtb, MmpL3, MmpL7 and MmpL8 transport TMM, PDIM and SL-1 respectively. The translocation of DAT and biosynthesis of PAT is likely due to MmpL10. MmpL and MmpS proteins are involved in other processes such as drug efflux (MmpL5 and MmpL7), siderophore export (MmpL4/MmpS4 and MmpL5/MmpS5), and heme uptake (MmpL3 and MmpL11). Altogether, these proteins can be regarded as new potential targets for antituberculosis drug development. We will review recent advances in developing inhibitors of MmpL proteins, in the challenging context of targeting membrane proteins and the future prospects for potential antituberculosis drug candidates.

© 2015 Elsevier Inc. All rights reserved.

1. Tuberculosis along history

Mycobacterium tuberculosis (Mtb), the causative agent of tuberculosis, has been present in the human population since antiquity. Initially, it was thought that during the domestication of animals in the Neolithic period, *Mycobacterium bovis* strains from infected cattle evolved and acquired the capability of infecting humans, hence originating human tuberculosis [1]. However, it is now widely accepted that the ancients Mtb strains were originated from environmental mycobacteria 70,000 years ago in Africa [2,3]. The introduction of agriculture, civilization and the increase in human population density led to the selection of virulent and transmissible Mtb strains. These modern Mtb strains spread throughout the world causing the tuberculosis epidemics that ravaged mankind for centuries [4].

Nowadays, 9 million people fell ill with tuberculosis and 1.5 million died in 2013 (including 360,000 deaths among HIV-positive people) according to the most recent report of the World Health Organization (WHO) [5]. At present, tuberculosis is the second leading cause of death from an infectious agent worldwide, after the Human Immunodeficiency Virus (HIV), in spite of the fact that we have powerful tools in order to face tuberculosis: vaccination, diagnostics and treatments.

2. Tuberculosis treatment and drug resistance

Drug treatment is the only effective therapy for tuberculosis. Drugs are classified into three groups (Table 1) based on evidence of efficacy, potency and experience of use [6].

* Corresponding author at: Grupo de Genética de Micobacterias, Departamento de Microbiología, Facultad de Medicina, Universidad de Zaragoza, c/Domingo Miral s/n, 50009-Zaragoza, Spain. Tel.: +34 876 554343.
E-mail address: ainsa@unizar.es (J.A. Aínsa).

Table 1
Drugs used in the treatment of tuberculosis.

Groups of drugs	Drugs
First-line drugs	Isoniazid
	Rifampicin
	Pyrazinamide
	Ethambutol
	Rifapentine
	Rifabutin
Second-line drugs	Aminoglycosides
	(Streptomycin, Kanamycin, Amikacin)
	Polypeptides (Capreomycin, Viomycin)
	Fluoroquinolones (Ciprofloxacin,
	Levofloxacin, Moxifloxacin, Ofloxacin, Gatifloxacin)
	Para-aminosalicylic acid
	Cycloserine
	Terizidone
	Ethionamide
	Prothionamide
	Thioacetazone
	Linezolid
Third-line drugs	Clofazimine
	Linezolid
	Amoxicillin plus clavulanate
	Imipenem plus cilastatin
	Clarithromycin

- First-line antituberculosis drugs are the most effective and widely used drugs for the treatment of drug-susceptible tuberculosis.
- Second-line antituberculosis drugs are reserved for treating bacilli resistant to first-line therapy. A drug may be classed as second-line instead of first-line for being less effective than the first-line drugs (e.g. para-aminosalicylic acid), having toxic side-effects (e.g. cycloserine) or being effective, but unavailable in many developing countries (e.g. fluoroquinolones).
- Third-line antituberculosis drugs are characterized for being less effective (e.g. clarithromycin) or because their efficacy has not been fully proven (e.g. clofazimine).

With appropriate antibiotic treatment, around 90% of HIV-negative patients with drug-susceptible tuberculosis can be cured in 6 months using a combination of rifampicin (Rif), isoniazid (Inh), pyrazinamide (Pza) and ethambutol (Emb) for 2 months, followed by a four-month continuation phase of Rif and Inh [5]. The main reason for prescribing this combination of medicines in the treatment of tuberculosis is because the likelihood of the emergence of multiple drug resistance bacteria is virtually impossible [7], apart from the fact that the distinct antituberculosis drugs have different modes of action: Inh is bactericidal against replicating bacteria; Emb is bacteriostatic at low doses, but is used in tuberculosis treatment at higher, bactericidal doses; Rif is bactericidal and has a sterilizing effect; and Pza is only weakly bactericidal, but is very effective against bacteria located in acidic environments, inside macrophages, or in areas of acute inflammation, where they enter into a non-replicative condition. Thus, the combination of all these drugs targets all subpopulations of Mtb, i.e. those actively replicating and those in a non-replicative state.

Monotherapy, irregular drug supply, poor drug quality, inappropriate prescription, poor adherence to treatment and unsuitable supervision and support on the part of health personnel, can contribute to appearance and selection of drug-resistant Mtb strains that can disseminate and cause drug resistant tuberculosis. Depending on the drug resistance pattern, three major categories have been defined:

- Multidrug-resistant (MDR) strains are those resistant to Inh and Rif. In 2013, the highest levels of MDR tuberculosis were found in Eastern Europe and central Asia, where in some countries more than 20% of new tuberculosis cases and more than 50% of those previously treated for tuberculosis have MDR tuberculosis [5].
- Extensively drug-resistant (XDR) strains are MDR strains (i.e., resistant to Inh and Rif) that are also resistant to a quinolone and one of the second-line injectable drugs (kanamycin, amikacin or capreomycin). In 2006, the first XDR tuberculosis outbreak was described in KwaZulu-Natal in South Africa. The mortality rate among HIV-positive patients, with limited or no access to highly active antiretroviral therapy was 98%, after a median survival period from diagnosis of only 16 days [8].
- Totally drug-resistant (TDR) refers to strains that are resistant to all available tuberculosis drugs, although the number and level of resistance to each drug has not yet been precisely defined. To date, only a limited number of TDR tuberculosis cases have been confirmed in Iran, India, South Africa and Italy [9].

All these are cases of acquired resistance [7]. The mechanisms by which bacteria in general acquired drug resistance are: barrier mechanisms (decreased permeability/increased efflux), degrading/inactivating enzymes, modification of pathways involved in drug activation/metabolism, and drug target modification (mutations) or target amplification [10]. Mtb in particular is able to acquire drug resistance by spontaneous mutations in chromosomal genes then leading to target modification, target amplification, reduced ability for activating drugs, or increased capacity for inactivating drugs (Table 2); no horizontal transfer of resistance genes has been reported [11].

3. Mycobacterial cell envelope: biochemically complex, pharmacologically interesting

The mycobacterial envelope is unique, both in molecular composition and in the architectural arrangement of its constituents (Fig. 1; adapted from [12,13]). Its complex structure is composed of a typical phospholipid bilayer plasma membrane, an outer membrane called mycomembrane, and an outermost layer known as the capsule. The plasma membrane is composed mainly of anionic phospholipids in a bilayer arrangement with proteins. The mycomembrane consists of an asymmetric lipid bilayer made of long chain (C60-C90) mycolic fatty acids in the inner leaflet, and free intercalating glycolipids and waxy components on the outer leaflet. Cryo-electron microscopy images support a folded or compact configuration of these mycolic chains, which reminiscent of Gram-negative bacterial cell walls [14–16], and also confirm that the measured thickness of the outer membrane is consistent with the size of mycobacterial porins, such as MspA from *M. smegmatis*, which may therefore form channels in this bilayer [14]. The outer and inner membrane form a periplasmic space, with the presence of a thin layer of peptidoglycan covalently linked to arabinogalactan and lipoarabinomannan, which in turn are bound to mycolic acids. Peptidoglycan, arabinogalactan and mycolic acids form the cell wall skeleton. The capsule is mainly composed of polysaccharides, proteins and small amounts of lipids, and it is considered to have a different molecular composition in pathogenic and non-pathogenic species [17]. The outermost layer is visible in conventional electron microscopy preparations only when cultures have been grown in free detergent medium. It is thought that mycobacterial growth under laboratory routine culturing conditions (with a detergent as Tween-80) promotes removing of this layer [13].

The mycobacterial envelope is involved in important roles, such as defining the shape of the cell and providing mechanical and osmotic protection. Its unusual high hydrophobicity makes it an efficient barrier for chemotherapeutic agents. Other important function is the transport of molecules, including nutrients, ions and

Table 2

The commonly used antituberculosis drugs with the genes associated with their respective resistance and major mechanism.

Drug or drug class	Mechanism of action	Genes associated with drug resistance	Gene number[*]	Protein function	Mechanism of drug resistance
Rifamycins (rifampicin, rifabutin, etc.)	Inhibition of RNA synthesis	rpoB	Rv0667	RNA polymerase ß-subunit	Target modification
Isoniazid	Inhibition of mycolic acid biosynthesis and multiple effects in DNA, lipids, carbohydrates, and NAD metabolism	katG	Rv1908c	Catalase-peroxidase enzyme	Decreased drug activation
		inhA	Rv1484	NADH-dependent enoyl-acyl carrier protein	Target amplification or modification
Pyrazinamide	Depletion of membrane energy and other effects	pncA	Rv2043c	Pyrazinamidase	Decreased drug activation
Ethambutol	Inhibition of arabinogalactan synthesis	embCAB	Rv3793-5	Arabinosyltransferases	Target modification
Streptomycin	Inhibition of protein synthesis	rpsL rrs gidB	Rv0682 MTB000019 Rv3919c	12S ribosomal protein 16S rRNA 7-Methylguanosine methyltransferase	Target modification Target modification Target modification
Kanamycin/amikacin	Inhibition of protein synthesis	rrs eis	MTB000019 Rv2416c	16S rRNA Aminoglycoside acetyltransferase	Target modification Increased drug inactivation
Capreomycin	Inhibition of protein synthesis	rrs tlyA	MTB000019 Rv1694	16S rRNA rRNA methyltransferase	Target modification Target modification
Quinolones	Inhibition of DNA gyrase	gyrA gyrB	Rv0006 Rv0005	DNA gyrase A DNA gyrase B	Target modification Target modification
Ethionamide	Inhibition of mycolic acid synthesis	ethA	Rv3854c	Mono-oxygenase	Decreased drug activation
		ethR	Rv3855	Transcriptional regulatory repressor protein (TetR family)	Decreased drug activation
		inhA	Rv1484	NADH-dependent enoyl-acyl carrier protein	Target amplification and modification
Para-aminosalicylic acid	Inhibition of folic acid and iron metabolism	thyA	Rv2764c	Thymidylate synthase	
		ribD	Rv2671	Enzyme in riboflavin biosynthesis	
Cycloserine	Peptidoglycan biosynthesis	alr ddl cycA	Rv3423c Rv2981c Rv1704c	Alanine racemase D-Alanine-D-alanine ligase Bacterial D-serine/L- and D-alanine/glycine/D-cycloserine proton symporter	
Bedaquiline	Inhibition of ATP synthesis	atpE	Rv1305	ATP synthase	Target modification
Linezolid	Inhibition of protein synthesis	rrl rplC	MTB000020 Rv0701	23S rRNA 50S ribosomal protein L3	Target modification Target modification

[*]Gene numbers are given according to Tuberculist database (http://tuberculist.epfl.ch/).

toxic metabolites. During infection, cell-wall compounds have been shown to trigger a set of biological effects including adjuvanticity, toxicity, immune down-modulation, and arrest of phagosome maturation [18]. For these reasons, antitubercular drugs acting by inhibiting biosynthesis or assembly of mycobacterial cell envelope components are very effective antituberculosis drugs. This is the case of Inh, one of the two major drugs in tuberculosis treatment, and ethionamide: both are prodrugs that need activation by catalase-peroxidase (KatG) and mono-oxygenase (EthA), and their active products inhibit InhA, and enzyme involved in mycolic acids biosynthesis; similarly, Emb directly blocks biosynthesis of arabinan and its assembly into the bacterial arabinogalactan. Since these three drugs (Inh, ethionamide, and Emb) inhibit biosynthesis of cell wall components that are exclusive of mycobacteria and a few related genera, these drugs are extremely specific for mycobacterial pathogens, having little (if any) activity against other bacterial pathogens.

In addition to mycolic acids, there are many other lipids that are also very important components of the mycobacterial cell wall, most of them being exclusive for mycobacteria. Among them can be found trehalose dimycolate (TDM), often referred as cord factor, trehalose monomycolate (TMM), glucose monomycolate (GMM), glycerol monomycolate, diacyl trehaloses (DAT), triacyl trehaloses (TAT), pentacyl trehaloses (PAT), the recently characterized family of mannosyl-β-1-phosphomycoketides, sulpholipids (SLs), phenolic glycolipids (PGLs) and phthiocerol dimycocerosate (PDIM). Other major glycolipids are lipomannan (LM), lipoarabinomannan (LAM) and phosphatidylinositol mannosides (PIMs). The importance of lipids for mycobacteria must be regarded from a double point of view: on the one hand, they contribute to the structure of the mycobacterial cell envelope, and in addition, many lipids have important roles in pathogenesis. A well-known example of this is PDIM, which is found only in pathogenic mycobacteria; PDIM is essential during the early step of infection when bacilli encounter
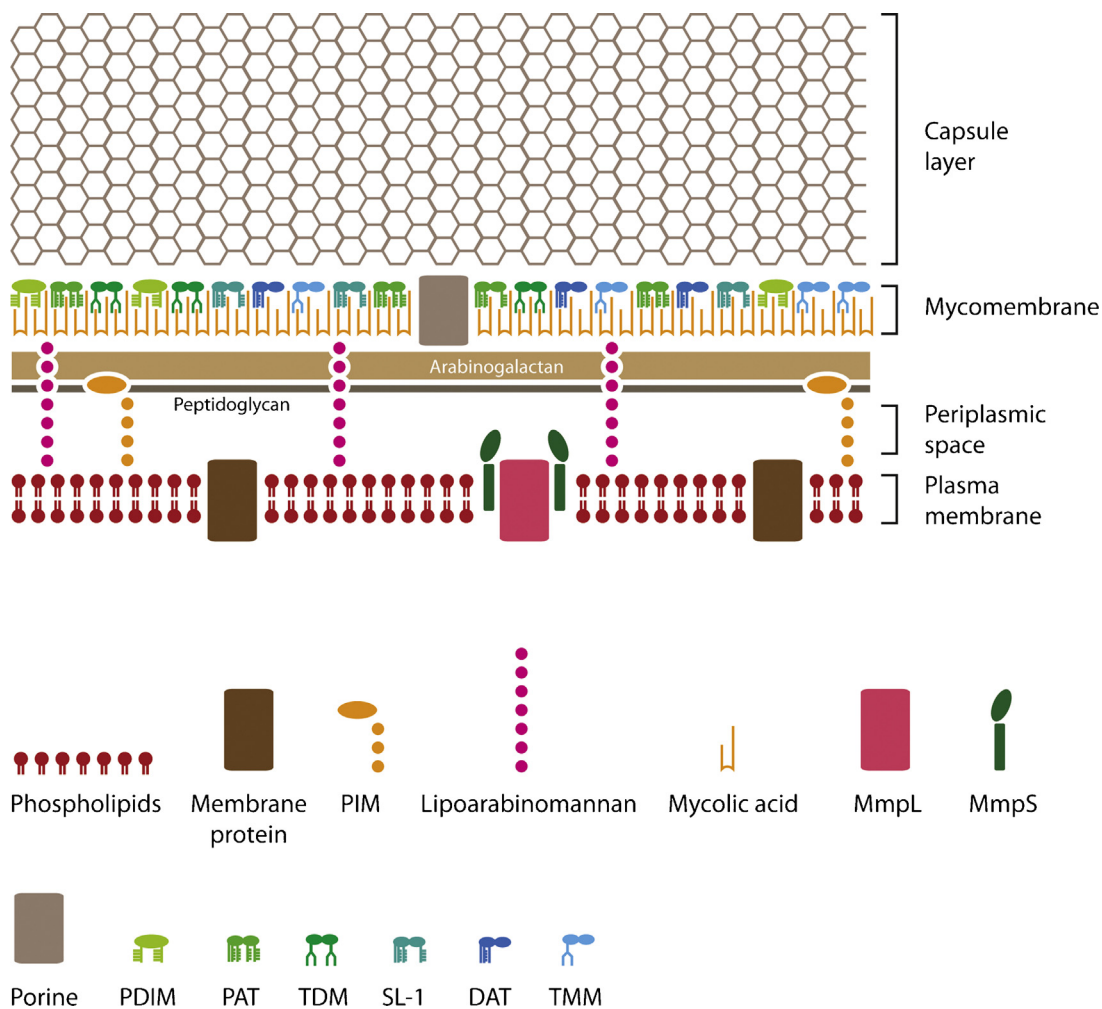
Fig. 1. Cell envelope of *Mycobacterium tuberculosis*.

their host macrophages. In fact, mutant Mtb strains defective in genes encoding enzymes that take part in biosynthesis of PDIM (such as FadD26, FadD28 enzymes in cooperation with polyketide synthases) or in PDIM transport (such as DrrC protein, which forms an ABC transporter along with DrrA and DrrB) showed attenuated phenotypes in mice [19,20]. Similarly, PIMs and mannose-capped lipoarabinomannan (Man-LAM) both interfere with phagosome maturation [21].

In summary, proper localization of lipids in the mycobacterial cell wall, mostly in the outermost layer, is needed for their role in pathogenicity, thus making transport of lipids an essential process in mycobacterial cells. Proteins transporting lipids are therefore important virulence factors and attractive drug targets.

4. Proteins for lipid transport in *M. tuberculosis*

Efflux pumps are membrane proteins that transport actively a wide variety of compounds across bacterial envelope. They have been classified into five superfamilies: ATP-binding cassette (ABC), major facilitator super-family (MFS), resistance nodulation division (RND), small multidrug resistance (SMR) and multidrug and toxic-compound extrusion (MATE). While MFS, SMR, RND and MATE members are secondary transporters, typically energized by the proton motive force (H^+ or Na^+), members of the ABC superfamily use ATP as the energy source and are considered as primary transporters [22]. Whereas efflux pumps are mostly known because of the transport of drugs from the cytoplasm, other efflux pump substrates are sugars, lipids, proteins, synthetic compounds, toxic metabolites, host-defence molecules, virulence factors, etc. Such a heterogeneous substrate profile allows bacterial efflux pumps to play diverse roles in drug resistance, virulence, bacterial cell physiology, and detoxification [22], among others.

Mce proteins are ABC transporters implicated in virulence. The Mce proteins are encoded by the *mce1*, *mce2*, *mce3* and *mce4* operons in the genome of Mtb. The involvement of Mce4 transport system in cholesterol import and intracellular survival has been confirmed [23,24], but the role of *mce1*, *mce2* and *mce3* operons is not clearly established, especially in the case of the *mce3* operon. As regards to *mce1* operon, it has been suggested that these proteins may serve as a mycolic acid re-importer [25], and *mce2* operon might be related in sulpholipid transport [26]. Due to their most probable implication in lipid metabolism, the Mce proteins may modulate pathogenicity through changes in Mtb lipid pathways.

5. A special case for lipid transport: the MmpL and MmpS families of proteins

The transport of lipids in Mtb is predominantly via a family of proteins termed MmpL proteins (Mycobacterial Membrane Protein Large) belonging to the RND family of membrane proteins. The Mtb genome possesses 15 different genes encoding for RND proteins [27], 13 of which belong to MmpL (Table 3) protein family. Mutants with disruptions in *mmpL2*, *mmpL4*, *mmpL5*, *mmpL7*, *mmpL8*,

Table 3
MmpL and MmpS proteins of *Mycobacterium tuberculosis* H37Rv.

Name	Rv number	Protein length (amino acids)
MmpL1	Rv0402c	958
MmpL2	Rv0507	968
MmpL3	Rv0206c	944
MmpL4	Rv0450c	967
MmpL5	Rv0676c	964
MmpL6	Rv1557	397
MmpL7	Rv2942	920
MmpL8	Rv3823c	1089
MmpL9	Rv2339	962
MmpL10	Rv1183	1002
MmpL11	Rv0202c	966
MmpL12	Rv1522c	1146
MmpL13a	Rv1145	303
MmpL13b	Rv1146	470
MmpS1	Rv0403c	142
MmpS2	Rv0506	147
MmpS3	Rv2198c	299
MmpS4	Rv0451c	140
MmpS5	Rv0677c	142

mmpL10, and *mmpL11* showed significant attenuation for growth in mice lungs [20,28–30]. Notably, the first Mtb genome also revealed that many clusters harbouring polyketide synthase genes with a known or putative role in lipid biosynthesis also contained an *mmpL* gene suggesting that the function of the *mmpL* gene was associated with the cognate lipid species produced by the enzymes encoded by the cluster. The first role for MmpLs in lipid transport was demonstrated by Cox et al. [31] who isolated an *mmpL7* mutant from a signature-tag mutagenesis screen. The mutant was found to be defective in PDIM transport and found to accumulate the complex lipid intracellularly [31]. *mmpL7* is present in the same cluster that encodes enzymes responsible for the biosynthesis of the pthiocerol (*ppsA-E*) and mycocerosic acid (*mas*) moieties of PDIM. Subsequently, another MmpL protein, MmpL8 was shown to be involved in the transport of SLs [29,32]. Interestingly, while no sulpholipid-1 (SL-1) was detected in the cell envelope of Mtb, the *mmpL8* mutant accumulated an intermediate of SL-1, termed SL-1278, indicating that some, if not all MmpLs were involved in transporting intermediates, which were consequently processed further outside the cell [29,32].

More recently, the functions of other *mmpL* genes have been deciphered. MmpL10 was shown to be involved in the translocation of acylated trehaloses; loss of *mmpL10* function led to intracellular accumulation of DATs [33]. Additionally, PATs were missing from the cell surface, indicating that the translocation of DATs by MmpL10 was likely required for the subsequent acylation of DAT substrates to yield extracellular PATs. MmpL proteins are also involved in the transport of mycolic acid derived lipids. *mmpL3*, the only essential *mmpL* gene in Mtb was shown to be involved in the transport of TMM [34,35] using a conditional mutant of the *mmpL3* homologue of *Mycobacterium smegmatis*. Furthermore, *mmpL11*, located in the same cluster as *mmpL3* was shown to be involved in the export of monomeromycolyl diacylglycerol (MMDAG) [36].

There is also a growing line of evidence that suggests the MmpLs are not just transporters, but may be involved in the formation of membrane-associated scaffolds that facilitate the coupling of lipid biosynthesis with transport. Four *mmpL* containing clusters in Mtb also contain a gene encoding an MmpS protein (Mycobacterial Membrane Protein Small). In *M. smegmatis*, MmpS4 was shown to be required for biosynthesis and export of a surface exposed glycopeptidolipid [37]. A domain of MmpL7 was shown to interact PpsE, an enzyme involved in PDIM biosynthesis [38]. MmpL3 was also shown to co-localise

with meromycolate producing FAS-II complex components at the septa and poles of the mycobacterial cell [39].

6. Other roles for MmpL and MmpS proteins in *M. tuberculosis*

Besides lipid transport, MmpL and MmpS proteins are involved in other bacterial processes, including drug resistance and siderophore export [40] (MmpL4/MmpS4 and MmpL5/MmpS5), and heme uptake [41,42] (MmpL3 and MmpL11); the acquisition of iron is an essential attribute of pathogenic bacteria so as to establish a successful infection.

6.1. Drug resistance

Early studies suggested that MmpL proteins did not play a significant role in intrinsic resistance to drugs in Mtb [30]; although this seems to be the general case, a few examples have been reported recently involving MmpL proteins in resistance to certain drugs. The MmpL5-MmpS5 proteins were originally characterised for their contribution to drug resistance in Mtb, which was mediated by active efflux of econazole and other substrates from cells [43]. In recent years, these proteins were linked to cross-resistance between clofazimine (a traditional drug to treat leprosy, which is also considered as a third-line drug for use against drug resistant tuberculosis) and bedaquiline (a recently approved drug for treatment of MDR tuberculosis) [44,45]. In all cases, drug resistance was mediated by increased transcription of these two genes, mediated by mutations in a regulatory protein encoded by *rv0678* gene; the latter could probably regulate as well expression of *mmpL4–mmpS4* and *mmpL2–mmpS2* [46].

Evidences about a role for MmpL7 transporter in isoniazid resistance are still controversial: isoniazid readily increases transcription of *mmpL7* gene in Mtb [47], although overexpression of *mmpL7* gene only resulted in resistance to isoniazid in the heterologous host *M. smegmatis* [48].

The link between MmpL3 and drug resistance seems to be indirect and has not been fully characterised yet. MmpL3 interacts with Wag31 protein as a part of a large network of interactions between proteins involved in fatty acid metabolism; as a consequence of Wag31 knock-down, resistance to lipophilic drugs was altered [49].

6.2. Iron acquisition

Mtb has developed two strategies for acquiring iron when infecting the human host, and MmpL proteins play an important role in both pathways. First, a secreted protein, Rv0203, binds heme groups (an abundant iron source in mammalian tissues and proteins) in the outside of the bacteria, and then transfer it to MmpL3 and MmpL11 proteins that will transport iron-containing heme groups through the mycobacterial membrane into the cytoplasm, where MhuD protein will degrade heme group releasing its iron content [41]. Second strategy consists on producing and exporting siderophores (mycobactins and carboxymycobactins) that will bind non-heme iron outside the bacterial cell. MmpS4 and MmpS5 proteins resulted essential for producing and releasing siderophores, hence indicating a role for MmpL4-MmpS4 and MmpL5-MmpS5 protein complexes in exporting siderophores in Mtb [40]. Iron-containing siderophores are subsequently uptaken by a pathway independent of MmpL4-MmpS4 and MmpL5-MmpS5, which complete the siderophore recycling system; in those mutants lacking MmpS4 and MmpS5 proteins, siderophores then accumulate in the cytoplasm resulting in lethality for the bacteria [50].
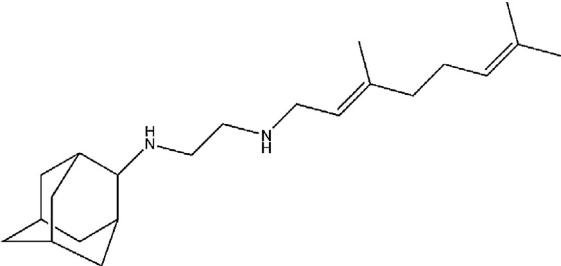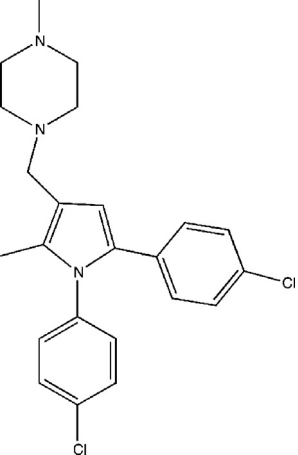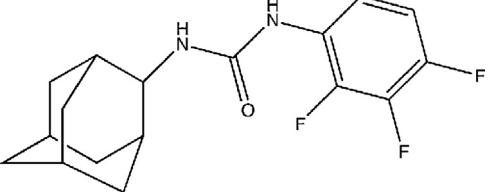
6   R. Bailo et al./Biochemical Pharmacology xxx (2015) xxx–xxx

Table 4
Inhibitors of MmpL3.
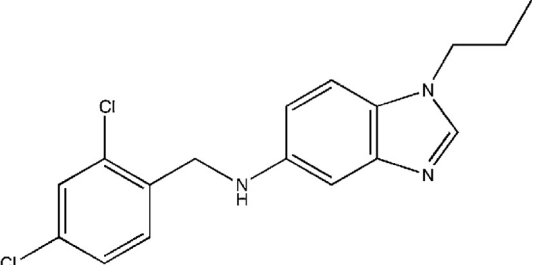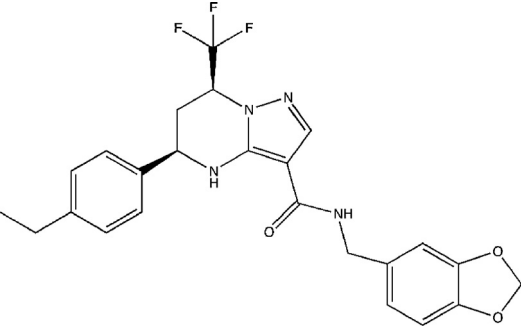
Drug	Structure	References
SQ109		[54]
1,5-diarylpyrrole derivatives (BM212)		[55,58]
Adamantyl ureas (AU1235)		[34,57,61]
Benzimidazole (C215)		[62]
Tetrahydropyrazolo[1,5-a]pyrimidine-3-carboxamides (THPPs)		[60]

Table 4 (*Continued*)

Drug	Structure	References
N-benzyl-6′,7′-dihydrospiro [piperidine-4,4′-thieno[3,2-c]pyrans]		[60]
Indolecarboxamides		[56,59]

7. Inhibitors of MmpL proteins: new drugs for the future?

MmpL proteins have been investigated for their contribution to virulence, drug resistance, and other processes in Mtb for more than a decade, but it was just in the last three years when MmpL3 (that had been predicted to be the only essential protein of this family [30]) emerged as a drug target. From 2012, several families of structurally different chemical entities have been shown to inhibit MmpL3 (Table 4) opening a new field in the inhibition of mycolic acids transport [34,51–62]. Notably, compound SQ109, which was identified a decade ago in a combinatorial chemistry-based search for ethambutol analogues, currently on phase III of clinical trials, was revealed as an inhibitor of MmpL3 [54].

Discovering a brand new drug target in Mtb along with 7 new families of potential inhibitory compounds in such a short period of time seemed like a success in antituberculosis drug discovery never before seen. Further investigation into their mechanism of action demonstrated that most of these compounds are also targeting several enzymes in the menaquinone biosynthesis pathway and electron transport chain; as a consequence, respiration and ATP synthesis were inhibited and the transmembrane electrochemical proton gradient (the energy source in many transport processes) were abolished [63,64]. Then, since multiple protein targets can be affected simultaneously, the probability of selection of resistant mutants remains very low for most of these compounds. Also, given that the electrochemical gradient, a general process in many cells, is targeted, compounds in this group such as SQ109, BM212 [55,58] and the THPPs [60] have shown to be active against other bacterial and fungal pathogens lacking mycolic acids and MmpL3-related targets. In any case, the activity of these compounds against drug resistant and MDR isolates of Mtb and their synergy with current antituberculosis therapy (notably in the case of SQ109) makes conceivable the possibility to shorten current antituberculosis treatment, one of the key points that will be essential in the near future to control this terrible disease.

8. Future directions: the impact of MmpL proteins and lipid transport in antituberculosis drug discovery

For decades, the role of transport proteins in drug resistance in Mtb was considered to be marginal. While most of resistant strains, isolated from clinical specimens or selected under laboratory conditions, carried mutations in genes encoding target proteins or activating enzymes, concerning efflux pumps the situation was far distant to that in Gram-negative bacteria, where efflux-mediated drug resistance is prominent in many pathogens [65].

Being enthusiastic about the role of transport proteins in drug resistance, we suggested that efflux pumps could have a role in transporting new drugs in development, and hence they should be taken into account in antituberculosis drug discovery programmes [66]. Recently, several publications have confirmed this hypothesis, and transport proteins were genetically related with resistance to peptidoglycan synthesis inhibitors [67] and several other families of new compounds with antituberculosis activity [68,69]. Notably, among a series of spectinomycin derivatives, the most active molecules were those that escaped transport by the Rv1258c efflux pump [70]. Similarly, this has been the case for the MmpL5 protein since it has been demonstrated to transport bedaquiline [44,45]. Altogether, it becomes clear that efflux transporters must be taken into consideration in any tuberculosis drug discovery programs in order to estimate the likelihood of the new molecules for being transported out of bacterial cells.

One of the most successful approaches in antimicrobial therapy has been the combination of beta-lactam antibiotics with inhibitors of beta-lactamases, and this has inspired a similar strategy for drug transport proteins [66,71]. For years, this approached seemed unrealistic, given the toxicity of most efflux inhibitors, which remained useful only under laboratory conditions to demonstrate efflux mechanism. However, discovery of several MmpL3 inhibitors on recent years has brought the attention back to this field. Being a transport protein of the RND superfamily, MmpL3 is however rather distinct from conventional efflux pumps of the same family such as AcrAB-TolC from *E. coli*, in

terms of substrate specificity and transport activity: whereas AcrAB-TolC has a clear role in detoxification by transporting out antibiotics and other noxious products, MmpL3 has a major role as both a trehalose monomycolate (TMM) transporter (hence contributing to the assembly of mycobacterial cell envelope) and a heme importer [34,35,42]. It is tempting to believe that inhibiting a protein involved in two such different and important pathways is like having found the Achilles' heel of Mtb. In addition, since several of these MmpL3 inhibitors act by dissipating the proton gradient, which is the energy source used by MmpL3 itself and many other transport proteins [63,64], it is expected that lipid transport in general (not only TMM transport) would be greatly affected, given the implication of other MmpL proteins in the transport of other essential lipids (PDIM in the case of MmpL7, sulpholipid-1 in the case of MmpL8, acylated trehaloses in the case of MmpL10, and monomeromycolyl diacylglycerol in the case of MmpL11).

In summary, MmpL proteins have emerged also as attractive drug targets in Mtb, given their pivotal role in lipid transport (and other essential processes) in this pathogen. Including specifically MmpL proteins in drug discovery programmes could be challenging, given the intrinsic difficulty to work with membrane proteins, but this should be overcome by the expectations of finding a new effective drug candidate against tuberculosis.

Conflicts of interest

The authors declare no conflicts of interest.

Acknowledgements

References

[1] A.G. Nerlich, S. Losch, Paleopathology of human tuberculosis and the potential role of climate, Interdiscip. Perspect. Infect. Dis. 2009 (2009) 437187.
[2] I. Comas, M. Coscolla, T. Luo, S. Borrell, K.E. Holt, M. Kato-Maeda, et al., Out-of-Africa migration and Neolithic coexpansion of Mycobacterium tuberculosis with modern humans, Nat. Genet. 45 (2013) 1176–1182.
[3] P. Supply, M. Marceau, S. Mangenot, D. Roche, C. Rouanet, V. Khanna, et al., Genomic analysis of smooth tubercle bacilli provides insights into ancestry and pathoadaptation of Mycobacterium tuberculosis, Nat. Genet. 45 (2013) 172–179.
[4] S. Gagneux, Host-pathogen coevolution in human tuberculosis, Philos. Trans. R. Soc. Lond. B Biol. Sci. 367 (2012) 850–859.
[5] WHO. Global tuberculosis report 2014. World Health Organization, 2014.
[6] A. Zumla, P. Nahid, S.T. Cole, Advances in the development of new tuberculosis drugs and treatment regimens, Nat. Rev. Drug Discov. 12 (2013) 388–404.
[7] WHO/IUATLD. Anti-tuberculosis drug resistance in the world. Report no. 2. Prevalence and Trends, 2000.
[8] N.R. Gandhi, A. Moll, A.W. Sturm, R. Pawinski, T. Govender, U. Lalloo, et al., Extensively drug-resistant tuberculosis as a cause of death in patients co-infected with tuberculosis and HIV in a rural area of South Africa, Lancet 368 (2006) 1575–1580.
[9] K. Dheda, T. Gumbo, N.R. Gandhi, M. Murray, G. Theron, Z. Udwadia, et al., Global control of tuberculosis: from extensively drug-resistant to untreatable tuberculosis, Lancet Respir. Med. 2 (2014) 321–338.
[10] K.A. Cohen, W.R. Bishai, A.S. Pym, Molecular basis of drug resistance in Mycobacterium tuberculosis, Microbiol. Spect. (2014) 2.
[11] Almeida Da Silva PE, Palomino JC. Molecular basis and mechanisms of drug resistance in Mycobacterium tuberculosis: classical and new drugs. J. Antimicrob. Chemother. 2011;66:1417–1430.
[12] H. Ouellet, J.B. Johnston, P.R. de Montellano, Cholesterol catabolism as a therapeutic target in Mycobacterium tuberculosis, Trends Microbiol. 19 (2011) 530–539.
[13] M. Sani, E.N. Houben, J. Geurtsen, J. Pierson, K. de Punder, M. van Zon, et al., Direct visualization by cryo-EM of the mycobacterial capsular layer: a labile structure containing ESX-1-secreted proteins, PLoS Pathog. 6 (2010) e1000794.
[14] C. Hoffmann, A. Leis, M. Niederweis, J.M. Plitzko, H. Engelhardt, Disclosure of the mycobacterial outer membrane: cryo-electron tomography and vitreous sections reveal the lipid bilayer structure, Proc. Natl. Acad. Sci. U.S.A. 105 (2008) 3963–3967.
[15] B. Zuber, M. Chami, C. Houssin, J. Dubochet, G. Griffiths, M. Daffe, Direct visualization of the outer membrane of mycobacteria and corynebacteria in their native state, J. Bacteriol. 190 (2008) 5672–5680.
[16] W. Groenewald, M.S. Baird, J.A. Verschoor, D.E. Minnikin, A.K. Croft, Differential spontaneous folding of mycolic acids from Mycobacterium tuberculosis, Chem. Phys. Lipids 180 (2014) 15–22.
[17] A. Lemassu, A. Ortalo-Magne, F. Bardou, G. Silve, M.A. Laneelle, M. Daffe, Extracellular and surface-exposed polysaccharides of non-tuberculous mycobacteria, Microbiology 142 (Pt 6) (1996) 1513–1520.
[18] L.M. Lopez-Marin, Nonprotein structures from mycobacteria: emerging actors for tuberculosis control, Clin. Dev. Immunol. 2012 (2012) 917860.
[19] M.A. Forrellad, L.I. Klepp, A. Gioffre, Sabio, J. Garcia, H.R. Morbidoni, M. de la Paz Santangelo, et al., Virulence factors of the Mycobacterium tuberculosis complex, Virulence 4 (2012) 3–66.
[20] L.R. Camacho, D. Ensergueix, E. Perez, B. Gicquel, C. Guilhot, Identification of a virulence gene cluster of Mycobacterium tuberculosis by signature-tagged transposon mutagenesis, Mol. Microbiol. 34 (1999) 257–267.
[21] A.K. Mishra, N.N. Driessen, B.J. Appelmelk, G.S. Besra, Lipoarabinomannan and related glycoconjugates: structure, biogenesis and role in Mycobacterium tuberculosis physiology and host-pathogen interaction, FEMS Microbiol. Rev. 35 (2011) 1126–1157.
[22] X.Z. Li, H. Nikaido, Efflux-mediated drug resistance in bacteria: an update, Drugs 69 (2009) 1555–1623.
[23] A.K. Pandey, C.M. Sassetti, Mycobacterial persistence requires the utilization of host cholesterol, Proc. Natl. Acad. Sci. U.S.A. 105 (2008) 4376–4380.
[24] M.D. Miner, J.C. Chang, A.K. Pandey, C.M. Sassetti, D.R. Sherman, Role of cholesterol in Mycobacterium tuberculosis infection, Indian J. Exp. Biol. 47 (2009) 407–411.
[25] M.A. Forrellad, M. McNeil, L. Santangelo Mde, F.C. Blanco, E. Garcia, L.I. Klepp, et al., Role of the Mce1 transporter in the lipid homeostasis of Mycobacterium tuberculosis, Tuberculosis (Edinb) 94 (2014) 170–177.
[26] O. Marjanovic, A.T. Iavarone, L.W. Riley, Sulfolipid accumulation in Mycobacterium tuberculosis disrupted in the mce2 operon, J. Microbiol. 49 (2011) 441–447.
[27] I.T. Paulsen, TransportDB, 2002 http://www.membranetransport.org/.
[28] G. Lamichhane, S. Tyagi, W.R. Bishai, Designer arrays for defined mutant analysis to detect genes essential for survival of Mycobacterium tuberculosis in mouse lungs, Infect. Immun. 73 (2005) 2533–2540.
[29] S.E. Converse, J.D. Mougous, M.D. Leavell, J.A. Leary, C.R. Bertozzi, J.S. Cox, MmpL8 is required for sulfolipid-1 biosynthesis and Mycobacterium tuberculosis virulence, Proc. Natl. Acad. Sci. U.S.A. 100 (2003) 6121–6126.
[30] P. Domenech, M.B. Reed, C.E. Barry 3rd., Contribution of the Mycobacterium tuberculosis MmpL protein family to virulence and drug resistance, Infect. Immun. 73 (2005) 3492–3501.
[31] J.S. Cox, B. Chen, M. McNeil, W.R. Jacobs Jr., Complex lipid determines tissue-specific replication of Mycobacterium tuberculosis in mice, Nature 402 (1999) 79–83.
[32] P. Domenech, M.B. Reed, C.S. Dowd, C. Manca, G. Kaplan, C.E. Barry 3rd., The role of MmpL8 in sulfatide biogenesis and virulence of Mycobacterium tuberculosis, J. Biol. Chem. 279 (2004) 21257–21265.
[33] J.M. Belardinelli, G. Larrouy-Maumus, V. Jones, L.P. Sorio de Carvalho, M.R. McNeil, M. Jackson, Biosynthesis and translocation of unsulfated acyltrehaloses in Mycobacterium tuberculosis, J. Biol. Chem. 289 (2014) 27952–27965.
[34] A.E. Grzegorzewicz, H. Pham, V.A. Gundi, M.S. Scherman, E.J. North, T. Hess, et al., Inhibition of mycolic acid transport across the Mycobacterium tuberculosis plasma membrane, Nat. Chem. Biol. 8 (2012) 334–341.
[35] C. Varela, D. Rittmann, A. Singh, K. Krumbach, K. Bhatt, L. Eggeling, et al., MmpL genes are associated with mycolic acid metabolism in mycobacteria and corynebacteria, Chem. Biol. 19 (2012) 498–506.
[36] S.A. Pacheco, F.F. Hsu, K.M. Powers, G.E. Purdy, MmpL11 protein transports mycolic acid-containing lipids to the mycobacterial cell wall and contributes to biofilm formation in Mycobacterium smegmatis, J. Biol. Chem. 288 (2013) 24213–24222.
[37] C. Deshayes, H. Bach, D. Euphrasie, R. Attarian, M. Coureuil, W. Sougakoff, et al., MmpS4 promotes glycopeptidolipids biosynthesis and export in Mycobacterium smegmatis, Mol. Microbiol. 78 (2010) 989–1003.
[38] M. Jain, J.S. Cox, Interaction between polyketide synthase and transporter suggests coupled synthesis and export of virulence lipid in M. tuberculosis, PLoS Pathog. 1 (2005) e2.
[39] C. Carel, K. Nukdee, S. Cantaloube, M. Bonne, C.T. Diagne, F. Laval, et al., Mycobacterium tuberculosis proteins involved in mycolic acid synthesis and transport localize dynamically to the old growing pole and septum, PLoS One 9 (2014) e97148.
[40] R.M. Wells, C.M. Jones, Z. Xi, A. Speer, O. Danilchanka, K.S. Doornbos, et al., Discovery of a siderophore export system essential for virulence of Mycobacterium tuberculosis, PLoS Pathog 9 (2013) e1003120.
[41] C.P. Owens, N. Chim, A.B. Graves, C.A. Harmston, A. Iniguez, H. Contreras, et al., The Mycobacterium tuberculosis secreted protein Rv0203 transfers heme to membrane proteins MmpL3 and MmpL11, J. Biol. Chem. 288 (2013) 21714–21728.
[42] M.V. Tullius, C.A. Harmston, C.P. Owens, N. Chim, R.P. Morse, L.M. McMath, et al., Discovery and characterization of a unique mycobacterial heme acquisition system, Proc. Natl. Acad. Sci. U.S.A. 108 (2011) 5051–5056.
[43] A. Milano, M.R. Pasca, R. Provvedi, A.P. Lucarelli, G. Manina, A.L. Ribeiro, et al., Azole resistance in Mycobacterium tuberculosis is mediated by the MmpS5-MmpL5 efflux system, Tuberculosis (Edinb) 89 (2009) 84–90.

[44] K. Andries, C. Villellas, N. Coeck, K. Thys, T. Gevers, L. Vranckx, et al., Acquired resistance of *Mycobacterium tuberculosis* to bedaquiline, PLoS One 9 (2014) e102135.

[45] R.C. Hartkoorn, S. Uplekar, S.T. Cole, Cross-resistance between clofazimine and bedaquiline through upregulation of MmpL5 in *Mycobacterium tuberculosis*, Antimicrob. Agents Chemother. 58 (2014) 2979–2981.

[46] A. Radhakrishnan, N. Kumar, C.C. Wright, T.H. Chou, M.L. Tringides, J.R. Bolla, et al., Crystal structure of the transcriptional regulator Rv0678 of *Mycobacterium tuberculosis*, J. Biol. Chem. 289 (2014) 16526–16540.

[47] L. Rodrigues, D. Machado, I. Couto, L. Amaral, M. Viveiros, Contribution of efflux activity to isoniazid resistance in the *Mycobacterium tuberculosis* complex, Infect. Genet. Evol. 12 (2011) 695–700.

[48] M.R. Pasca, P. Guglierame, E. De Rossi, F. Zara, G. Riccardi, *mmpL7* gene of *Mycobacterium tuberculosis* is responsible for isoniazid efflux in *Mycobacterium smegmatis*, Antimicrob. Agents Chemother. 49 (2005) 4775–4777.

[49] W.X. Xu, L. Zhang, J.T. Mai, R.C. Peng, E.Z. Yang, C. Peng, et al., The Wag31 protein interacts with AccA3 and coordinates cell wall lipid permeability and lipophilic drug resistance in *Mycobacterium smegmatis*, Biochem. Biophys. Res. Commun. 448 (2014) 255–260.

[50] C.M. Jones, R.M. Wells, A.V. Madduri, M.B. Renfrow, C. Ratledge, D.B. Moody, et al., Self-poisoning of *Mycobacterium tuberculosis* by interrupting siderophore recycling, Proc. Natl. Acad. Sci. U.S.A. 111 (2014) 1945–1950.

[51] T.R. Ioerger, T. O'Malley, R. Liao, K.M. Guinn, M.J. Hickey, N. Mohaideen, et al., Identification of new drug targets and resistance mechanisms in *Mycobacterium tuberculosis*, PLoS One 8 (2013) e75245.

[52] E.J. North, M. Jackson, R.E. Lee, New approaches to target the mycolic acid biosynthesis pathway for the development of tuberculosis therapeutics, Curr. Pharm. Des. 20 (2013) 4357–4378.

[53] G. Riccardi, M.R. Pasca, Trends in discovery of new drugs for tuberculosis therapy, J. Antibiot. (Tokyo) 67 (2014) 655–659.

[54] K. Tahlan, R. Wilson, D.B. Kastrinsky, K. Arora, V. Nair, E. Fischer, et al., SQ109 targets MmpL3, a membrane transporter of trehalose monomycolate involved in mycolic acid donation to the cell wall core of *Mycobacterium tuberculosis*, Antimicrob. Agents Chemother. 56 (2012) 1797–1809.

[55] V. La Rosa, G. Poce, J.O. Canseco, S. Buroni, M.R. Pasca, M. Biava, et al., MmpL3 is the cellular target of the antitubercular pyrrole derivative BM212, Antimicrob. Agents Chemother. 56 (2011) 324–331.

[56] S. Lun, H. Guo, O.K. Onajole, M. Pieroni, H. Gunosewoyo, G. Chen, et al., Indoleamides are active against drug-resistant *Mycobacterium tuberculosis*, Nat. Commun. 4 (2013) 2907.

[57] E.J. North, M.S. Scherman, D.F. Bruhn, J.S. Scarborough, M.M. Maddox, V. Jones, et al., Design, synthesis and anti-tuberculosis activity of 1-adamantyl-3-heteroaryl ureas with improved in vitro pharmacokinetic properties, Bioorg. Med. Chem. 21 (2013) 2587–2599.

[58] G. Poce, R.H. Bates, S. Alfonso, M. Cocozza, G.C. Porretta, L. Ballell, et al., Improved BM212 MmpL3 inhibitor analogue shows efficacy in acute murine model of tuberculosis infection, PLoS One 8 (2013) e56980.

[59] S.P. Rao, S.B. Lakshminarayana, R.R. Kondreddi, M. Herve, L.R. Camacho, P. Bifani, et al., Indolcarboxamide is a preclinical candidate for treating multidrug-resistant tuberculosis, Sci. Transl. Med. 5 (2013) 214ra168.

[60] M.J. Remuinan, E. Perez-Herran, J. Rullas, C. Alemparte, M. Martinez-Hoyos, D.J. Dow, et al., Tetrahydropyrazolo[1,5-a]pyrimidine-3-carboxamide and N-benzyl-6',7'-dihydrospiro[piperidine-4,4'-thieno[3,2-c]pyran] analogues with bactericidal efficacy against *Mycobacterium tuberculosis* targeting MmpL3, PLoS One 8 (2013) e60933.

[61] M.S. Scherman, E.J. North, V. Jones, T.N. Hess, A.E. Grzegorzewicz, T. Kasagami, et al., Screening a library of 1600 adamantyl ureas for anti-*Mycobacterium tuberculosis* activity in vitro and for better physical chemical properties for bioavailability, Bioorg. Med. Chem. 20 (2012) 3255–3262.

[62] S.A. Stanley, S.S. Grant, T. Kawate, N. Iwase, M. Shimizu, C. Wivagg, et al., Identification of novel inhibitors of *M. tuberculosis* growth using whole cell based high-throughput screening, ACS Chem. Biol. 7 (2012) 1377–1384.

[63] K. Li, L.A. Schurig-Briccio, X. Feng, A. Upadhyay, V. Pujari, B. Lechartier, et al., Multitarget drug discovery for tuberculosis and other infectious diseases, J. Med. Chem. 57 (2014) 3126–3139.

[64] W. Li, A. Upadhyay, F.L. Fontes, E.J. North, Y. Wang, D.C. Crans, et al., Novel insights into the mechanism of inhibition of MmpL3, a target of multiple pharmacophores in *Mycobacterium tuberculosis*, Antimicrob. Agents Chemother. 58 (2014) 6413–6423.

[65] J.M. Blair, M.A. Webber, A.J. Baylay, D.O. Ogbolu, L.J. Piddock, Molecular mechanisms of antibiotic resistance, Nat. Rev. Microbiol. 13 (2014) 42–51.

[66] L. Rodrigues, J.A. Ainsa, L. Amaral, M. Viveiros, Inhibition of drug efflux in mycobacteria with phenothiazines and other putative efflux inhibitors, Recent Pat. Antiinfect. Drug Discov. 6 (2011) 118–127.

[67] N. Dinesh, S. Sharma, M. Balganesh, Involvement of efflux pumps in the resistance to peptidoglycan synthesis inhibitors in *Mycobacterium tuberculosis*, Antimicrob. Agents Chemother. 57 (2013) 1941–1943.

[68] M. Balganesh, N. Dinesh, S. Sharma, S. Kuruppath, A.V. Nair, U. Sharma, Efflux pumps of *Mycobacterium tuberculosis* play a significant role in antituberculosis activity of potential drug candidates, Antimicrob. Agents Chemother. 56 (2012) 2643–2651.

[69] M. Balganesh, S. Kuruppath, N. Marcel, S. Sharma, A. Nair, U. Sharma, Rv1218c, an ABC transporter of *Mycobacterium tuberculosis* with implications in drug discovery, Antimicrob. Agents Chemother. 54 (2010) 5167–5172.

[70] R.E. Lee, J.G. Hurdle, J. Liu, D.F. Bruhn, T. Matt, M.S. Scherman, et al., Spectinamides: a new class of semisynthetic antituberculosis agents that overcome native drug efflux, Nat. Med. 20 (2014) 152–158.

[71] M. Viveiros, M. Martins, L. Rodrigues, D. Machado, I. Couto, J. Ainsa, et al., Inhibitors of mycobacterial efflux pumps as potential boosters for anti-tubercular drugs, Expert. Rev. Anti Infect. Ther. 10 (2012) 983–998.